



**Università
degli Studi
di Ferrara**



**ISTITUTO
ITALIANO DI
TECNOLOGIA**

DOCTORAL COURSE IN

Translational Neuroscience and Neurotechnologies

CYCLE **XXXVI**

DIRECTOR Prof. Luciano Fadiga

Hebbian-like plasticity induction in ventral premotor–
primary motor network reveals its dynamics during
different prehension actions.

Scientific/Disciplinary Sector (SDS) BIO/09

Research funded by Fondazione Istituto Italiano di Tecnologia

Candidate

Dott. Andrea Casarotto

Supervisor

Prof. Alessandro D'Ausilio

Co-Supervisor

Prof. Thierry Pozzo

Years 2020/2023

SUMMARY

Abstract.....	5
1. INTRODUCTION.....	8
Neural basis of reach-to-grasp movements	8
PMv neurons properties	13
The relevance of PMv-M1 network.....	14
From the study of connectivity to its manipulation	17
The legacy of Donald Olding Hebb	17
The <i>cortico-cortical paired associative stimulation</i> (cc-PAS)	18
The plasticity induction in the PMv-M1 network	19
2. MECHANISMS OF HEBBIAN-LIKE PLASTICITY IN THE VENTRAL PREMOTOR – PRIMARY MOTOR NETWORK	21
Abstract.....	22
Key points.....	24
Introduction	24
Methods	25
Ethical approval.....	25
Participants	26
Electromyography recording	26
TMS.....	27
cc-PAS	27
Neurophysiological indices.....	28
Connectivity protocol.....	30
Experimental procedure	30
Analysis and results.....	32
Data treatment	33
Results.....	33
Discussion	39
Conclusion	44
3. CORTICO-CORTICAL PAIRED ASSOCIATIVE STIMULATION CONDITIONING SUPERFICIAL VENTRAL PREMOTOR CORTEX–PRIMARY MOTOR CORTEX CONNECTIVITY INFLUENCES MOTOR CORTICAL ACTIVITY DURING PRECISION GRIP.....	46

Abstract.....	48
Key points.....	50
Introduction.....	50
Methods.....	52
Ethical approval.....	52
Participants.....	52
Experimental task.....	52
EMG recording.....	54
TMS.....	54
cc-PAS.....	55
Data analysis.....	56
Results.....	57
Corticospinal excitability.....	57
Corticospinal silent period.....	60
Motor-evoked potential latency.....	62
Discussion.....	65
Effects of PMv-to-M1 cc-PAS on corticospinal motor drive.....	65
Effects of PMv-to-M1 cc-PAS on MEP latency.....	68
Limitations and future perspectives.....	69
Conclusion.....	70
Supplementary Analyses.....	71
4. VENTRAL PREMOTOR CORTEX–PRIMARY MOTOR CORTEX PLASTICITY INDUCTION LEADS TO THE MODULATION OF PRECISION GRIP KINEMATICS.....	80
Introduction.....	82
Methods.....	85
Participants.....	85
Experimental task.....	85
Kinematic data recording.....	87
Transcranial Magnetic Stimulation.....	87
Cortico-cortical paired associative stimulation.....	88
EMG recording.....	88
Data Analysis.....	88
Corticospinal Excitability.....	88

Kinematics.....	89
Results.....	90
Corticospinal Excitability.....	90
Acceleration Profile Analyses	91
Standard Deviation Analysis.....	94
Macroscopic Features Analyses.....	95
Discussion	98
Action Preparation.....	98
Kinematic Modulation	100
Conclusion	101
5. DISCUSSION AND FUTURE PERSPECTIVES.....	104
Discussion	104
Future perspectives	108
Clinical implications	110
BIBLIOGRAPHY	113

Abstract

I will present here a series of studies carried out during the three years of my PhD. The theoretical rationale stems from the rather general assumption that every function expressed by the brain must be based on a complex and dynamic network of cortical and subcortical regions and that no integrative function can emerge from the contribution of a single area. Along these lines and, for the sake of operationalizing such a complexity into directly testable hypothesis, we focused our attention towards one particular segment of the extended network responsible for goal-directed actions. More specifically, we conducted a number of experiments on the ventral premotor cortex (PMv)-primary motor cortex (M1) connectivity by means of Transcranial Magnetic Stimulation (TMS), electromyography (EMG) and motion capture (MoCap). All studies employed a relatively recent approach in the domain of non-invasive brain stimulation which is the administration of protocols aimed at inducing plasticity between two anatomically connected brain areas – cortico-cortical Paired Associative Stimulation (cc-PAS). In fact, the ultimate goal of my thesis was to discern whether it was possible to modulate the activity of the ventral premotor cortex (PMv)-primary motor cortex (M1) network to obtain functionally-relevant neurophysiological and behavioural change in reaching and grasping actions.

The first chapter contains a brief introduction on the key aspects that will later become important for the experimental chapters (2, 3 and 4). The introduction will indeed sketch the theoretical framework from which this research originated, including the organisation of the brain network that supports grasping actions. In particular, here I focused on the PMv-M1 network and how it can be studied in humans through TMS. Then, I moved to the description of Hebbian-like plasticity and how it can be promoted via TMS. The chapter closes with a description of the few recent studies applying cc-PAS protocols to the PMv-M1 network. The general take home message of this chapter is that the cc-PAS might be a very powerful tool to investigate the PMv-M1 connectivity and its plastic properties. At the same time, however, we lack fundamental information to fine-tune its properties and to understand why and how it works.

The first study (Chapter 2) is specifically motivated by this lack of neurophysiological understanding of how the cc-PAS impacts on PM-M1 connectivity. In five experiments, we tested different cc-PAS protocols with different coil orientations. We analysed their effects on the connectivity between PMv and M1 and on M1 excitatory and inhibitory intracortical circuits through a number of different neurophysiological indices. Beside shedding new light on the putative circuitry mediating the connectivity between these two areas, the key result was that different coil orientations preferentially recruit different M1 populations, potentially providing different contributions to different motor task.

As a consequence, the second set of experiments (Chapter 3), was aimed at testing whether we could modulate the descending motor output during different grasping actions. In particular, during the execution of a precision and a power grip. Here we tested the effect of two different cc-PAS protocols, one administered with a posterior-anterior (PA) and one with an anterior-posterior (AP) coil orientation, on the motor drive during the isometric execution of a precision and power grip. This study adds one fundamental pieces of information: AP coil orientation preferentially modulates the M1 motor output during the precision grip action and, consequently, we have now access to the neural populations preferentially involved in the execution of this action. This fact opens to a number of possible expansions of our work if we take into consideration how relevant this type of action could be in humans. However, first we had to explore the impact of PMv-M1 cc-PAS on real goal directed actions. Indeed, one of the main goals of my project was to understand whether we could non-invasively manipulate ecological reach to grasp actions.

The last experimental chapter (4) describes experiment that was designed with this goal in mind. This study made use of cc-PAS protocols, as refined in our previous studies, and MoCap recordings to accurately quantify motor performance changes after brain stimulation. In fact, differently from the few studies investigating the impact of PMv-M1 cc-PAS on motor performance, we here set to understand *how* naturalistic motor performance was affected. Our data shows that PMv-M1 cc-PAS affect the relative balance between feedforward and feed-back control processes during the reaching phase of precision grip actions. This is probably one of the most relevant results obtained so far, as it bridges the gap

between physiological modulations and clearly measurable behavioural proxies of fundamental principles of how actions are planned, executed and eventually corrected.

The last chapter (5) will expand on this latter aspect, first by returning to the key results obtained so far and then moving towards areas in need of further research. In particular, I wish to stress here that the goal on my PhD has always been that bridging the gap existing between neurophysiology and behaviour. The last chapter will indeed open a window on what could be the next steps in this direction. I will briefly sketch the two lines of research I'm now pursuing and namely, the role of the PMv-M1 network in guiding goal directed social actions (i.e., when two participants have to coordinate towards a shared motor goal) and to explore the potential that PMv-M1 cc-PAS might have for the rehabilitation of fractioned finger control in stroke patients.

1. INTRODUCTION

Neural basis of reach-to-grasp movements

Reaching and grasping an object is a fundamental aspect of our daily interactions with the environment. Skilled hand function is essential for this ability, and its loss can be devastating. The process of reaching and grasping an object involves the integration of visual information about its location and intrinsic features, such as shape and size, with sensorimotor information about the effector to be used, which is then transformed into an appropriate motor plan. The transformation of purely visual information into a motor plan is a complex process that requires further investigation.

Decades of research on the planning and execution of prehension movements in human and monkeys have led to the definition of a network that supports the performance of these actions (Jeannerod *et al.*, 1995; Raos *et al.*, 2006; Castiello & Begliomini, 2008; Prabhu *et al.*, 2009; Davare *et al.*, 2011). This network, responsible for planning and online control of visually guided grasping actions, connects different regions of the posterior parietal cortex (PPC) and inferior parietal lobe (IPL) with the motor-related areas in the frontal cortex. The dorsal stream connects these regions and is classically divided into two interconnected pathways: the dorsolateral pathway and the dorsomedial pathway. The dorsolateral pathway is responsible for encoding grasping, while the dorsomedial pathway is responsible for encoding reaching (Caminiti *et al.*, 1991; Culham *et al.*, 2003; Culham & Valyear, 2006).

In monkeys, the dorsolateral pathway connects the anterior part of the intraparietal sulcus (AIP) within IPL and the area F5, the rostral part of the ventral premotor cortex (PMv; Murata *et al.*, 1997; Raos *et al.*, 2006). This network supports visual-guided grasping actions by transforming the object's intrinsic visual features into an appropriate motor plan for grasping (Brochier & Umiltà, 2007; Umiltà *et al.*, 2007). The neurophysiological basis of this process is uncertain. However, it may rely on the activation of a specific class of visuomotor neurons known as "canonical".

These neurons have been found in the area F5 (Murata *et al.*, 1997), and have the peculiar property of activating during both the execution of an action and the simple observation of a graspable object. This property led to the concept that these “canonical” neurons in F5 form a motor repertoire of possible grasping actions (Rizzolatti & Luppino, 2001). Furthermore, it is important to note that not only the spike activity, but also the local field potentials (LFPs), of the F5 neurons were found to be grasp-specific during the steady hold of an object (Spinks *et al.*, 2008).

Lesional studies have shown that inactivating the AIP (Gallese *et al.*, 1994) or F5p (Fogassi *et al.*, 2001) area affects the hand-preshaping, while leaving the reach component unaltered (Gallese *et al.*, 1994).

More specifically, abnormalities in hand-shaping and wrist orientation were only evident when more precise prehension was required, such as prehension requiring fractioned finger coordination. Similar results were obtained in human by disturbing the activity of AIP and PMv through protocols of repetitive TMS (rTMS). The application of rTMS protocols on AIP disrupts the online adjustment during grasping actions (Tunik *et al.*, 2005; Rice *et al.*, 2006). Conversely, disrupting the activity of PMv leads to deficits in planning an accurate hand configuration (Davare *et al.*, 2006; Dafotakis *et al.*, 2008).

The dorsomedial pathway connects the area V6A (Bosco *et al.*, 2010) and the medial intraparietal (MIP) cortex (Johnson *et al.*, 1996) with the area F2vr in the dorsal premotor cortex (PMd; Caminiti *et al.*, 1991). This pathway encodes the information necessary for planning and controlling the effector during the transport phase. Planning and control occur through the integration of visual and somatosensory information (Rizzolatti *et al.*, 1998). Additionally, areas PF, PFG and PG on the convexity of the IPL exhibit object-related sensorimotor properties related to the mouth, hand and arm, respectively (Rozzi *et al.*, 2008).

However, the classical description of this network has been deemed too rigid. Indeed, just as in movement reaching and hand-preshaping components are interconnected rather than being strictly segregated, so are their neural bases. In monkeys, neurons in the regions previously identified as the substrates of the reaching phase, V6A and F2 area, have also shown activity related to grasping (Raos *et al.*, 2004; Fattori *et al.*, 2010). Lesional studies have also provided

evidence for a non-complete segregation of these two networks. A lesion of the V6A area in monkeys resulted in an inability to correctly perform an object-directed grasping action. The monkeys exhibit misreaching of the targets, abnormal wrist orientation, and incorrect hand-preshaping (Battaglini *et al.*, 2002; Galletti *et al.*, 2003). Neuroimaging studies in human have also demonstrated that areas V6A and PMd are strongly coupled during grasping, similar to the coupling of AIP and PMv areas (Grol *et al.*, 2007).

Similarly, the core areas encoding grasping (i.e. AIP and F5), have been shown to host neural populations that are also active during the reaching phase (Stark & Abeles, 2007; Lehmann & Scherberger, 2013).

These results suggest that both sub-networks are causally involved in grasping encoding. Nevertheless, lesions in the dorsolateral stream primarily impair the grasping element, whereas lesions of the dorsomedial stream may only affect the reaching component (e.g. lesion of medial intraparietal area - MIP) but can also affect both the reaching and grasping component (e.g. lesion of V6A; Andersen & Buneo, 2002; Turella & Lingnau, 2014). Considering these factors, it is reasonable to argue for only a partial dissociation of these pathways.

Based on the investigations conducted in monkeys, several studies have set themselves the goal of finding the homologous network that supports reach-to-grasp actions in humans. Obviously, in this case is more difficult to have evidence from lesional studies and almost impossible from intracranial recording. However, neuroimaging and non-invasive brain stimulation (NIBS) techniques, as well as clinical studies on patients have provided evidence supporting homologue networks in humans.

Considering the dorsolateral pathway and, consequently, the hand-preshaping component, neuroimaging studies have suggested that the anterior intraparietal sulcus (aIPS; Culham *et al.*, 2003) and the PMv (Cavina-Pratesi *et al.*, 2010) could represent the human homologue of the dorsolateral system. In summary, this stream appears to be left-lateralized, projecting medially from the occipital lobe to the left inferior parietal lobe (IPL) and ultimately terminating in the PMv, which is the human homologue of the monkey F5 area.

On the other hand, the dorsomedial pathway showed reaching-related activation in the medial intraparietal sulcus (mIPS; (Prado *et al.*, 2005; Filimon *et al.*, 2009), in

the superior parietal occipital cortex (SPOC), in the praecuneus (Connolly *et al.*, 2003; Prado *et al.*, 2005; Filimon *et al.*, 2009; Cavina-Pratesi *et al.*, 2010) and in the dorsal premotor cortex (PMd; Filimon *et al.*, 2007, 2009). This pathway runs bilaterally from the occipital cortex to the PPC and superior parietal lobe (SPL) before arriving in the frontal PMd, which is the human homologue of monkey F2 area.

As previously mentioned, in human complementary information on the organization of these networks comes from studies on patients. A lesion in the parieto-occipital junction (POJ), usually bilaterally but also unilaterally, can lead to the onset of a clinical condition known as “optic ataxia”. Patients with this condition exhibit a disorder of visually guided action. They make gross errors when attempting to reach a visible object and demonstrate inadequate online control, failing to make prompt corrections if the target of a reaching movement is unexpectedly displaced (Pisella *et al.*, 2000). Despite this deficit in visuomotor coordination, these patients retain the ability to correctly grasp objects.

However, as for monkeys, the classical distinction between reach-related and grasp-related areas proved to be too rigid also for humans. Indeed, recent studies have shown that several regions, including the PMv, the inferior PMd, the anterior SPL and the aIPS encode both reaching and grasping elements (Fabbri *et al.*, 2014). These results do not detract from the concept of networks that are, to some extent, specialised in encoding the reaching and hand-preshaping elements. However, it would be oversimplifying to view them as completely segregated networks. Instead, they seem to be closely interconnected. Through a mutual connection in the IPL, these two sub-streams can integrate perceptual information into a congruent action plan that enable the grasping of object for use (Rizzolatti & Matelli, 2003; Binkofski & Buxbaum, 2013; Vingerhoets, 2014).

Despite decades of investigation and numerous identified areas, it remains unclear how visual information is transformed, integrated with somatosensory and proprioceptive information, and previous knowledge to build a congruent motor plan.

Regarding the dorsolateral stream, it is currently sustained that the AIP encodes a sensorimotor representation of an object’s visual properties. This information is then transmitted to the PMv (Luppino *et al.*, 1999; Borra *et al.*, 2008), which in turn

directly projects to the primary motor cortex (M1). It can be imagined that the premotor cortices form the motor plan and send it to the M1. The M1 neurons receive and process this information before it is conveyed to the spinal cord by the pyramidal tract neurons (PTNs). **Figure 1.1** provides a complete representation of the described network.

The following sections will focus on the AIP-PMv-M1 network and the properties of the PMv neuronal populations.

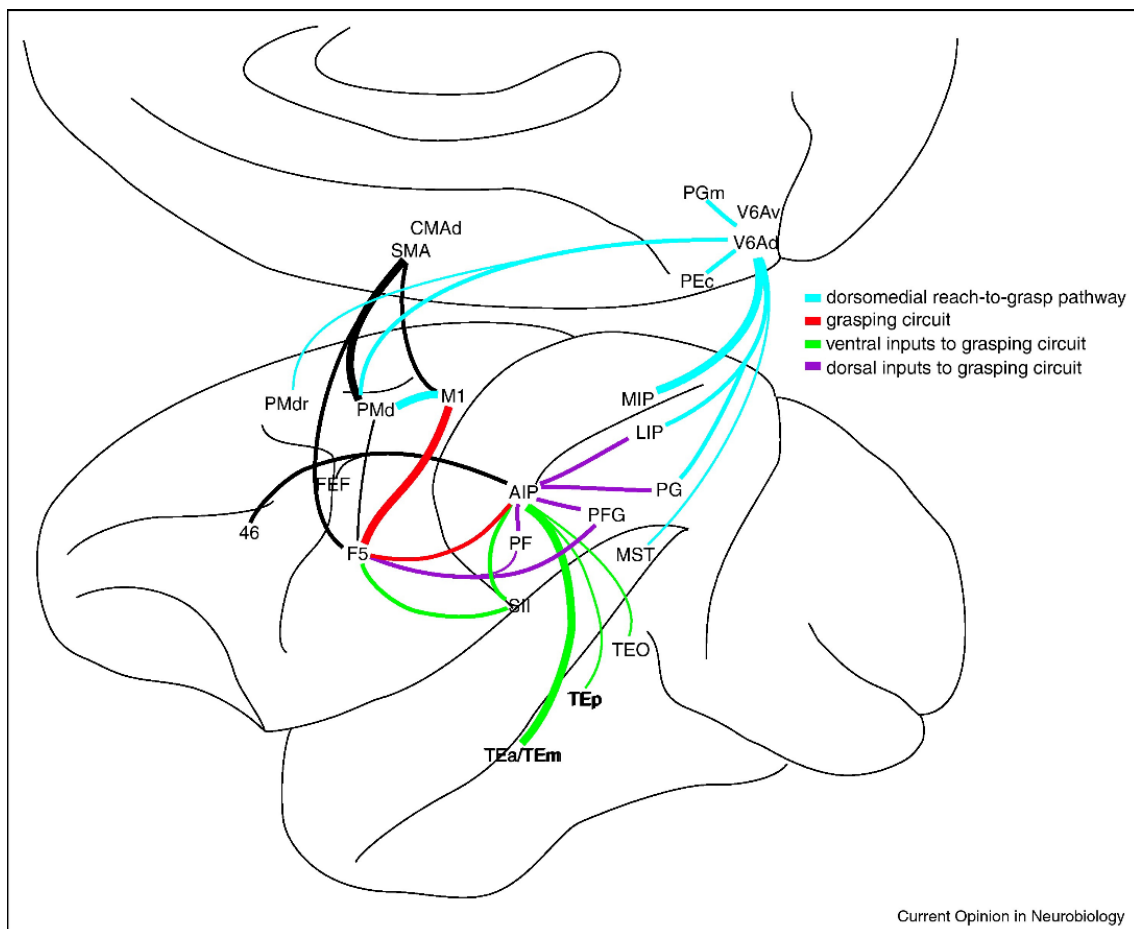


Figure 1.1 Anatomical connections of the cortical grasping network in non-human primates (Grafton, 2010; Davare *et al.*, 2011). AIP-F5-M1 represent the key nodes of the grasping circuit (here linked in *red*). AIP processes the grasp-related object properties and received inputs from different areas (i.e. PF, PFG, PG in the IPL and LIP) located in the dorsal stream (here, in *purple*) and in the ventral stream (i.e. SII, TEa/TEm, TEp, Teo and from the MST; here, in *green*). All these connections provide AIP with information on the properties of an object and the knowledge stored within it. In *blue* is highlighted the dorsomedial circuits that connect the area V6A with the area MIP, LIP, PG, MST, the medial parietal areas (Pec and PGm) and the PMd.

PMv neurons properties

As previously described, the PMv serves as the convergence area of the dorsolateral network that supports hand-preshaping during reach-to-grasp movements. In this section, we will provide a brief summary of the properties of the different neuronal populations of PMv to highlight the importance of this area in our research project.

In the monkey's F5, both motor and sensorimotor (i.e. visuomotor) neurons have been identified. The motor neurons discharge in association with specific types of grasping movements. In other words, different objects grasped similarly determined similar F5 motor neuron responses (Rizzolatti *et al.*, 1998).

The previously cited visuomotor neurons, also known as “canonical” neurons, were found to fire not only during an active grasping movement but also during the simple presentation of 3-D objects. The prevalence of these neurons has been shown to selectively discharge for one or few objects (Murata *et al.*, 1997; Raos *et al.*, 2006). Moreover, the neurons that were activated for a specific object were also activated during the grasping of that object (Murata *et al.*, 1997). These findings imply that the object shapes are encoded by the F5 neurons even when a motor action is not required.

These neurons are complemented by another visuomotor neuronal population, known as “mirror” neurons. These neurons are activated both when the monkey performs a specific action and when it observes another individual performing the same action (di Pellegrino *et al.*, 1992; Gallese *et al.*, 1996).

This class of neurons will not be discussed in detail here, but they highlight the visuomotor nature of the F5 area. However, we may mention that this mirroring behaviour has led to speculation about a role of mirror neurons in understanding and imitating the actions of others (Rizzolatti & Craighero, 2004).

At this point, we have examined the neural organization of the reach-to-grasp network and the relevant properties of the PMv area. Next, we will focus on the most relevant part of this network for the research conducted during my PhD course: the PMv-M1 connections.

The relevance of PMv-M1 network

In this section, we will briefly consider the connections of the AIP-PMv-M1 network before focusing on the connections between PMv-M1 in monkeys and humans.

The AIP receives different inputs from various regions, including the infero-temporal and medio-superior temporal (MST) lobe regions (i.e. TEa/TE_m, TE_p and TEO) in the ventral stream, as well as from IPL (i.e. PF, PFG, and PG) and lateral intraparietal area (LIP) in the dorsal stream. Finally, both AIP and PMv receive connections from the secondary somatosensory cortex (SII; Davare *et al.*, 2011). These inputs provide AIP with real-time information about the properties of an object, along with stored previous knowledge about its identity.

The AIP is reciprocally connected with PMv, which is in turn reciprocally connected to M1.

In monkeys, electrical stimulation of the premotor cortex elicits two types of response in M1 PTNs: a pure inhibition response or an early excitatory response followed by an inhibitory response (Tokuno & Nambu, 2000). This response pattern is common for both PTNs located in M1 layer III and those in layer V (Ghosh & Porter, 1988).

Subsequent studies have analysed the effect of PMv input on M1 motor output in more detail. Indeed, the M1 motor output consists of a sequence of descending discharges, also known as descending *volleys*, sculpted by inputs from other areas. These discharges are classified as an early direct wave (D-wave), a first indirect wave (I₁-wave) and later indirect waves (I₂-, I₃-wave; Di Lazzaro *et al.*, 2012).

These descending *volleys* are clearly visible stimulating the M1 and registering directly from the spinal cord or via an intramuscular electrode (Shimazu *et al.*, 2004; Di Lazzaro *et al.*, 2012).

In monkeys, the stimulation of the F5 area (PMv) was found to cause a clear modulation of the M1 descending discharges. When the stimulation of M1 neurons was preceded by the stimulation of the F5 area neurons, there was a strong facilitation of I₂- and I₃-wave (Cerri *et al.*, 2003; Shimazu *et al.*, 2004). These results highlight the capability of PMv to modulate the M1 motor output.

In humans, the connections between different areas have been studied using a paired-pulse TMS approach (pp-TMS). In this protocol, a conditioning stimulus

(CS) is released in the first area studied, followed by a test stimulus (TS) released in M1. The first stimulus activated the projections of the studied area toward M1, while the second stimulus activates M1, generating the MEP. This approach allows for the observation of the effect of the first area on M1.

Through this approach, several studies have explored the influence of PMv on M1 during rest and actions execution and observation.

At rest, PMv stimulation 4, 6 or 8 ms before M1 with an intensity of 80% of the active motor threshold (AMT) facilitated the ipsilateral M1. When the CS intensity was increased to 90% RMT the PMv exerted an inhibitory effect on the ipsilateral M1 when stimulated 2, 4 or 6 ms before. Further increasing the CS intensity to 110% RMT it was observed an inhibitory effect of PMv on M1 with an interstimulus interval (ISI) of 2, 4 or 10 ms (Bäumer *et al.*, 2009). This first study suggests that different CS intensities may recruit different neuronal populations within M1, which could exert different effects on M1.

Davare and colleagues (2008) replicated the inhibitory influence exerted by PMv on M1 with an ISI of 6 ms. Moreover, they also observed that this influence disappeared during the execution of a power grip action and was converted into strong facilitation during the precision grip execution. Therefore, the effect exerted by PMv on M1 appears to be dependent on the specific type of grasp performed. However, in this study, the MEPs were recorded from the first dorsal interosseus (FDI) muscle, which is more functionally involved in the execution of precision rather than power grip. This may have in part contributed to the facilitation effect observed during the precision grip execution.

Studying the effect exerted by PMv on M1 during the action preparation it was possible to extend these results. During the preparation of different prehension actions (precision vs. power), it was observed that PMv exerts a facilitatory influence on the muscle subsequently involved in the actions. The study by Davare *et al.* (2009) found that the MEPs in FDI were facilitated during precision grip preparation, but not during power grip preparation. Conversely, MEPs in the abductor digiti minimi (ADM) muscle were facilitated during power grip preparation, but not during precision grip preparation. The degree of facilitations was correlated with the amount of muscle activity expressed later during the prehension.

Considering a wider network, facilitatory influence exerted by PMv on M1 during action preparation results to be significantly reduced following the disruption of AIP's activity (Davare *et al.*, 2010). This finding remarks the centrality of AIP-PMv interactions in grasping programming and execution.

Similar results were obtained when studying the influence of PMv on M1 during action observation, where PMv exerts a muscle-specific positive influence on M1. During the observation of execution of a precision grip, there was a facilitation of the MEPs recorded in the FDI muscle. Conversely, during the observation of a power grip there was a facilitation in the ADM muscle. This effect was only present when the hand configuration was congruent with the object to be grasped. If the hand-shape conflicts with the object to be grasped (e.g., the hand-shape of a pinch to grasp a glass that required a whole hand configuration) the facilitation was absent (Koch *et al.*, 2010b). The same effect was observed when it was tested a specific intracortical circuit in M1 responsible for the I₂-wave generation, which reflects the activity of the cortico-cortical connections transmitting inputs from PMv to M1 (Koch *et al.*, 2010b).

Overall, these results provide an overview of the relevance and current knowledge regarding the role of the PMv-M1 pathway as a neural substrate for grasping actions. These studies also provided the methodological basis for subsequent studies aimed at inducing plasticity in this network. In other words, they provided the methodological basis for the studies conducted during my PhD course.

In the upcoming session, we will discuss the phenomenon of neural plasticity and its induction through the TMS, specifically in the PMv-M1 connections.

From the study of connectivity to its manipulation

The legacy of Donald Olding Hebb

The plasticity protocols used to manipulate neural connectivity are based on the Hebbian principle according to which:

“When an axon of cell A is near enough to excite cell B and repeatedly or persistently takes part in firing it, some growth process or metabolic change takes place in one or both cells such that A’s efficiency, as one of the cells firing B, is increased” (Hebb, 1949).

In other words, repeated activation of the presynaptic neurons immediately before the postsynaptic neurons induces synaptic strengthening leading to a condition known as long-term potentiation (LTP). Although Hebb did not propose an inverse rule for inverse neuronal activation, the repeated activation of a presynaptic cell immediately after the postsynaptic one leads to synaptic weakening. This phenomenon is known as long-term depression (LTD) (Malenka, 1994; Brzosko *et al.*, 2019). This synaptic learning rule is also known as spike-timing-dependent plasticity (STDP).

The neurophysiological basis of synaptic plasticity remains unclear and may depend on the type of synapses involved (e.g. glutamatergic, GABAergic), their location (i.e. near the soma or dendritic arbour of the neuron) or the frequency of the stimulation.

Generally, inducing an LTP state requires presynaptic input activation a few milliseconds before the backpropagating action potential (BAP) in the postsynaptic dendrites. In this way, the BAP can facilitate the release of Mg^{2+} from NMDA and leading to Ca^{2+} influx in the postsynaptic cell and inducing the LTP. Conversely, if the excitatory post-synaptic potential (EPSP) of the presynaptic neuron coincides with the afterdepolarizations of the postsynaptic cell a moderate Ca^{2+} influx occurs, leading to the LTD state. In excitatory synapses onto inhibitory neurons and in GABAergic synapses, the learning rules appear to have a more variable temporal window. For example, some synapses show an asymmetrical timing to induce the LTP effect compared to the LTD effect. Other cells exhibit a totally opposite timing, where the stimulation of the postsynaptic neuron before the presynaptic one leads to the LTP and vice versa (for a complete view, see Caporale & Dan, 2008).

A shared characteristic among these various STDPs is that the establishment of plasticity depends on the modulation of Ca^{2+} influx in the postsynaptic neurons, regardless of differences in time windows.

The cortico-cortical paired associative stimulation (cc-PAS)

In humans, the first attempt to manipulate neural plasticity was made by Stefan and colleagues (Stefan *et al.*, 2000). They repeatedly paired a TMS single pulse (spTMS) over M1 with peripheral median nerve electrical stimulation with an ISI of 25 ms. It is known that MNS activates the primary somatosensory cortex (S1) after approximately 20 ms (Allison *et al.*, 1991). Considering a few additional milliseconds, the signal travels from S1 to M1 and arrives here just before the trans-synaptic excitation of corticospinal neurons by the TMS pulse. The pairing of these two stimuli 100 times led to a long-lasting enhancement of corticospinal excitability (CSE). Conversely, if the ISI between the MNS and the M1 stimulations was set at 10 ms, the reverse effect was obtained: a long-lasting depression of the CSE (Wolters *et al.*, 2003).

Starting from this first protocol, several others were developed, including the *cortico-cortical paired associative stimulation (cc-PAS)*. The cc-PAS is a dual-sites TMS (ds-TMS) protocol thought to promote Hebbian STDP (Hebb, 1949; Markram *et al.*, 1997, 2011) by mimicking the neuronal pre- and postsynaptic coupling pattern that induces STDP. This is achieved through a series of TMS pairs on two interconnected areas with a specific and constant ISI. In each couple of pulses the first is delivered to the first brain area, and after a few milliseconds, the second is delivered to the second region.

This protocol was first proposed by Rizzo and colleagues (2009), and since then, several pieces of evidence have supported its capability to modulate neural connectivity between different brain regions.

The following section provides a brief analysis of the results obtained by the application of the cc-PAS protocol in the PMv-M1 network.

The plasticity induction in the PMv-M1 network

PMv is directly connected to M1 and can exert both inhibitory and excitatory effects. Neural projections from PMv target both the superficial layers (L2-L3) and the deeper layers (L5) of M1, targeting both glutamatergic corticospinal neurons and GABAergic interneurons (Ghosh & Porter, 1988; Tokuno & Nambu, 2000).

The first study that applied the cc-PAS protocol on PMv-M1 network was conducted by Buch and colleagues (Buch *et al.*, 2011). After the cc-PAS, opposing effects on the CSE were reported based on the subjects' state. At rest, there was a reduction of the CSE; conversely, during a task execution there was an increment in the CSE.

Since this initial study, further investigation delved into the neurophysiological and behavioural modulations induced by the application of different PMv-M1 cc-PAS protocols (Johnen *et al.*, 2015; Fiori *et al.*, 2018; Casarotto *et al.*, 2023a, 2023b; Turrini *et al.*, 2023b). These results will be discussed in the following chapters.

2. MECHANISMS OF HEBBIAN-LIKE PLASTICITY IN THE VENTRAL PREMOTOR – PRIMARY MOTOR NETWORK

In the present chapter will be reported the first experiment conducted during my PhD course. At the time of the experiment, only two papers had been published that used a cc-PAS protocol to induce plasticity in the PMv-M1 network (Buch *et al.*, 2011; Johnen *et al.*, 2015). However, neither of these papers investigated in depth the neurophysiological modulations induced by the cc-PAS in the cited network. For this reason, before investigating possible behavioural modulations, we decided to explore the neurophysiological modulations induced by the application of the cc-PAS protocol in this network.

In five different TMS experiments we tested different cc-PAS protocols with the coil in posterior-anterior (PA) and anterior-posterior (AP) coil orientation over M1. To understand the after-effect induced, we collect several single-pulse (sp-TMS) and paired-pulses (pp-TMS) neurophysiological indices necessary to elucidate the modulation induced in M1 local circuitry. Moreover, through a ds-TMS protocol we studied the effect of plasticity induction on the PMv-M1 connectivity. After these multiple experiments, we proposed a neurophysiological model to explain our results. This neurophysiological model will form the basis of our subsequent works.

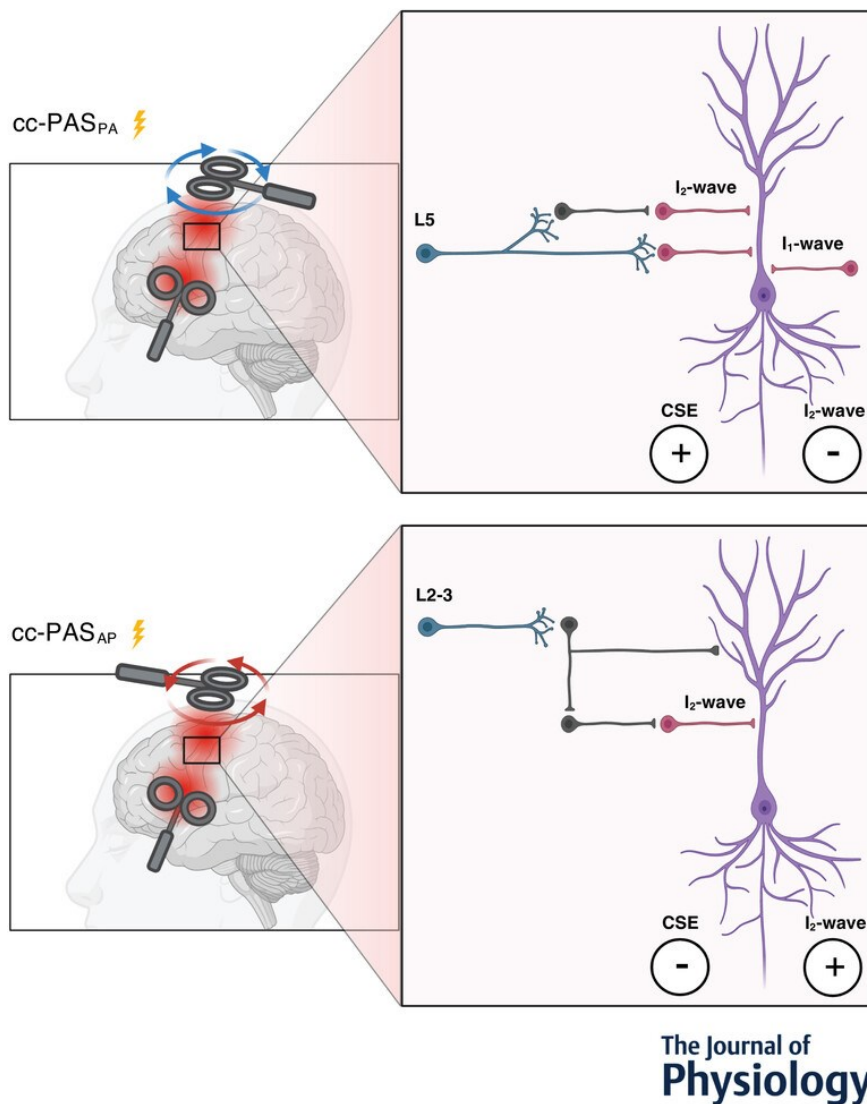
The following results were initially presented at the XXIX CONGRESSO NAZIONALE SIPF "BEYOND THE LOCKDOWN OF THE BRAIN" in Palermo (Italy; 30/09/2021 - 2/10/2021) and then at the Brain Stimulation: Basic, Translational, and Clinical Research in Neuromodulation in Lisbon (Portugal; 19/02/2023 – 22/02/2023).

It is published in *The Journal of Physiology* as:

Casarotto, A., Dolfini, E., Cardellicchio, P., Fadiga, L., D'Ausilio, A., & Koch, G. (2023). Mechanisms of Hebbian-like plasticity in the ventral premotor – Primary motor network. *The Journal of Physiology*, 601(1), 211–226.

Abstract

The functional connection between ventral premotor cortex (PMv) and primary motor cortex (M1) is critical for the organization of goal-directed actions. Repeated activation of this connection by means of cortico-cortical paired associative stimulation (cc-PAS), a transcranial magnetic stimulation (TMS) protocol, may induce Hebbian-like plasticity. However, the physiological modifications produced by Hebbian-like plasticity in the PMv-M1 network are poorly understood. To fill this gap, we investigated the effects of cc-PAS on PMv-M1 circuits. We hypothesized that specific interactions would occur with I₂-wave interneurons as measured by the short intracortical facilitation protocol (SICF). We used different paired-pulse TMS protocols to examine the effects of PMv-M1 cc-PAS on SICF, on GABAergic circuits as measured by short (SICI) and long (LICI) intracortical inhibition protocols and varied the current direction in M1 to target different M1 neuronal populations. Finally, we examined the effects of cc-PAS on PMv-M1 connectivity using a dual coil approach. We found that PMv-M1 cc-PAS induces both a long-term potentiation (LTP)- or long-term depression (LTD)-like after-effect in M1 neuronal activity that is strongly associated with a bidirectional-specific change in I₂-wave activity (SICF = 2.5 ms ISI). Moreover, cc-PAS induces a specific modulation of the LICI circuit and separately modulates PMv-M1 connectivity. We suggest that plasticity within the PMv-M1 circuit is mediated by a selective mechanism exerted by PMv on M1 by targeting I₂-wave interneurons. These results provide new mechanistic insights into how PMv modulates M1 activity that are relevant for the design of brain stimulation protocols in health and disease.



Abstract Figure.

The neural circuits involved in plasticity induction after the ventral premotor cortex to primary motor cortex (PMv-to-M1) cortico-cortical paired associative stimulation (cc-PAS). Left, the cc-PAS coil orientations: postero-anterior (PA) and antero-posterior (AP). Right blocks show the neural circuits preferentially activated by the different coil orientations. The pyramidal neuron (PN) (purple) receives both excitatory (red) and inhibitory (grey) synaptic inputs responsible for the generation of I₂-waves. The PMv projections (light blue) contact the interneurons within M1 in both layers 2–3 (L2–3) and in L5. The cc-PASPA protocol preferentially target the deep neuron populations in L5, increasing the corticospinal excitability (CSE) and inhibiting the I₂-wave circuits (top block). On the other side, AP stimulation activates the more superficial neuronal populations in L2–3, inhibiting the dendritic arbour of the PN, leading to a reduction of CSE and a simultaneous increase in the activity of the I₂-wave circuit (bottom block).

Key points

- The I₂-wave is specifically modulated by the induction of ventral premotor cortex – primary motor cortex (PMv-M1) plasticity.
- After PMv-M1 cortico-cortical paired associative stimulation (cc-PAS), corticospinal excitability correlates negatively with I₂-wave amplitude.
- Different cc-PAS coil orientations can lead to a long-term potentiation- or long-term depression-like after-effect in M1.

Introduction

Human goal-directed actions are guided by a parieto-frontal network in which the ventral premotor cortex (PMv) represents a critical hub (Murata *et al.*, 1997; Fogassi *et al.*, 2001; Raos *et al.*, 2006; Grol *et al.*, 2007; Umiltà *et al.*, 2007; Turella & Lingnau, 2014). The Parieto - PMv – M1 network is crucial in transforming object properties (e.g. size, shape and texture) into appropriate grasping actions (Murata *et al.*, 1997, 2000; Davare *et al.*, 2010).

Dual-site transcranial magnetic stimulation (ds-TMS) at rest shows that the PMv exerts either an inhibitory or an excitatory influence on M1, depending on the intensity of PMv stimulation (Davare *et al.*, 2008; Bäumer *et al.*, 2009; de Beukelaar *et al.*, 2016). This influence is also relevant during action preparation or action observation (Davare *et al.*, 2008; Lago *et al.*, 2010; de Beukelaar *et al.*, 2016).

Input from the PMv probably interacts with a specific set of interneurons located in M1. In monkeys, when a single stimulus delivered to F5 (homologous of PMv) conditioned a test M1 stimulus, the late indirect (I) waves of the resulting corticospinal volley are selectively facilitated (Cerri *et al.*, 2003; Shimazu *et al.*, 2004). In humans, the I-wave interactions during grasping preparation (Cattaneo *et al.*, 2005) show a selective grasp-related activation of the late I₂-wave prior to movement onset, confirming that this specific circuit mediates the functional input from PMv.

Recently, cortico-cortical paired associative stimulation (cc-PAS) has been used to modulate PMv-M1 functional connectivity (Buch *et al.*, 2011; Fiori *et al.*, 2018). cc-PAS is a ds-TMS protocol thought to promote Hebbian spike-timing-dependent plasticity (STDP) (Hebb, 1949; Markram *et al.*, 2011). The cc-PAS protocol mimics

the neuronal pre- and postsynaptic coupling pattern that induces STDP, via a series of TMS pairs on two interconnected areas with a specific interstimulus interval (ISI). Strengthening of PMv-M1 connectivity appears to lead to a larger inhibitory influence exerted by the PMv on M1, at rest. At the same time, during action preparation, the excitatory influence exerted by the PMv is also increased (Buch *et al.*, 2011).

However, the physiological modifications produced by cc-PAS in the PMv-M1 network and in the M1 intracortical circuitry are poorly understood.

To investigate the effect of PMv-M1 plasticity induction on the PMv-M1 circuit and M1 local circuitry, we measured the impact of the cc-PAS protocol on different M1 intracortical circuits. We hypothesized an influence of cc-PAS in specific circuits mediating the input from M1: in particular, in those with a specific interaction with I₂-wave interneurons (Cattaneo *et al.*, 2005). We evaluated changes in short intracortical facilitation (SICF) and the effects on GABAergic interneurons by measuring short-interval intracortical inhibition (SICI; 1 and 3 ms) and long-interval intracortical inhibition (LICI; 100 ms). In another set of experiments, we explored whether PMv-to-M1 cc-PAS would also modulate PMv-M1 connectivity. In a fourth experiment, we varied the current direction (postero-anterior or PA and antero-posterior or AP) of M1 stimulation during cc-PAS, hypothesizing opposite long-term potentiation (LTP)- or long-term depression (LTD)-like after-effects due to the activation of different synaptic inputs to the corticospinal neurons (Ni *et al.*, 2011b; Koch *et al.*, 2013; Federico & Perez, 2017). Indeed, while PA stimulation activates neurons in deep M1 layers, AP is more likely to stimulate superficial layers (Koch *et al.*, 2013; Sommer *et al.*, 2013).

Methods

Ethical approval

All the participants were informed about the experimental procedure and gave their written consent according to the last update of the Declaration of Helsinki, except for the registration in a database. The experiment was approved by the ethics committee 'Comitato Etico Unico della Provincia di Ferrara' (approval No. 170 592). The participants were compensated for their participation with €30.00 for

their first TMS session and €15.00 if they took part in one of the subsequent experimental sessions.

Participants

A total of 39 healthy (mean age = 26 years; $SD = 4.5$; males: 17) volunteers took part in the study: 14 participants completed the first experimental session (*Experiment 1*); 22 subjects took part in the second experimental session (*Experiment 2, Experiment 3*); 17 subjects were recruited for the third experimental session (*Experiment 4*) and 10 subjects completed the fourth experimental session (*Experiment 5*). In the second session, due to technical problems with data acquisition, 21 participants completed *Experiment 2* while 18 completed *Experiment 3* (see **Table 2.1**). The sample size is in line with previous studies using similar experimental manipulations (Rizzo *et al.*, 2009; Chiappini *et al.*, 2018; Fiori *et al.*, 2018).

Experiment	Subjects (males)	Age	M1 rMT _{PA} 70 mm coil	M1 rMT _{PA} 50 mm coil ₁	M1 rMT _{PA} 50 mm coil ₂	M1 rMT _{AP}
1	14 (9)	27.3 ± 4.7	49.1 ± 8.8	44.8 ± 8.1	46.9 ± 8.7	
2	21 (6)	26.4 ± 4.5	47 ± 7.7	42.4 ± 7.8	44.3 ± 7.7	
3	18 (5)	26.9 ± 4.6	47.1 ± 7.1	42.5 ± 7.8	44.5 ± 7.5	
4	17 (8)	25.4 ± 5.3	47.5 ± 7.3	41.2 ± 6.7	44.4 ± 7.2	50.6 ± 7.3
5	10 (5)	25.1 ± 4.5	54.2 ± 10.1	46.5 ± 9.6	50 ± 10.7	

Table 2.1. For each experiment, the number of subjects, their age and rMT (mean ± SD).

The rMT value indicates the percentage of the maximum stimulator output and is reported for all coils used. During the cc-PAS protocol and acquisition of connectivity, the 50 mm coil₁ was positioned on M1 while the 50 mm coil₂ was on PMv.

Electromyography recording

Surface electromyography (EMG) was recorded from the right first dorsal interosseous (FDI) muscle by means of a wireless system (Zerowire EMG, Aurion, Italy) with a tendon-belly montage. EMG signals were digitized (2 kHz) and acquired with a CED Power1401-3A board (Cambridge Electronic Design,

Cambridge, UK). All the acquired data were stored for offline analysis using the Signal 3.09 software (Cambridge Electronic Design, Cambridge, UK).

TMS

Participants were seated on a comfortable armchair, during all experimental sessions, with their right arm on an armrest. They remained relaxed and they did not observe any videos or perform any actions. Single-pulse and paired-pulse TMS protocols were administered through a 70 mm figure-of-eight focal coil connected to a Magstim BiStim2 monophasic stimulator (The Magstim Company, Whitland, UK). By contrast, for the cc-PAS protocols and PMv-M1 connectivity evaluations we used two 50 mm figure-of-eight focal coils connected to the same Magstim BiStim2 monophasic stimulator.

The FDI optimal scalp position (OSP) was found by moving the coil in 0.5 cm steps over the left M1 hand area and using a slightly suprathreshold stimulus. Resting motor threshold (rMT) was defined as the lowest intensity that evoked a motor-evoked potential (MEP) with $>50 \mu\text{V}$ amplitude in 5 out of 10 consecutive trials while the participants kept the FDI muscle relaxed (Rossi *et al.*, 2009; Rossini *et al.*, 2015). **Table 2.1** gives a summary of the rMT in each experiment and coil. The individual OSP and rMT were defined for each coil used in each experiment (50 or 70 mm) and separately for the different coil orientations as later specified in the description of each experiment.

cc-PAS

In the cc-PAS protocol, dsTMS repeatedly activates the connection between left PMv and left M1. One-hundred pairs of pulses were delivered at a frequency of 0.25 Hz for ~6 min. The left PMv was stimulated at 90% of individual rMT while the left M1 was stimulated at 120% of rMT (Koch *et al.*, 2013). In each pair, M1 stimulation followed the PMv stimulation by 6 ms (Davare *et al.*, 2008, 2009; Koch *et al.*, 2010*b*; Lago *et al.*, 2010). The coil over the left M1 was placed tangentially to the scalp on the FDI OSP, at $\sim 45^\circ$ with respect to the midline, to induce a PA current flow (Experiment 1-2-3-5); from this position the coil was rotated 180° to induce an AP current flow (*Experiment 4*). To estimate the position of the left PMv we used the SofTaxic Navigator System (Electro Medical System, Bologna, Italy).

The skull landmarks (nasion,inion, right, and two preauricular points) and 23 points on the scalp were digitized through a Polaris Vicra optical tracker (Northern Digital, Waterloo, Canada). To stimulate the left PMv, the coil was placed over a scalp region corresponding to Montreal Neurological Institute (MNI) coordinates: $x = -52.8$, $y = 11.6$, $z = 25.1$ (Koch *et al.*, 2010b).

Neurophysiological indices

Motor-evoked potential

MEPs were collected with a single pulse protocol (sp-TMS) with a suprathreshold stimulus at 120% of the individual rMT. The amplitude of the MEP provides a global readout of corticospinal excitability (CSE) (Aguiar & Baker, 2018; Derosiere *et al.*, 2020).

Short-interval intracortical inhibition at 1 and 3 ms

SICI is measured via a paired-pulse (pp-TMS) paradigm with a first subthreshold conditioning stimulus (CS) followed, 1–5 ms later by a second suprathreshold test stimulus (TS). Here we set the CS at 80% and the TS at 120% of individual rMT. We tested two different ISIs, 1 and 3 ms, since previous studies suggest the existence of two phases, or two inhibition peaks, respectively at 1 ms and at 2.5–3 ms (Fisher *et al.*, 2002; Roshan *et al.*, 2003; Vucic *et al.*, 2011; Hannah *et al.*, 2020; Cardellicchio *et al.*, 2021). Pharmacological studies suggest that SICI at 3 ms ISI reflects GABA_A receptor-mediated fast intracortical inhibition in M1 (Ziemann *et al.*, 1996a, 2015; Di Lazzaro *et al.*, 2006). In particular, it has been proposed that it may represent short-lasting IPSPs in corticospinal neurons (Ilić *et al.*, 2002; Ziemann *et al.*, 2015). In contrast, the origin of SICI at 1 ms is still debated. Some authors propose that it does not derive from inhibitory synaptic input, but rather originates from the axonal refractoriness of neurons recruited by the CS (Hannah *et al.*, 2020; Fong *et al.*, 2021), whereas others suggest that it originates from synaptic mechanisms (Fisher *et al.*, 2002; Roshan *et al.*, 2003).

Long-interval intracortical inhibition at 100 ms

LICI is measured via a pp-TMS paradigm consisting of two suprathreshold stimuli; the MEPs elicited by the TS (second pulses) are inhibited by the CS (first pulses).

We set both the CS and the TS at 120% of the individual rMT with an ISI of 100 ms. It has been proposed that the LICl reflects GABA_B receptor-mediated slow inhibition in M1 (McDonnell *et al.*, 2006; Ziemann *et al.*, 2015) and, in particular, slow IPSPs (Werhahn *et al.*, 1999).

Intracortical facilitation (ICF) at 15 ms

Here ICF was elicited by a pp-TMS protocol where the CS was set at 80% and the TS at 120% of the rMT, with an ISI of 15 ms. This protocol normally shows a facilitation, which is believed to be mediated by NMDA glutamatergic receptors (Ziemann *et al.*, 1998; Schwenkreis *et al.*, 2000). This effect seems to reflect the activity of a circuit, at least in part, distinct from that responsible for the SICl (Ziemann *et al.*, 1996b, 1996a, 2015).

Short-interval intracortical facilitation (SICF)

To study changes in M1 intracortical circuits that are thought to receive direct input from PMv, we measured the SICF (Cattaneo *et al.*, 2005; Koch *et al.*, 2010b; Di Lazzaro *et al.*, 2012). The SICF was obtained by a pp-TMS protocol, with the first stimulus at 120% followed by a second stimulus at 80% of the rMT, with 1.3, 2.5 and 4.1 ms ISIs. When a TMS pulse is applied over M1, it produces a repetitive discharge of the corticospinal neurons, resulting in a series of descending volleys called 'waves'. The first, called 'direct-wave' (D-wave), results from direct activation of corticospinal neurons. The subsequent descending discharges, called 'indirect-waves' (I-waves), appear to depend on trans-synaptic excitation of intracortical interneurons that project to the corticospinal neurons (Amassian & Stewart, 2003; Di Lazzaro *et al.*, 2012; Ziemann, 2020). Later I-waves reveal cortico-cortical pathways targeting M1, and an ISI of 2.5 ms corresponds to the peak of the I₂-wave that probably reflects inputs from the premotor cortex (Shimazu *et al.*, 2004; Cattaneo *et al.*, 2005; Di Lazzaro *et al.*, 2006). The resulting facilitation is produced because the peaks of the I-waves evoked by the two subsequent pulses are in phase (Di Lazzaro *et al.*, 2012; Federico & Perez, 2017).

Connectivity protocol

The ds-TMS protocol is a well-established method to assess the functional connectivity between brain sites. A first CS was delivered over PMv to activate the projections towards M1 followed by TS over M1, 6 ms later (Davare *et al.*, 2008, 2009; Koch *et al.*, 2010b). However, previous studies suggest that different CS intensities over the premotor cortex may induce either a facilitatory or an inhibitory influence on M1 (Davare *et al.*, 2008; Bäumer *et al.*, 2009). These opposite effects may be due to activation of different neuronal populations. Here we used different CS intensities (30, 50, 70 and 90% of the individual rMT) and a fixed TS intensity set at 120% of the rMT.

Experimental procedure

Experiment 1: effect of PMv-to-M1 cc-PASPA on M1 neurophysiological indexes (n = 14)

To investigate the neurophysiological modifications induced by conditioning the PMv-to-M1 connectivity, we collected different excitatory and inhibitory indices before and after the cc-PAS protocol. More specifically, we measured the MEP, LICI, SICI (with an ISI of 1 and 3 ms), ICF and SICF (only at an ISI of 2.5 ms). A total of 120 trials were collected, that is 20 repetitions for each index. Previous work has shown how the LICI protocol influences subsequent SICI acquisition (Ni *et al.*, 2011b) while it does not interact with ICF. The LICI protocol was administered at least 6 s before the SICI/ICF protocols. In the present study, all indexes were acquired in a randomized order to avoid order effects and with an interval of 5 s to avoid carryover effects between the different protocols. All indexes were acquired before the cc-PAS protocol as well as 10 min (post-10) and 30 min (post-30) after the end of the cc-PAS protocol (see **Fig. 2.1**).

Experiment 2: SICF modulations induced by PMv-to-M1 cc-PASPA (n = 21)

To investigate if the reduction observed in the SICF (*Experiment 1*) was specific for the tested ISI (2.5 ms), we measured the SICF before and after the PMv-to-M1 cc-PAS protocol with different ISIs. Specifically, we used 1.3, 2.5 and 4.1 ms ISIs, which correspond to the timing of the different I-waves (Cattaneo *et al.*, 2005). At the same time, we also tested the 2.1 and 3.3 ms ISIs, which do not target specific

I-waves and offer a clear baseline, beside the single-pulse MEPs (Cattaneo *et al.*, 2005). A total of 60 trials were collected, 10 for each condition. All the conditions were randomized within each block. All measures were obtained before the cc-PAS protocol and 30 min later (post-30; **Fig. 2.1**).

Experiment 3: connectivity modulation induced by PMv-to-M1 cc-PASPA (n = 18)

We investigated the modification induced by the PMv-to-M1 cc-PAS protocol on the connectivity between left PMv and M1. We explored different CS intensities (30, 50, 70 and 90% of the individual rMT) as well as single-pulse MEPs as a reference condition. Ten trials for each condition were acquired, for a total of 50 trials. All the conditions were randomized within each block. All measures were obtained before the cc-PAS protocol and 30 min later (post-30; **Fig. 2.1**).

Experiment 4: effects of PMv-to-M1 cc-PASAP on M1 neurophysiological indexes and PMv-M1 connectivity (n = 17)

In this experiment, we changed the direction of the induced current over M1 during the cc-PAS protocol from PA to AP. The cc-PAS protocol was applied as reported in Experiment 1 except that the coil over M1 was rotated 180° to induce an AP current (M1: 120% of FDI rMT_{AP}; PMV: 90% of FDI rMT_{PA}). We recorded the MEPs and the SICF (2.5 ms ISI). We also measured the connectivity between PMv and M1 by using two CS intensities over PMv (30 or 70% of rMT_{PA}) while the TS over M1 was applied at 120% of rMT_{PA} with the coil in PA orientation. Fifteen trials were collected for each measure. All measures were obtained before the cc-PAS protocol and 30 min later (post-30; **Fig. 2.1**).

Experiment 5: M1-to-PMv cc-PASPA (n = 10)

The aim of this experiment was to evaluate if the modulations observed in M1 intracortical circuits were specific for the conditioning exerted by PMv onto M1. The cc-PAS protocol was administered as reported in the TMS section above but now the M1 stimulation preceded the left PMv stimulation by 6 ms. The coil over M1, FDI hotspot, was positioned with PA orientation. Fifteen trials were collected for each measure, MEPs and the SICF (ISI of 2.5 ms), before and 30 min after the cc-PAS protocol (see **Fig. 2.1**).


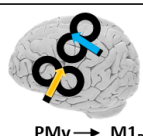

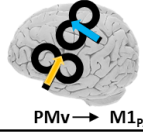

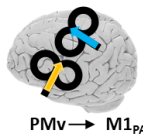

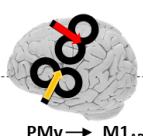


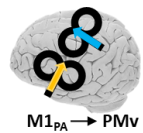
	pre-PAS	cc-PAS	post-10	post-30
Experiment 1 	<ul style="list-style-type: none"> MEP_{PA} SICI 1 and 3 ms of ISIs LICI 100 ms of ISI ICF 15 ms of ISI SICF 2.5 ms of ISI 	 PMv → M1 _{PA}	<ul style="list-style-type: none"> MEP_{PA} SICI 1 and 3 ms of ISIs LICI 100 ms of ISI ICF 15 ms of ISI SICF 2.5 ms of ISI 	<ul style="list-style-type: none"> MEP_{PA} SICI 1 and 3 ms of ISIs LICI 100 ms of ISI ICF 15 ms of ISI SICF 2.5 ms of ISI
Experiment 2 	SICF (ISIs) <ul style="list-style-type: none"> 1.3 ms 2.1 ms 2.5 ms 3.3 ms 4.1 ms 	 PMv → M1 _{PA}		SICF (ISIs): <ul style="list-style-type: none"> 1.3 ms 2.1 ms 2.5 ms 3.3 ms 4.1 ms
Experiment 3 	Connectivity, CS (% of rMT) <ul style="list-style-type: none"> 30% 50% 70% 90% 	 PMv → M1 _{PA}		Connectivity, CS (% of rMT) <ul style="list-style-type: none"> 30% 50% 70% 90%
Experiment 4 	<ul style="list-style-type: none"> MEP_{PA} MEP_{AP} SICF 2.5 ms of ISI 	 PMv → M1 _{AP}		<ul style="list-style-type: none"> MEP_{PA} MEP_{AP} SICF 2.5 ms of ISI
	Connectivity, CS (%rMT) <ul style="list-style-type: none"> 30% 70% 			Connectivity, CS (%rMT) <ul style="list-style-type: none"> 30% 70%
Experiment 5 	<ul style="list-style-type: none"> MEP_{PA} SICF 2.5 ms of ISI 	 M1 _{PA} → PMv		<ul style="list-style-type: none"> MEP_{PA} SICF 2.5 ms of ISI

Figure 2.1. Table summarizing all experimental procedures.

cc-PAS was preceded by the baseline acquisition (pre-PAS) and followed by the reacquisition (post-10 and post-30) of the same indices to evaluate the modulation caused by the plasticity-inducing protocol. For each experiment, the first column specifies the coil position for the acquired indices, while the cc-PAS column shows the coil position for the cc-PAS administration and the induced current direction (arrows).

Analysis and results

We excluded from the analysis all trials that presented a peak-to-peak MEP amplitude ≤ 0.05 mV. Moreover, for each subject we calculated the mean and standard deviations of the background pre-TMS EMG (100 ms) over all trials. We removed from the analysis those trials that presented a pre-trigger EMG activity exceeding the mean by 2 SD. All trials were visually inspected for artefacts. All analyses were conducted on STATISTICA 12 (StatSoft, Inc., Tulsa, OK, USA). Finally, although approximately 2 weeks elapsed between experimental sessions, we analysed the MEPs recorded in 13 participants who took part in one or more

sessions to avoid any interference effects. No significant differences were found between these groups ($t_{13} = 0.02$; $p = 0.96$).

Data treatment

MEPs amplitudes are given in millivolts. Neurophysiological indices based on pp-TMS (ICF, SICI and SICF) are expressed as the ratio between their mean MEP amplitude and the mean MEP size in the sp-TMS protocol. The LICI, by contrast, is expressed as the ratio between the TS and CS amplitudes in every trial, to avoid modulations driven by local excitability changes in M1. In *Experiments 3 and 4* connectivity (ds-TMS) is expressed as the ratio between mean MEP size (obtained when PMv was stimulated before M1) and the mean MEP amplitude obtained via the sp-TMS protocol.

Results

Experiment 1

We computed a one-way repeated-measures ANOVA with 'Time' as factor on three levels (pre-PAS/post-10/post-30), separately for each neurophysiological index. The ANOVA did not show any effect of Time for the ICF ($F_{1,13} = 0.43$; $p = 0.65$), for the SICI with an ISI of 1 ms ($F_{1,13} = 0.61$; $p = 0.54$) or for the SICI with an ISI of 3 ms ($F_{1,13} = 0.78$; $p = 0.46$). In contrast, a significant effect of Time was found for the SICF ($F_{1,13} = 5.04$; $p = 0.01$). The post hoc analyses, with Bonferroni correction, revealed a significant reduction of the SICF at post-10 (mean (M) = 1.21; $SD = 0.18$; $p = 0.03$) and at post-30 ($M = 1.21$; $SD = 0.23$; $p = 0.03$) with respect to the pre-PAS acquisition ($M = 1.38$; $SD = 0.23$). No significant difference was found between post-10 and post-30 ($p = 0.99$). The ANOVA on the sp-TMS MEPs showed a significant effect of Time ($F_{1,13} = 4.28$; $p = 0.02$). The *post hoc* analyses, with Bonferroni correction, revealed a significant CSE increment at post-30 ($M = 2.40$ mV; $SD = 1.40$, $p = 0.03$) compared to the pre-PAS acquisition ($M = 1.87$ mV, $SD = 1.16$). No significant difference was present between pre-PAS and post-10 ($M = 2.27$ mV, $SD = 1.43$, $p = 0.13$) or between post-10 and post-30 ($p = 0.99$). The ANOVA on LICI showed a significant effect of Time ($F_{1,13} = 4.99$, $p = 0.01$). The post hoc analyses, with Bonferroni correction, showed a significantly larger inhibition for post-10 ($M = 0.14$, $SD = 0.11$, $p = 0.03$) and post-30 ($M = 0.15$,

$SD = 0.14$, $p = 0.04$) compared to the pre-PAS acquisition ($M = 0.29$, $SD = 0.27$). No significant difference was present between post-10 and post-30 ($p = 0.99$). All results are reported in **Fig. 2.2**.

We then calculated the individual relative change induced by cc-PAS on the MEP, SICF and LICI as the ratio between the post-30 and pre-PAS acquisitions. The data were then subjected to a Pearson correlation analysis to test whether a change in one index was associated with a stable change in another one. We found a significant negative correlation between the increment of the MEP ($M = 1.39$, $SD = 0.46$) and the reduction of the SICF ($M = 0.88$, $SD = 0.15$, $r = -0.62$, $p = 0.02$). No significant correlation was found between the MEP and the LICI ($M = 0.95$, $SD = 0.85$) modulation ($r = -0.09$, $p = 0.77$) or between the SICF and LICI modulation ($r = 0.08$, $p = 0.77$).

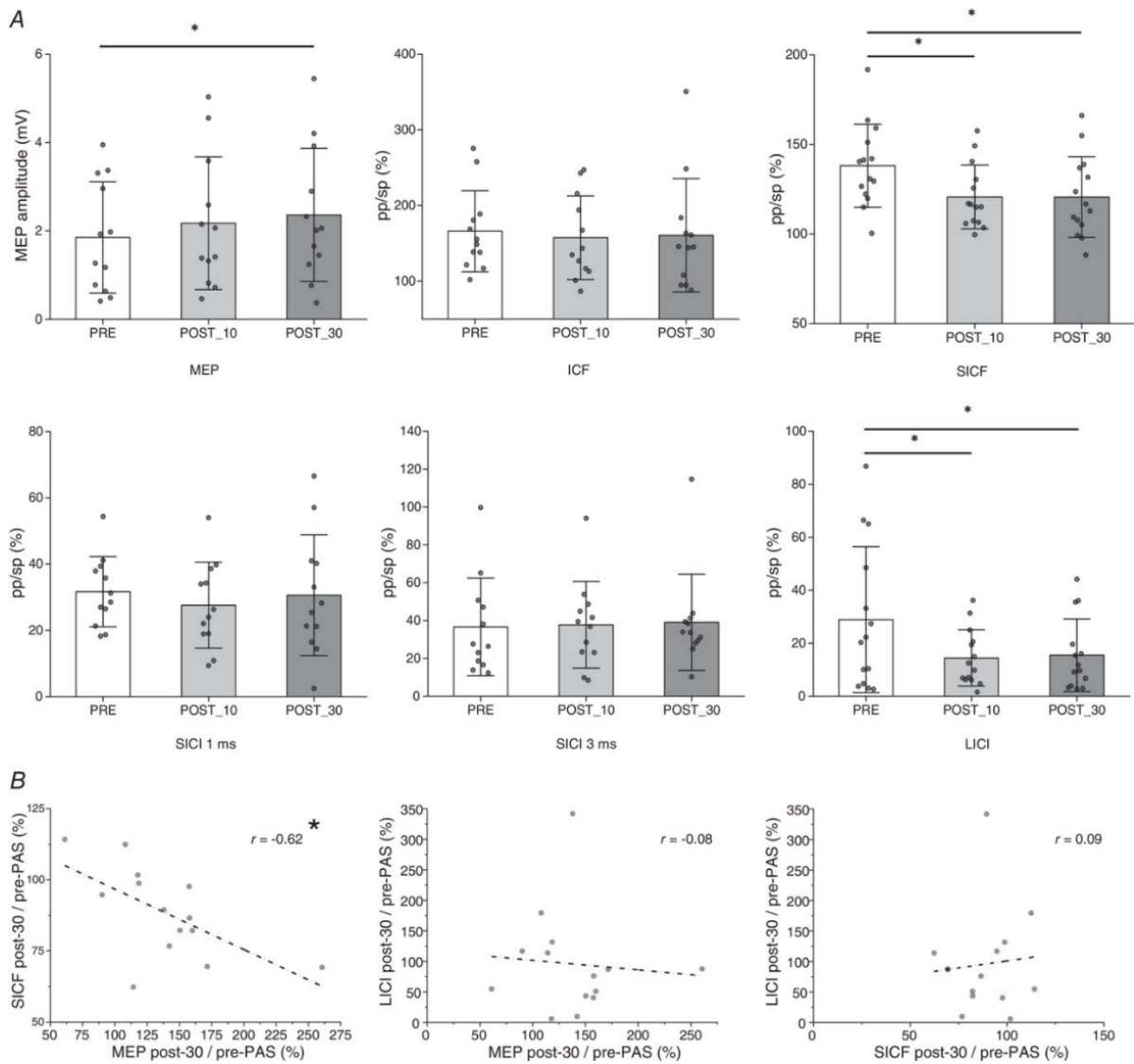


Figure 2.2. Results of Experiment 1 (previous page).

A, the effect of the PMv-to-M1 cc-PAS protocol on the different indices. SICI, ICF and SICF are expressed as the ratio of the mean MEP amplitude (pp-TMS/sp-TMS). The error bars on the histograms represent the standard deviation (SD). B, correlation results between the significantly modulated indices. * $p < 0.05$.

Experiment 2

We computed five Bonferroni-corrected paired-sample two-tailed t tests between the pre-PAS and the post-30 acquisition on the SICF data. No significant results were found for the SICF with an ISI of 1.3 ms ($t_{21} = 0.49$, $P = 0.62$) and 4.1 ms ($t_{21} = 0.39$, $p = 0.70$). In contrast, a significant reduction of the SICF was found with an ISI of 2.5 ms between pre-PAS ($M = 1.3$, $SD = 0.30$) and post-PAS acquisition ($M = 1.11$, $SD = 0.32$) ($t_{21} = 2.98$, $p = 0.007$). No significant modulations were found for an ISI of 2.1 ms ($t_{21} = -0.44$, $p = 0.66$) or 3.3 ms ($t_{21} < 0.0001$, $p = 0.99$). We replicated and extended the previous result, obtained in *Experiment 1*, on the SICF. Indeed, the reduction of the SICF was specific for the ISI of 2.5 ms. The results are reported in **Fig. 2.3**.

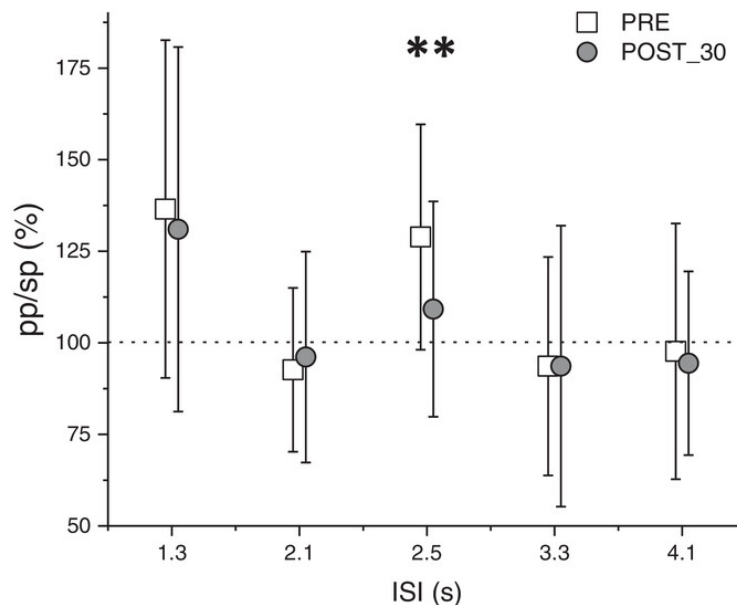


Figure 2.3. Results of Experiment 2; the effect of the PMv-to-M1 cc-PAS on the SICF at different ISIs, each reflecting different I-waves.

A selective modulation of the I₂-wave is observable. The error bars represent the SD. ** $p < 0.01$, in a t -test with Bonferroni correction for multiple comparisons.

Experiment 3

We first evaluated the connectivity between PMv and M1 before cc-PAS with four Bonferroni-corrected one-sample two-tailed t tests, between the conditioned MEP (pp-TMS with different stimulation intensities on PMv followed by a constant stimulus intensity on M1), and the sp-TMS protocol. No significant difference was found when the PMv was stimulated at 30% ($t_{18} = -0.18, p = 0.86$), 50% ($t_{18} = -0.81, p = 0.43$) or 90% of the rMT ($t_{18} = -0.12, p = 0.91$). When the CS on the PMv was set at 70% of the rMT, the MEPs were significantly reduced ($M = 1.91, SD = 1.30, t_{18} = -3.33, p = 0.007$).

We then evaluated if the cc-PAS modulated the PMv-M1 connectivity by comparing the conditioned MEPs before (pre-PAS) and after (post-30), through four two-tailed paired-sample t tests, with Bonferroni correction. No significant modulation on the connectivity was found when the CS on PMv was at 30% ($t_{18} = -0.38, p = 0.71$), 50% ($t_{18} = -0.94, p = 0.36$) or 90% of rMT ($t_{18} = -0.19, p = 0.85$). In contrast, the inhibitory effect exerted by the PMv when the CS was set at 70% of the rMT disappeared and the difference between the pre-PAS ($M = 0.86, SD = 0.17$) and the post-30 ($M = 1.04, SD = 0.18$) was significant ($t_{18} = -3.05, p = 0.007$). The results are reported in **Fig. 2.4**.

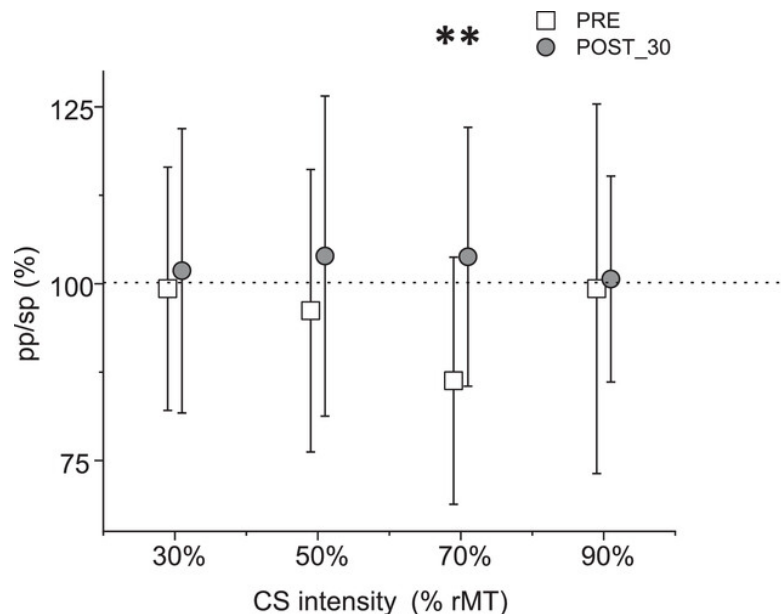


Figure 2.4. Results of Experiment 3.

The PMv expressed an inhibitory influence on M1 only when it was stimulated at 70% of the rMT. This inhibitory influence was suppressed after the PMv-M1 cc-PAS protocol. The error bars represent the SD . $**p < 0.01$, in a t test with Bonferroni correction for multiple comparison.

Experiment 4

We first analysed MEP latencies elicited by the PA and AP TMS stimulation. A two-tailed paired-sample t test showed a significantly shorter latency ($t_{18} = 11.67$, $p < 0.0001$) for MEP_{PA} ($M = 21.76$ ms, $SD = 2.22$) with respect to MEP_{AP} ($M = 23.58$ ms, $SD = 1.87$). Accordingly, the different trans-synaptic set of input engaged in PA vs. AP should result in a constantly delayed MEP latency of about 1.5 ms (Di Lazzaro *et al.*, 2006; Ni *et al.*, 2011a; Koch *et al.*, 2013; Federico & Perez, 2017).

Then, by means of Bonferroni-corrected paired-sample two-tailed t tests, we found a significant reduction ($t_{17} = 3.48$, $p = 0.003$) of MEP_{PA} amplitude in post-30 ($M = 1.78$ mV, $SD = 1.05$) compared to pre-PAS ($M = 2.14$ mV, $SD = 1.12$). Note that this is the opposite pattern to that seen in *Experiment 1*. At the same time, we found no significant modulation of MEP_{AP} between pre-PAS ($M = 1.17$ mV, $SD = 0.70$) and post-30 ($M = 1.29$ mV, $SD = 1.03$, $t_{17} = -0.71$, $p = 0.49$). The SICF2.5ms showed a significant increment ($t_{17} = -2.36$, $p = 0.03$) in post-30 ($M = 2.03$, $SD = 1.74$) with respect to pre-PAS ($M = 1.23$, $SD = 0.69$). Note that this is the opposite pattern to that seen in *Experiment 1*. As in *Experiment 1* we evaluated if there was a correlation between the modulation of MEP and the modulation of the SICF, at the individual level. We found a significant negative correlation ($r = -0.75$, $p = 0.0004$) between the reduction of the MEP_{PA} and the increment of the SICF. This is the same pattern as that seen in *Experiment 1*. The results are reported in **Fig. 2.5**.

For the connectivity measures we applied the same statistical analyses used in *Experiment 3* and we replicated the results obtained in the pre-PAS acquisition of *Experiment 3*. Indeed, before the cc-PAS protocol when the PMv was stimulated at 70% of the rMT, we showed an inhibitory influence on M1 ($t_{17} = -2.81$, $p = 0.01$). However, no significant difference was found when the stimulation of PMv was set at 30% of the rMT ($t_{17} = -0.63$, $p = 0.53$). In addition, the cc-PAS_{AP} effect on connectivity was the same as in *Experiment 3*. More precisely, a significant modulation of the PMv-M1 connectivity was found between the pre-PAS ($M = 0.91$ mV, $SD = 0.13$) and post-30 ($M = 1.04$ mV, $SD = 0.19$) acquisition when the PMv was stimulated at 70% of the rMT ($t_{17} = -2.65$, $p = 0.01$). No significant change

was seen when PMv was stimulated at 30% of the rMT ($t_{17} = -0.41, p = 0.69$). The results are reported in **Fig. 2.5**.

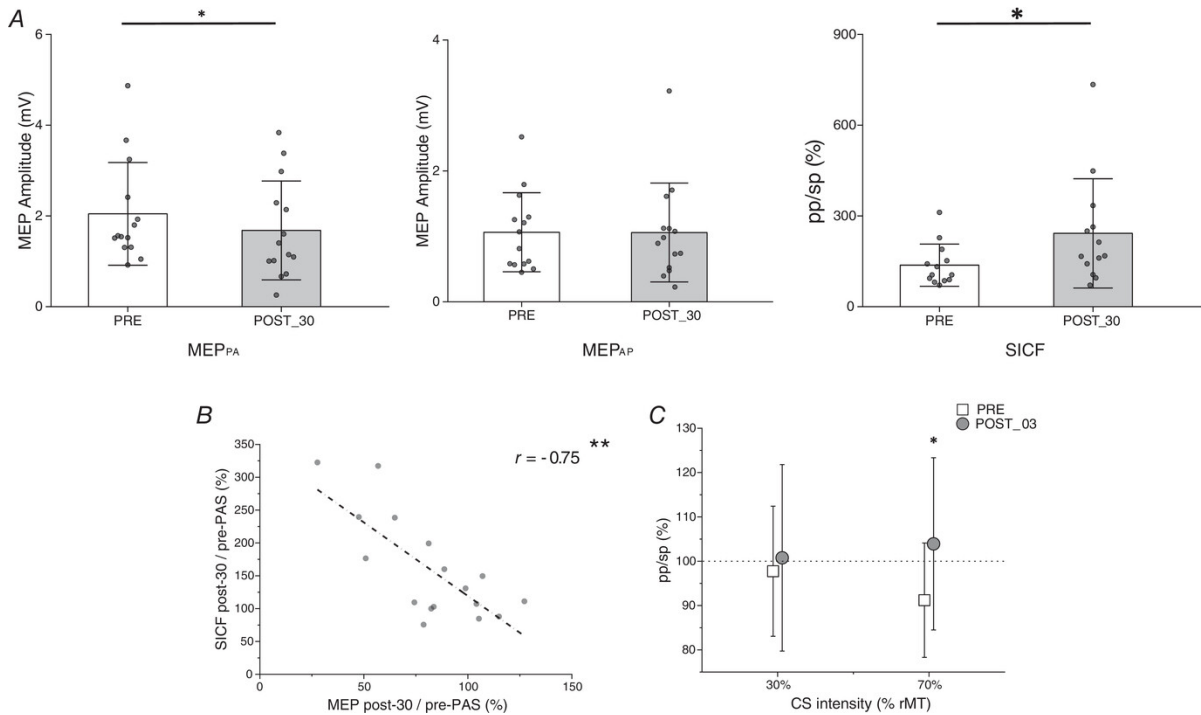


Figure 2.5. Results of Experiment 4.

A, the effect of cc-PAS in AP orientation. The modulations observed in the MEPPA and in the SICF are the opposite of those induced by cc-PAS in PA orientation (*Experiment 1*). **B**, correlation between the MEPPA and the SICF. **C**, effect induced by cc-PASAP on the connectivity between PMv and M1. The error bars represent the *SD*. * $P < 0.05$, ** $P < 0.01$.

Experiment 5

As in the control experiment, we applied cc-PAS in the opposite temporal order (M1 first). No significant modulation emerged in MEP amplitude between pre-PAS ($M = 1.83$ mV, $SD = 0.68$) and post-30 ($M = 1.95$ mV, $SD = 0.66$, $t_{10} = -0.50$, $p = 0.63$) acquisitions. In the same way, no significant modulation was found in the SICF (ISI = 2.5 ms) between the pre-PAS ($M = 1.63$, $SD = 0.49$) and the post-30 ($M = 1.84$, $SD = 0.80$, $t_{10} = -1.23$, $p = 0.25$) acquisition (**Fig. 2.6**).

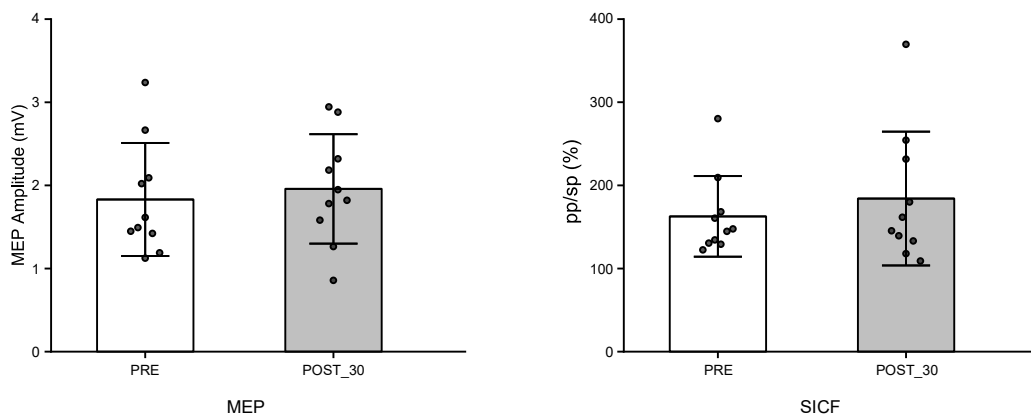


Figure 2.6. Results of Experiment 5.

The M1-to-PMv cc-PAS showed no modulation of the MEP or SICF after 30 min. The error bars represent the *SD*.

Discussion

To better understand the nature of PMv-M1 connectivity modulations, we believe it is essential to investigate the neurophysiological modulations reflecting complex intracortical reorganization within M1. Here, after cc-PAS, we observed in parallel: (i) long-lasting enhanced/decreased corticospinal excitability, as indexed by MEP amplitude changes, that was strongly associated with long-lasting enhanced/decreased I_2 -waves, as measured by SICF_{2.5ms} amplitude change; (ii) an independent long-lasting change of LICl; (iii) a cc-PAS-induced plasticity that is dependent on current direction in M1; and (iv) modulation of the strength of PMv-M1 connectivity.

Summing up, we show that conditioning the PMv-M1 network via a cc-PAS protocol induces a clear modulation of both the PMv-M1 connectivity and selective M1 local circuitry. These modulations evolve rapidly (after 10 min) and persist for at least 30 min.

Effects of PMv-to-M1 cc-PAS corticospinal excitability

In this work we systematically explored the effects of cc-PAS in the PMv-M1 network using a ds-TMS protocol to promote Hebbian-like STDP (Hebb, 1949; Markram *et al.*, 2011).

We found that at the corticospinal level, cc-PAS led to opposite LTP-like or LTD-like after-effects depending on the coil orientation, PA vs. AP respectively. This result is consistent with previous observations from our group in which similar dynamics were reported in the context of the posterior parietal cortex (PPC)-M1 network (Koch *et al.*, 2013; Veniero *et al.*, 2013). The PA orientation preferentially targets the deeper neural layers in M1, whereas the AP orientation probably targets the more superficial layers (Koch *et al.*, 2013; Sommer *et al.*, 2013). Previous works have demonstrated how plasticity in M1 can depend on the relative distance between the synaptic site and the soma of the pyramidal neurons (Sjöström & Häusser, 2006). Activation of the connection from layer 2 and layer 3 (L2 and L3), in other words the connection from a more superficial neuronal population projecting far from the soma of the pyramidal neurons, leads to LTD. In contrast, activation from layer 5 (L5), which is the connection from a deeper neural population that could project near to the soma of the pyramidal neurons, leads to LTP in M1 (Sjöström & Häusser, 2006; Kampa *et al.*, 2007).

cc-PAS_{PA} might preferentially target deeper neural populations in L5 projecting near to the soma of the pyramidal neurons in M1 (Sjöström & Häusser, 2006). This may lead to the larger CSE observed in *Experiment 1* (**Fig. 2.7A**).

Conversely, the reduction of the CSE in *Experiment 4* (cc-PAS_{AP}) might be due to the preferential recruitment of superficial neuronal populations, in L2 and L3, that project far from the soma of the pyramidal neurons situated in L5 (Sjöström & Häusser, 2006; Koch *et al.*, 2013). Indeed, it is possible that interneurons located in L2–L3 inhibit the dendritic arbour of the large pyramidal cells (Jiang *et al.*, 2013) (**Fig. 2.7B**). Together, this suggests that cc-PAS delivered with PA vs. AP induces opposite long-lasting effects, equivalent to LTP and LTD respectively.

Effects of PMv-to-M1 cc-PAS on I₂-wave activity

In *Experiment 1*, the PMv-to-M1 conditioning protocol in the PA direction determines specific modifications of the excitatory descending volleys as early as 10 min after cc-PAS. *Experiment 2* showed that the influence of the PMv is specific to the I₂-wave (SICF_{2.5ms}). This result is in line with previous non-human primate data, which identified the PMv as the site of origin of inputs to M1 that contribute to the generation of the late descending I-waves (Shimazu *et al.*, 2004). The

concurrent lack of modulation observed for the first I₁-wave supports the idea of a different circuit for the generation of the I₁- and the I₂-wave (Di Lazzaro *et al.*, 2012; Di Lazzaro & Rothwell, 2014).

In parallel with the reduction of the SICF_{2.5ms}, we showed an increase in the corticospinal excitability after the cc-PAS_{PA} protocol, as discussed above. More importantly, we found a robust negative correlation between MEP and SICF_{2.5ms}, which supports the idea that these two indices, although reflecting different circuits within M1, are functionally coupled at single-subject level.

To evaluate the nature of this correlation, in *Experiment 4* we applied the cc-PAS protocol in the AP direction. By changing the TMS current direction it is possible to target different synaptic inputs to the corticospinal neurons (Ni *et al.*, 2011a; Koch *et al.*, 2013; Hamada *et al.*, 2014; Federico & Perez, 2017; Fong *et al.*, 2021). The PA stimulation preferentially elicits the earliest I-waves, while the AP stimulation preferentially elicits late I-waves (Ni *et al.*, 2011a; Di Lazzaro & Rothwell, 2014). Here, reversing the current direction from PA to AP, we confirmed the strong correlation between the MEP and the SICF_{2.5ms} but with an inversion of the effects induced in *Experiment 1*. Specifically, we observed a reduction of the CSE paralleled by a larger I₂-wave (SICF_{2.5ms}). Finally, these modifications are specific for the cc-PAS protocol applied. When we reversed the timing, i.e. M1 stimulated 6 ms before the PMv, these effects were cancelled (*Experiment 5*).

The consistency of the correlation between CSE and I₂-waves, across different current directions, also suggests a mechanism-based on a simple circuit, formed by few interneurons, probably located in L2–L3, and differently influenced by the PMv projections to different M1 layers (**Fig. 2.7**). This correlation might reflect a fine push–pull control mechanism exerted by PMv to regulate the M1 activity state at rest or M1 output during action preparation (Johnson *et al.*, 2012).

Based on these results, we suggest that the neuronal populations responsible of the generation of the I₂-wave (SICF_{2.5ms}) can differentially be inhibited or disinhibited using different cc-PAS protocols (PA vs. AP; **Fig. 2.7**). The robust and selective modulation of the I₂-wave indicates the SICF_{2.5ms} as a preferential channel to investigate the interactions between these areas.

Although more specific studies will be needed to understand how these cc-PAS modulations could be linked to motor behaviour, previous studies have shown how

both the SICF_{2.5ms} (Cattaneo *et al.*, 2005) and the CSE was increased during action preparation (Leocani *et al.*, 2000; Klein *et al.*, 2012; Poole *et al.*, 2018). Federico & Perez (2017) demonstrated how less synchronized synaptic inputs, activated by AP stimulation, were preferentially recruited during the power grip. This suggests the possibility of targeting and conditioning the neural subpopulation within M1 preferentially recruited during a specific action. Future studies should investigate this opportunity and its implications for the field of motor rehabilitation.

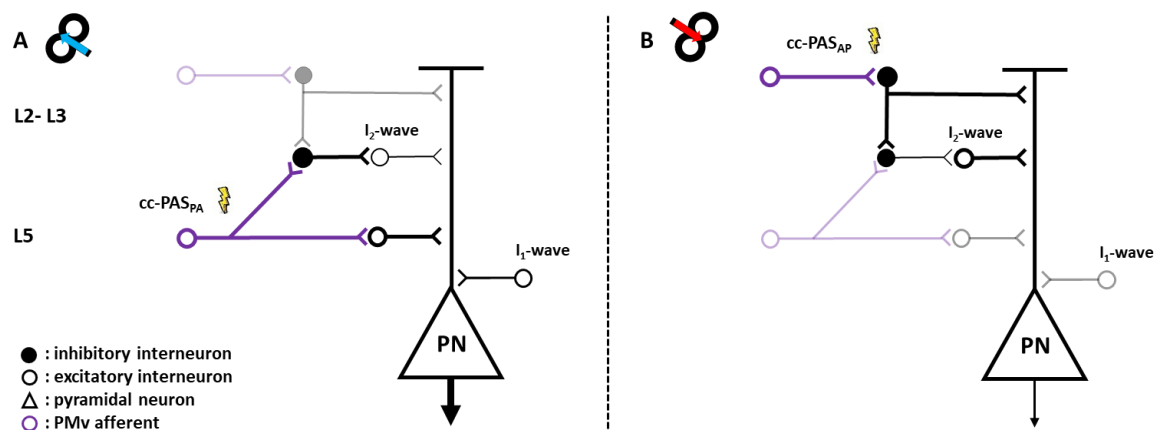


Figure 2.7. Model of the possible neural circuits involved in the plasticity changes after the PMv-to-M1 cc-PAS.

The large pyramidal neuron (PN) in L5 of M1, which projects to the spinal cord, receives both excitatory (white circle) and inhibitory (black circle) synaptic inputs responsible for the I₂-waves. The PMv projections (violet circle) contact the interneurons both in L2–3 and in L5 of M1 (Ghosh & Porter, 1988). The lightning bolt represents the preferential activation layers of the cc-PAS stimulation while the shaded circuits indicate the not preferential action sites of cc-PAS and the thickness of neurons indicates the increase or decrease in their activity. **A**, the PMv projection that synapses with the interneurons in the deepest layer (L5), preferentially enhanced by the cc-PAS in PA direction, excites the PN, leading to an increment of the CSE, and inhibits the circuit responsible for the I₂-waves. **B**, on the other side, the more superficial interneurons populations in L2-3, probably responsible for the I₂-wave and preferentially activated by the AP stimulation, can inhibit the dendritic arbour of the PN (Jiang *et al.*, 2013), leading to reductions of the CSE, and in parallel enhance the I₂-waves exciting the responsible circuitry.

Effects of PMv-to-M1 cc-PAS on GABAergic activity

We found that the cc-PAS protocol induced specific changes on local GABAergic interneuronal activity. Importantly, we show a dissociation between inhibitory indexes, with larger slow inhibitory activity (LICI; probably mediated by

metabotropic GABA_B receptors) (Werhahn *et al.*, 1999; McDonnell *et al.*, 2006) while the fast local one was unaltered (SICI; probably mediated by ionotropic GABA_A receptors) (Ziemann *et al.*, 1996a; Ilić *et al.*, 2002; Müller-Dahlhaus *et al.*, 2008). This result might be driven by the very nature of the cc-PAS stimulation, which is considered to produce a long-lasting potentiation. Indeed, according to Hebbian principles, a stable change in synaptic strength is driven by pre- and postsynaptic activities that, beside glutamate, can also be mediated by GABAergic metabotropic receptor pathways (Mott & Lewis, 1991). In fact, slow inhibitory control of neuronal excitability exerts its influence at both the pre- and the postsynaptic levels – presynaptically via Ca²⁺-mediated reduction of GABA and glutamate release, and postsynaptically through robust slow K⁺-mediated hyperpolarization (Dutar & Nicoll, 1988; Sanchez-Vives *et al.*, 2021). Together, our data suggest that slow GABAergic activity might be implicated in the regulation of LTP-like mechanisms independently from the interaction with the I₂ circuits described above.

Effects of PMv-to-M1 cc-PAS on connectivity

We observed that the cc-PAS protocol changes the strength of PMv-M1 connectivity. Previous findings suggest that stimulating the PMv at different intensities recruits different projections exerting different excitatory or inhibitory influences on M1 (Bäumer *et al.*, 2009). In particular, stimulation of the PMv at 80% or 90% of the rMT, 4–6 ms before M1, highlights an inhibitory drive to M1 (Davare *et al.*, 2008; Bäumer *et al.*, 2009) while stimulation at 80% of active motor threshold (aMT) produces an excitatory effect (note that 80% aMT roughly corresponds to 60–70% rMT) (Bäumer *et al.*, 2009). In the pre-PAS acquisition, our results clearly support the intensity-dependent inhibitory influence of PMv towards M1 at rest. We find that the peak of inhibition is recruited with a stimulus intensity of 70% of the rMT. At the same time, none of the intensities explored here (30, 50, 70 and 90% of rMT) show any excitatory effect on M1.

Yet, after cc-PAS, the PMv inhibitory drive towards M1 disappeared to switch, qualitatively, to a more facilitatory influence. This effect is not intensity-dependent and, appears to be non-specific but caused by the induction of plasticity. Indeed, previous studies showed similar suppression of the influence between areas after

different conditioning protocols (Koch *et al.*, 2010a; Pauly *et al.*, 2022). Moreover, measures of connectivity were not affected by current direction since we were able to replicate previous results (*Experiment 3*) also with cc-PAS_{AP} (*Experiment 4*). Consequently, the long-lasting Hebbian-like effects on PMv-to-M1 connectivity, due to the plasticity-induction protocol, is indirectly mediated by specific local M1 circuitry.

Conclusion

These data provide novel insight into the neurophysiological basis of the PMv-to-M1 cc-PAS protocol. The functional connectivity between PMv and M1 covers a key function in the visuomotor transformations necessary for goal-directed actions and, understanding how to manipulate it might become crucial for the application of cc-PAS in future research as well as in motor rehabilitation. We highlight that the PMv-to-M1 cc-PAS influences both the connectivity between these areas and the M1 local circuitry.

The modulations induced in M1 depend on the current direction induced by the stimulation. Indeed, the PA vs. AP stimulations appear to induce two different long-lasting effects in M1, respectively identifiable as LTP and LTD. At the same time, we found a specific modulation of the neuronal circuit responsible of the I₂-wave, highlighting PMv as the specific source of the input to M1 responsible for its generation. The selective modulations of the I₂-wave support the use of the SICF_{2.5ms} as a marker of the influence of PMv on M1. Moreover, we showed a significant negative correlation between the CSE and the I₂-wave modulation. We suggest that this correlation could reflect different circuits, functionally coupled, within M1. These circuits may create a fine control mechanism, influenced by PMv, responsible of the regulations of the M1 motor output drive. Future studies will need to investigate how these neurophysiological modifications are involved in different types of movement.

3. CORTICO-CORTICAL PAIRED ASSOCIATIVE STIMULATION CONDITIONING SUPERFICIAL VENTRAL PREMOTOR CORTEX–PRIMARY MOTOR CORTEX CONNECTIVITY INFLUENCES MOTOR CORTICAL ACTIVITY DURING PRECISION GRIP

This chapter reports the second study carried out during my PhD course. After defining the neurophysiological modulations induced by different PMv-M1 cc-PAS protocols (Chapter 2) the aim became to understand whether this protocol was able to modify the motor behaviour of subjects. In particular, the performance of a fine and precise grasping.

However, the literature presented conflicting results regarding which coil orientation (PA vs. AP) is more effective in targeting the M1 neural population involved in the execution of fractioned finger actions as opposed to grosser action. For this reason, prior to exploring the effect of cc-PAS on kinematic, we conducted an experiment to determine which protocol (PA vs. AP) was better suited to target the neural populations within M1 that are preferentially recruited during the execution of a precision grip action.

During the experiment, participants were asked to perform two different types of actions with an isometric contraction: one that was more precise and one that involved the whole hand. The M1 motor output was evaluated during these two actions before and after the application of the cc-PAS protocol, applied with a PA or an AP coil orientation over M1.

This experiment served as a necessary link between the neurophysiological results and the subsequent behavioural investigation, where actions were performed in a naturalistic manner. Indeed, it allowed us to understand which neuronal populations were most involved in the execution of a precision hand action and which coil orientation was able to modulate their activity. In the last section of this chapter, you will find the “Supplementary Analysis” section. This section reports further analysis (i.e., within-subject repeated measured ANOVAs and linear mixed effect model) supporting our findings.

At the end of this experiment, we proceeded to combine TMS and MoCap recording with more certainty about which type of cc-PAS protocol might be suitable for modulating the behavioural execution of a precision prehension.

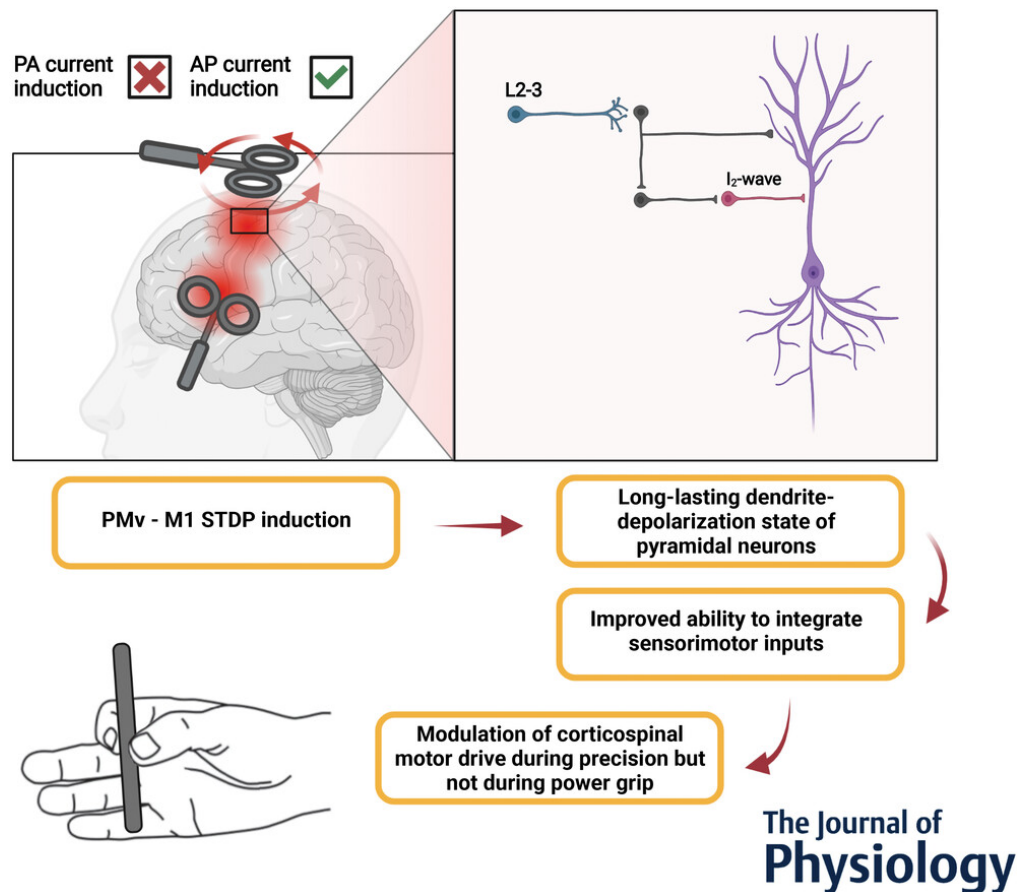
The results you will find below have been initially presented at the XXX CONGRESSO NAZIONALE SIPF "The developing brain" at Udine (Italy; 15/09/2022 -17/09/2022) and, subsequently at the Transcranial Brain Stimulation in Cognitive Neuroscience Workshop at Rovereto (Italy; 02/12/2022 - 03/12/2022), Brain Stimulation: Basic, Translational, and Clinical Research in Neuromodulation at Lisbon (Portugal; 19/02/2023 – 22/02/2023) and at the PROGRESS IN MOTOR CONTROL XIV at Rome (Italy; 27/09/2023 - 30/09/2023).

It is published in *The Journal of Physiology* as:

Casarotto, A., Dolfini, E., Fadiga, L., Koch, G. & D'Ausilio, A. (2023). Cortico-cortical paired associative stimulation conditioning superficial ventral premotor cortex–primary motor cortex connectivity influences motor cortical activity during precision grip. *The Journal of Physiology*, 601 (17), 3945-3960.

Abstract

The ventral premotor cortex (PMv) and primary motor cortex (M1) represent critical nodes of a parietofrontal network involved in grasping actions, such as power and precision grip. Here, we investigated how the functional PMv–M1 connectivity drives the dissociation between these two actions. We applied a PMv–M1 cortico-cortical paired associative stimulation (cc-PAS) protocol, stimulating M1 in both postero-anterior (PA) and antero-posterior (AP) directions, in order to induce long-term changes in the activity of different neuronal populations within M1. We evaluated the motor-evoked potential (MEP) amplitude, MEP latency and corticospinal silent period, in both PA and AP, during the isometric execution of precision and power grip, before and after the PMv–M1 cc-PAS. The repeated activation of the PMv–M1 cortico-cortical network with PA orientation over M1 did not change MEP amplitude or corticospinal silent period duration during both actions. In contrast, the PMv–M1 cc-PAS stimulation of M1 with an AP direction led to a specific modulation of precision grip motor drive. In particular, MEPs tested with AP stimulation showed a selective increase of corticospinal excitability during precision grip. These findings suggest that the more superficial M1 neuronal populations recruited by the PMv input are involved preferentially in the execution of precision grip actions.



Abstract Figure.

The ventral premotor cortex (PMv) and primary motor cortex (M1) represent critical nodes of a parietofrontal network involved in grasping actions, such as power and precision grip. Here, we investigated how the functional PMv–M1 connectivity drives the dissociation between these two actions. We applied a PMv–M1 cortico-cortical paired associative stimulation (cc-PAS) protocol, stimulating M1 in both postero-anterior (PA) and antero-posterior (AP) directions, in order to induce long-term changes in the activity of different neuronal populations within M1. We evaluated the motor-evoked potential (MEP) amplitude, MEP latency and corticospinal silent period, in both PA and AP, during the isometric execution of precision and power grip, before and after the PMv–M1 cc-PAS. The repeated activation of the PMv–M1 cortico-cortical network with PA orientation over M1 did not change MEP amplitude or corticospinal silent period duration during both actions. In contrast, the PMv–M1 cc-PAS stimulation of M1 with an AP direction led to a specific modulation of precision grip motor drive. In particular, MEPs tested with AP stimulation showed a selective increase of corticospinal excitability during precision grip. These findings suggest that the more superficial M1 neuronal populations recruited by the PMv input are involved preferentially in the execution of precision grip actions.

Key points

- Ventral premotor cortex (PMv)–primary motor cortex (M1) cortico-cortical paired associative stimulation (cc-PAS) with different coil orientation targets dissociable neural populations.
- PMv–M1 cc-PAS with M1 antero-posterior coil orientation specifically modulates corticospinal excitability during precision grip.
- Superficial M1 populations are involved preferentially in the execution of precision grip.
- A plasticity induction protocol targeting the specific PMv–M1 subpopulation might have important translational value for the rehabilitation of hand function.

Introduction

The control of fine finger movements is driven by the primary motor cortex (M1; Muir & Lemon, 1983), which uses information provided by the activity of a more complex network in which it is integrated. Within M1, multiple neuronal populations are involved specifically in the control of precision grip rather than power grip (Muir & Lemon, 1983). These different neuronal populations might be targeted preferentially by specific coil orientations of transcranial magnetic stimulation (TMS). In fact, despite their indirect nature, there are several pieces of evidence supporting partial dissociation for circuits targeted by different coil orientations (Ni *et al.*, 2011a; Di Lazzaro & Rothwell, 2014; Spampinato, 2020; Fong *et al.*, 2021). These orientations are believed to target partly dissociable neuronal populations projecting to the pyramidal layer V (L5) neurons, namely more superficial ones [layers 2–3 (L2–L3)] with antero-posterior (AP) and deeper ones with postero-anterior (PA) current directions (L5; Sommer *et al.*, 2013; Aberra *et al.*, 2020). Above all, circuits targeted by the two orientations might contribute in different ways to various motor tasks (Spampinato *et al.*, 2020; Davis *et al.*, 2021). Federico & Perez (2017) suggested that late synaptic input, targeted by AP TMS stimulation of M1, could be involved preferentially during power grip, whereas early synaptic input, targeted by the PA stimulation, might play a predominant role in precision grip. However, it has recently been shown that neuronal populations stimulated by

AP coil orientation are more sensitive to primary somatosensory cortex (S1)–M1 interaction, via thalamocortical pathways, during the execution of precision grip rather than power grip (Davis *et al.*, 2021).

The execution of a grasping action recruits a complex parietofrontal network, in which ventral premotor cortex (PMv)–M1 connections represent a critical node. In humans, PMv activity is crucial for the transformation of object-related visual properties into an appropriate motor plan (Murata *et al.*, 1997; Raos *et al.*, 2006; Prabhu *et al.*, 2009; Koch *et al.*, 2010*b*; Beukelaar *et al.*, 2016), and previous studies on PMv–M1 connectivity have shown how the PMv exerts an important influence on M1 during different grasping movements (Davare *et al.*, 2008; Koch *et al.*, 2010*b*; Beukelaar *et al.*, 2016). In addition, modulation of PMv–M1 connectivity via cortico-cortical paired associative stimulation (cc-PAS), a TMS protocol that promotes Hebbian spike timing-dependent plasticity (STDP) (Hebb, 1949; Markram *et al.*, 2011), influences the performance in several motor tasks (Buch *et al.*, 2011; Fiori *et al.*, 2018; Turrini *et al.*, 2023*a*). Nevertheless, little is known about the possibility of sustained modulation of corticospinal motor drive during the execution of specific actions. The aim of the present work was to investigate the cortical contribution of different M1 neural populations influenced by PMv input in precision and power grasping actions.

In two different sessions, we applied a PMv–M1 cc-PAS protocol with different M1 coil orientations (PA vs. AP current induction) to condition preferentially the neuronal populations that might be involved predominantly in precision or power grip. We assessed corticospinal excitability (CSE) and inhibition [corticospinal silent period (cSP)], in addition to motor-evoked potential (MEP) latency during isometric execution of precision and power grip, before and 30 min after the PMv–M1 cc-PAS protocol applied in the PA direction (*Session 1*, cc-PAS_{PA}) or the AP direction (*Session 2*, cc-PAS_{AP}). Considering the dense connections from PMv and S1 to the superficial M1 L2–L3; (Ghosh & Porter, 1988; Mao *et al.*, 2011), we hypothesized that the cc-PAS_{AP} might be more effective in modulating the corticospinal motor drive in grasping actions and, in particular, during precision grip, which might require the integration of more sensorimotor signals than power grip (Davis *et al.*, 2021).

Methods

Ethical approval

All the participants were informed about the experimental procedure and gave their written consent according to the last update of the *Declaration of Helsinki*, except for the registration in a database. The experiment was approved by the ethical committee 'Comitato Etico Unico della Provincia di Ferrara' (approval no. 170592). The participants were compensated for their participation with €30.00 for their first TMS session and with an additional €15.00 if they also took part in the second experimental session.

Participants

A total of 31 healthy volunteers (mean \pm SD age, 23.33 ± 2.37 years; 14 males) took part in this study (**Table 3.1**). The first experimental session was completed by 18 participants (*Session 1*, cc-PAS_{PA}), and 17 subjects took part in the second experimental session (*Session 2*, cc-PAS_{AP}). Four of 31 volunteers took part in both experimental sessions. The sample size of these *Sessions* are in line with previous studies using similar experimental manipulations (Rizzo *et al.*, 2009; Chiappini *et al.*, 2018; Fiori *et al.*, 2018; Casarotto *et al.*, 2023a).

Experimental task

At the beginning of the experimental session, subjects performed three short abductions of the right index finger, each separated by 30 s, in which they were asked to express the maximal voluntary contraction (MVC) for 3 s. Later, during the experiment, participants were asked to perform and maintain precision grip and power grip in randomized order, with their right hand. In the precision grip, participants were asked to grasp a cylinder (diameter, 1.18 cm; length, 10.9 cm; weight, 86 g) between the thumb and index finger. While performing the power grip, subjects were instructed to grasp the same cylinder with the whole hand, with all fingers flexed against the palm. During both these actions, the forearm and wrist were maintained in a natural position. Subjects were instructed to maintain ~10% of maximal voluntary contraction in the first dorsal interosseous (FDI) muscle (Davare *et al.*, 2008) and to keep the cylinder in a vertical position. Before

the start of each experiment, some practice trials ensured that participants were able to complete the tasks using the requested level of EMG activity. In addition, during all the experimental sessions, the EMG activity was monitored visually by the experimenter to provide verbal feedback about the correct level of muscle contraction. The FDI muscle was selected because it is consistently involved in both the examined actions and it is highly sensitive to task-dependent changes in corticospinal drive (Bunday *et al.*, 2014; Federico & Perez, 2017; Tazoe & Perez, 2017). Both motor tasks were performed before and 30 min after the application of the cc-PAS protocols (**Fig. 3.1**).

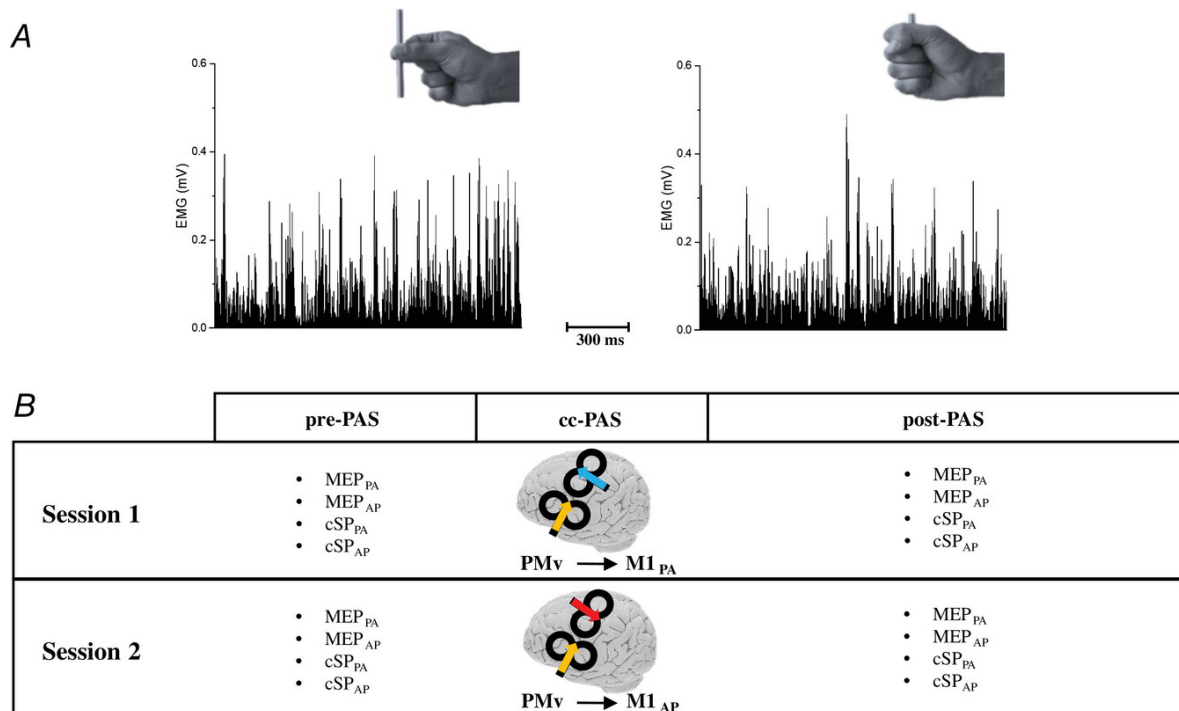


Figure 3.1. Table summarizing the experimental procedures.

A) representative hand posture during precision and power grip, with rectified EMG traces for the first dorsal interosseus (FDI) in a representative subject. **B)** summary of the experimental procedures. The cortico-cortical paired associative stimulation (cc-PAS) was preceded by the pre-PAS acquisition and followed by the post-PAS re-acquisition. All neurophysiological indices were acquired at rest (baseline) and during the precision and power grips. In the middle column, illustrating cc-PAS, the coil positions and induced current directions (arrows) are shown.

Session	Subject (males)	Age	M1 rMT _{PA} coil ₁	M1 rMT _{AP} coil ₁	M1 rMT _{PA} coil ₂	M1 aMT _{PA} coil ₂	M1 aMT _{AP} coil ₂
1	18 (8)	22.7 ± 1.7	48.3 ± 7.0	60.2 ± 8.5	51.6 ± 6.8	45.1 ± 5.5	54.6 ± 7.0
2	17 (7)	24 ± 3.0	46.1 ± 4.6	56.7 ± 4.5	49.2 ± 5.2	43.4 ± 4.0	53.0 ± 4.5

Table 3.1. For each experimental session is shown the number of subjects, their age, the resting motor threshold and the active motor threshold (means ± SD) in both postero-anterior and antero-posterior directions.

During the cortico-cortical paired associative stimulation (cc-PAS) protocol, coil₁ was positioned on the primary motor cortex, while coil₂ was positioned on the ventral premotor cortex. During the pre-PAS and post-PAS acquisition, coil₁ was used to acquire the neurophysiological indices at rest (baseline), while coil₂ was used to assess the neurophysiological indices during the execution of the action. The use of two coils during the acquisition of motor-evoked potentials was necessary to prevent them from overheating. Abbreviations: aMT, active motor threshold; AP, antero-posterior; PA, postero-anterior; rMT, resting motor threshold.

EMG recording

Surface EMG was recorded from the right FDI muscle by means of a wireless system (Zerowire EMG, Aurion, Italy) with a tendon–belly montage. EMG signals were digitized (2 kHz) and acquired by a CED Micro Power1401 mk II board (Cambridge Electronic Design, Cambridge, UK). All the acquired data were stored for offline analysis using the software Signal 6.05 (Cambridge Electronic Design).

TMS

Participants were seated on a comfortable armchair during all the experimental sessions. Single-pulse TMS and cc-PAS protocols were administered through a 50 mm figure-of-eight focal coil connected to a Magstim BiStim² monophasic stimulator (The Magstim Company, Whitland, UK).

The FDI optimal scalp position (OSP) was found by moving the coil in 0.5 cm steps over the left primary motor cortex hand area and using a slightly suprathreshold stimulus. Resting motor threshold (rMT) was defined as the lowest

intensity that evoked a MEP with $>50 \mu\text{V}$ amplitude in 5 of 10 consecutive trials while the participants kept the FDI muscle relaxed (Rossi et al., 2009; Rossini et al., 2015). Likewise, the active motor threshold (aMT) was determined as the minimum intensity required to elicit MEPs of $>200 \mu\text{V}$ (peak to peak) above the background EMG activity ($\sim 10\%$ of maximal voluntary contraction), in ≥ 5 of 10 consecutive trials (Davis et al., 2022). The individual OSP, rMT and aMT were defined for each coil used in each experiment, and separately for the different coil orientations (PA vs. AP). **Table 3.1** gives a summary of rMT and aMT in each experiment and coil.

A total of 90 trials were acquired before (pre-PAS) and 30 min (post-PAS) after the end of the cc-PAS protocol. Specifically, we recorded 15 MEPs for each action (precision grip vs. power grip) and for each coil orientation (PA vs. AP). In addition, 15 MEPs were also acquired at rest, with the coil in both PA and AP orientation.

cc-PAS

In the cc-PAS protocol, dual-sites TMS repeatedly activated the connection between the left PMv and left M1. One hundred couples of pulses were delivered at a frequency of 0.25 Hz for ~ 6 min. The left PMv was stimulated at 90% of individual rMT, while the left M1 was stimulated at 120% of rMT (Casarotto et al., 2023a). In each pair, the M1 stimulation followed the PMv stimulation by 6 ms (Davare et al., 2008, 2009; Koch et al., 2010b; Casarotto et al., 2023a). The coil over the left M1 was placed tangentially to the scalp on the FDI OSP, at $\sim 45^\circ$ with respect to the midline, to induce a PA current flow (*Session 1*, cc-PAS_{PA}); from this position, the coil was rotated 180° to induce an AP current flow (*Session 2*, cc-PAS_{AP}). To estimate the position of the left PMv, we used the SofTaxic Navigator System (Electro Medical System, Bologna, Italy). The skull landmarks (nasion, inion, right and two preauricular points) and 23 points on the scalp were digitalized through a Polaris Vicra optical tracker (Northern Digital, Canada). To stimulate the left PMv, the coil was placed over a scalp region corresponding to the Montreal Neurological Institute (MNI) coordinates $x = -52.8$, $y = 11.6$, $z = 25.1$ (Koch et al., 2010b).

Data analysis

As a first data check, we tested whether EMG activity was different before and after the cc-PAS protocol (pre-PAS vs. post-PAS) and across actions (precision vs. power), before the stimulus onset. We computed the root mean square (RMS) of the 100 ms pre-TMS window and, for each experimental session, we conducted a 2×2 repeated-measures ANOVA, with action (precision grip vs. power grip) and time (pre-PAS vs. post-PAS) as factors. The ANOVAs did not show any main effect or interaction between factors (*Session 1*, all $P > 0.24$; *Session 2*, all $P > 0.33$).

We then extracted the peak-to-peak amplitude of MEPs, the MEP latency and the duration of the cSP. The duration of the cSP was calculated, for each trial, from the offset of the MEP to the return of EMG activity according to literature standards (Hupfeld *et al.*, 2020). One participant was excluded from the cSP analysis in *Session 1* owing to a technical problem in calculating the duration of the cSP. The MEP latency was extracted from each trial as the time from the TMS pulse release to the MEP onset. The MEP amplitude was defined as the peak-to-peak difference of the first two major positive and negative deflections after MEP onset. We excluded from the analysis all trials that presented a peak-to-peak MEP amplitude of ≤ 0.05 mV. Then, we calculated for each subject the mean and *SD* of the background pre-TMS EMG (100 ms) over all trials. We removed from the analysis those trials in which mean EMG activity was ± 2 *SD* of the mean EMG. In *Session 1*, we excluded an average of 8.59% of the trials; in *Session 2*, 11.34%. At the single subject level, in *Session 1*, we excluded a minimum of 0% and a maximum of 17.7% of trials; in *Session 2*, we excluded a minimum of 2.22% and a maximum of 17.2% of trials. A minimum of 10 valid trials per condition was set to consider the data acquisition valid. All trials were inspected visually for artefacts.

The different trans-synaptic input engaged in PA vs. AP results in a constantly delayed MEP latency of ~ 1.5 ms, attributable to the recruitment of different M1 neural circuits in different layers (Ni *et al.*, 2011a; Federico & Perez, 2017). Therefore, as a second data check, we verified that this effect was also present in our data. We analysed the latencies of resting MEPs elicited by the PA and AP TMS stimulation before application of the cc-PAS protocol. In *Session 1*, Student's two-tailed paired-sample *t* test showed a significantly shorter latency ($t_{18} = -4.38$, $p = 0.0004$) for MEP_{PA} (mean = 0.021 s, *SD* = 0.001 s) with respect to

MEP_{AP} (mean = 0.023 s, *SD* = 0.002 s). The same result was obtained in the *Session 2* ($t_{17} = -6.66$, $P < 0.0001$; MEP_{PA}, mean = 0.020 s, *SD* = 0.002 s; MEP_{AP}, mean = 0.022 s, *SD* = 0.001 s).

To investigate the effects induced by different PMv–M1 cc-PAS protocols and the contributions of different M1 circuits (activated by single pulse PA or AP stimulation) during the execution of precision and power grip, we computed a 2×3×2×2 mixed ANOVA, with “cc-PAS protocol” (cc-PAS_{PA} vs. cc-PAS_{AP}) as a between factor and with “Action condition” (rest vs. precision grip vs. power grip), “Coil orientation” (PA vs. AP) and “Time” (pre-PAS vs. post-PAS) as within factors, on MEP amplitude and MEP latency data. Likewise, we computed a 2×2×2×2 mixed ANOVA, with “cc-PAS protocol” (cc-PAS_{PA} vs. cc-PAS_{AP}) as a between factor and “Action condition” (precision grip vs. power grip), “Coil orientation” (PA vs. AP) and “Time” (pre-PAS vs. post-PAS) as within factors, on cSP duration data. This analytical approach allowed us to compare the effect of different cc-PAS protocols on the three action conditions. Please note that the rest condition corresponds to the experimental scenario reported in our previous study (Casarotto *et al.*, 2023a) and thus can be used also to test the reliability of cc-PAS protocols. Any significant interaction was analysed further by Newman–Keuls corrected *post hoc* analysis. All analyses were conducted in STATISTICA 12 (StatSoft).

Results

Corticospinal excitability

The ANOVA on the MEP amplitude showed a significant main effect of “Action condition” ($F_{2,66} = 35.80$; $p < 0.0001$) and “Coil orientation” ($F_{1,33} = 20.95$; $p < 0.0001$). The interaction between “Action condition”, “Time” and “cc-PAS protocol” was also significant ($F_{2,66} = 17.48$; $p < 0.0001$). Furthermore, the interaction between “cc-PAS protocol”, “Action condition”, “Coil orientation” and “Time” was significant ($F_{2,66} = 15.87$; $p < 0.0001$). All the other interactions were not significant; for the complete ANOVA results, see **Table 3.2**. The *post hoc* analyses showed, that after the cc-PAS_{PA}, there was a significant increment of MEP_{PA} (pre-PAS, mean = 1.49 mV, *SD* = 0.69 mV; post-PAS, mean = 2.15 mV, *SD* = 1.23 mV; $P = 0.0003$) at rest. No significant differences emerged for the

MEP_{PA} during precision grip (pre-PAS, mean = 3.09 mV, *SD* = 1.30 mV; *p* = 0.07) and power grip (pre-PAS, mean = 2.35 mV, *SD* = 1.23 mV; post-PAS, mean = 2.19 mV, *SD* = 1.16 mV; *p* = 0.44) execution. Moreover, after the cc-PAS_{PA}, the MEP_{AP} did not show any significant modulation at rest (pre-PAS, mean = 1.33 mV, *SD* = 1.20 mV; post-PAS, mean = 1.36 mV, *SD* = 0.97 mV; *p* = 0.83), during the execution of precision grip (pre-PAS, mean = 2.19 mV, *SD* = 1.09 mV; post-PAS, mean = 2.12 mV, *SD* = 1.01 mV; *p* = 0.94) and the power grip (pre-PAS, mean = 1.80 mV, *SD* = 0.97 mV; post-PAS, mean = 1.64 mV, *SD* = 0.86 mV; *p* = 0.47, **Fig. 3.2**).

Effect	F	p
cc-PAS protocol	$F_{1,33} = 0.50$	$p = 0.48$
Action Condition	$F_{2,66} = 35.80$	$p < 0.0001$
Action Condition*cc-PAS protocol	$F_{2,66} = 0.93$	$p = 0.40$
Coil Orientation	$F_{1,33} = 20.95$	$p < 0.0001$
Coil Orientation*cc-PAS protocol	$F_{1,33} = 0.46$	$p = 0.50$
Time	$F_{1,33} = 0.39$	$p = 0.53$
Time*cc-PAS protocol	$F_{1,33} = 0.25$	$p = 0.62$
Action Condition*Coil Orientation	$F_{2,66} = 0.05$	$p = 0.95$
Action Condition*Coil Orientation*cc-PAS protocol	$F_{2,66} = 1.46$	$p = 0.24$
Action Condition*Time	$F_{2,66} = 0.69$	$p = 0.51$
Action Condition*Time*cc-PAS protocol	$F_{2,66} = 17.47$	$p < 0.0001$
Coil Orientation*Time	$F_{1,33} = 1.57$	$p = 0.22$
Coil Orientation*Time*cc-PAS protocol	$F_{1,33} = 0.11$	$p = 0.75$
Action Condition*Coil Orientation*Time	$F_{2,66} = 1.83$	$p = 0.17$
Action Condition*Coil Orientation*Time*cc-PAS protocol	$F_{2,66} = 4.72$	$p = 0.01$

Table 3.2. Complete results of mixed ANOVA on corticospinal excitability data
Significant results are shown in bold.

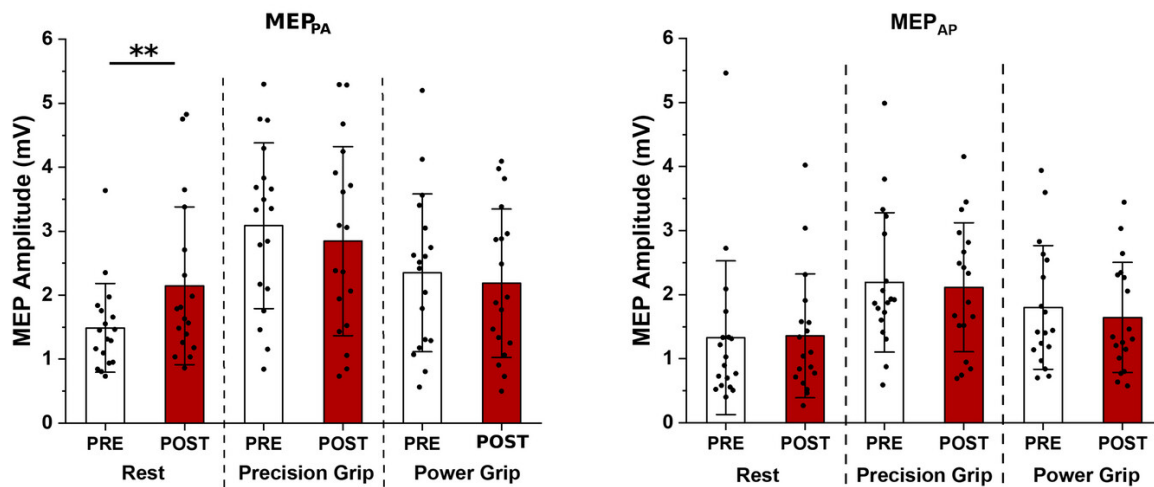


Figure 3.2. Motor-evoked potential results in Session 1.

The left panel shows the effects of the PMv-to-M1 cc-PAS_{PA} protocol on motor-evoked potentials (MEPs) tested with a postero-anterior (PA) coil orientation; the right panel reports the results of the MEP data acquired with an antero-posterior (AP) coil orientation. The error bars represent the SD; ** $p < 0.01$.

After the cc-PAS_{AP}, we found a significant reduction of the MEP_{PA} at rest (pre-PAS, mean = 2.00, SD = 1.05 mV; post-PAS, mean = 1.68; SD = 0.88 mV; $p = 0.05$). Differently, there was no significant modulation of the MEP_{PA} during the execution of precision grip (pre-PAS, mean = 2.79 mV, SD = 0.98; post-PAS, mean = 3.15 mV; SD = 0.86 mV; $p = 0.06$) and power grip (pre-PAS, mean = 2.38 mV, SD = 0.94 mV; post-PAS, mean = 2.68 mV, SD = 1.03 mV; $p = 0.06$). In this case, the MEP_{AP} was modulated selectively during the execution of precision grip (pre-PAS, mean = 2.48 mV, SD = 1.04 mV; post-PAS, mean = 2.84 mV; SD = 1.12 mV; $p = 0.04$). No significant modulation was observed in the MEP_{AP} at rest (pre-PAS, mean = 1.37 mV, SD = 0.64 mV; post-PAS, mean = 1.14 mV, SD = 0.46 mV; $p = 0.35$) and during the power grip execution (pre-PAS, mean = 2.09 mV, SD = 1.08 mV; post-PAS, mean = 2.04 mV, SD = 0.98 mV; $p = 0.66$; **Fig. 3.3**).

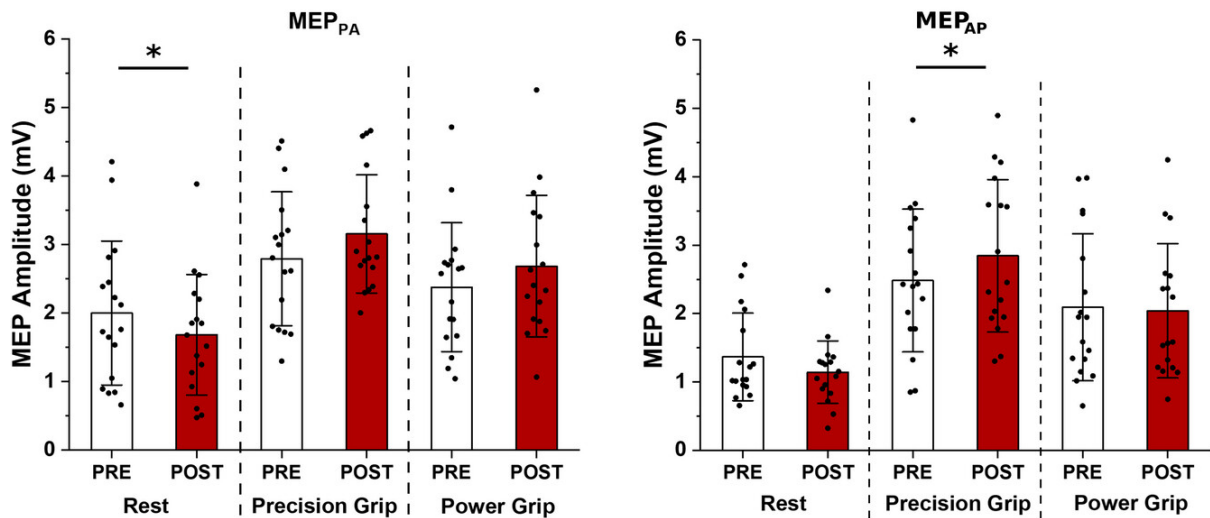


Figure 3.3. Motor-evoked potential results in Session 2.

The left panel shows the effects on motor-evoked potentials (MEPs) amplitude tested with a postero-anterior (PA) coil orientation; the right panel reports the results of MEPs acquired with an antero-posterior (AP) coil orientation. The error bars represent the *SD*; * $p < 0.05$.

Corticospinal silent period

The $2 \times 2 \times 2 \times 2$ ANOVA on the cSP duration showed a significant main effect of “Action condition” ($F_{1,32} = 11.71$; $p = 0.002$; precision grip, mean = 0.09 s, $SD = 0.02$ s; power grip, mean = 0.08 s, $SD = 0.02$ s) and “Coil orientation” ($F_{1,32} = 6.45$; $p = 0.02$; PA, mean = 0.08 s, $SD = 0.02$ s; AP, mean = 0.09 s; $SD = 0.02$ s). The interaction between “Coil orientation” and “cc-PAS protocol” was significant ($F_{1,32} = 4.26$; $p = 0.04$). The *post hoc* analyses revealed a significant difference between the cSP_{PA} and the cSP_{AP} (PA, mean = 0.07 s, $SD = 0.02$ s; AP, mean = 0.08 s, $SD = 0.03$ s; $p = 0.003$) in Session 2 (**Fig. 3.5**), in other words when the cc-PAS_{AP} was applied. This difference was not present when the cc-PAS_{PA} was applied (PA, mean = 0.08 s, $SD = 0.03$ s; mean = 0.08 s; $SD = 0.02$ s; $p = 0.74$ **Fig. 3.4**). Considering that no main effect or interaction with the factor “Time” was present, these results will not be discussed further. The complete results of ANOVA are reported in **Table 3.3**.

Effect of cc-PAS_{PA} on cSP length

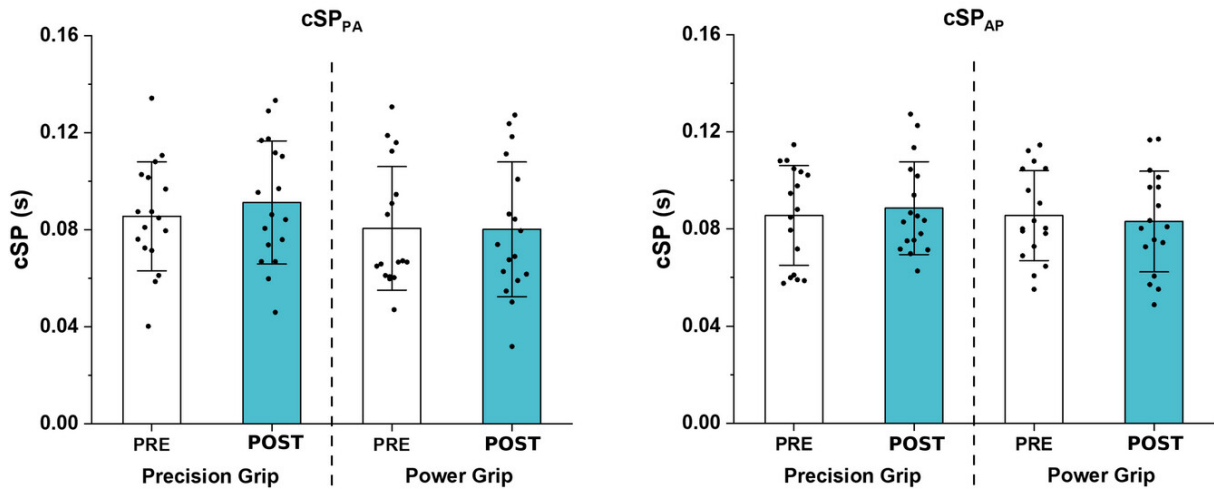


Figure 3.4. Corticospinal silent period results in Session 1.

The left panel shows the effects of the PMv-to-M1 cc-PAS_{PA} protocol on corticospinal silent period (cSP) tested with a postero-anterior (PA) coil orientation; the right panel report the results on cSP acquired with an antero-posterior (AP) coil orientation. Error bars represent the *SD*.

Effect of cc-PAS_{AP} on cSP length

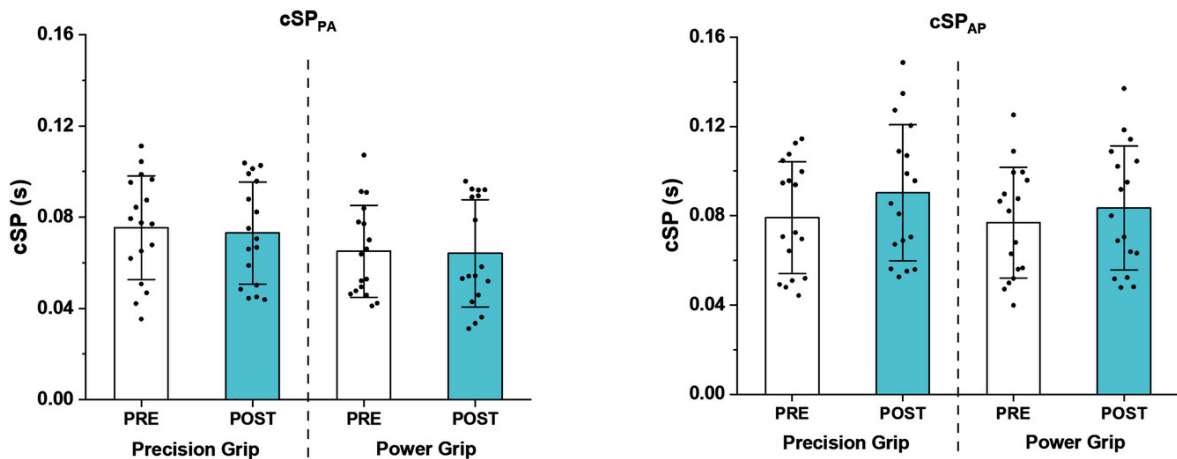


Figure 3.5. Corticospinal silent period results in Session 2.

The left panel shows the effects of the PMv-to-M1 cc-PAS_{PA} protocol on the corticospinal period (cSP) tested with a postero-anterior (PA) coil orientation; the right panel reports the results on cSP recorded with an antero-posterior (AP) coil orientation. Error bars represent the *SD*.

Effect	F	p
cc-PAS protocol	$F_{1,32} = 1.86$	$p = 0.18$
Action Condition	$F_{1,32} = 11.71$	$p = 0.002$
Action Condition*cc-PAS protocol	$F_{1,32} = 0.21$	$p = 0.65$
Coil Orientation	$F_{1,32} = 6.45$	$p = 0.02$
Coil Orientation*cc-PAS protocol	$F_{1,32} = 4.26$	$p = 0.05$
Time	$F_{1,32} = 3.10$	$p = 0.09$
Time*cc-PAS protocol	$F_{1,32} = 0.56$	$p = 0.46$
Action Condition*Coil Orientation	$F_{1,32} = 3.56$	$p = 0.07$
Action Condition*Coil Orientation*cc-PAS protocol	$F_{1,32} = 0.0004$	$p = 0.98$
Action Condition*Time	$F_{1,32} = 1.56$	$p = 0.22$
Action Condition*Time*cc-PAS protocol	$F_{1,32} = 0.51$	$p = 0.48$
Coil Orientation*Time	$F_{1,32} = 1.53$	$p = 0.23$
Coil Orientation*Time*cc-PAS protocol	$F_{1,32} = 3.82$	$p = 0.06$
Action Condition*Coil Orientation*Time	$F_{1,32} = 0.30$	$p = 0.58$
Action Condition*Coil Orientation*Time*cc-PAS protocol	$F_{1,32} = 0.44$	$p = 0.51$

Table 3.3. Complete results of mixed ANOVA on corticospinal silent period duration data. Significant results are shown in bold.

Motor-evoked potential latency

The $2 \times 3 \times 2 \times 2$ ANOVA conducted on the latency data showed a significant main effect of “Action condition” ($F_{2,66} = 41.31$; $p < 0.0001$) and “Coil orientation” ($F_{2,66} = 109.94$; $p < 0.0001$). A significant interaction emerged between “Coil orientation”, “Time” and “cc-PAS protocol” ($F_{1,33} = 6.85$ $p = 0.01$). We found no other significant interactions or main effect; the complete results are reported in **Table 3.4**.

The *post hoc* analyses on the interaction showed a significant difference in the latencies of the MEPs acquired with a PA coil orientation after the cc-PAS_{PA} (pre-

PAS, mean = 0.020 s, SD = 0.001 s; post-PAS, mean = 0.021 s, SD = 0.002 s; $p = 0.01$; **Fig. 3.6**). No difference was observed in the latencies of the MEPs acquired with the AP coil orientation (pre-PAS, mean = 0.022 s, SD = 0.001 s; post-PAS, mean = 0.022 s, SD = 0.001 s; $p = 0.99$). After the cc-PAS_{AP}, a significant difference was present in the latencies of the MEPs acquired with an AP coil orientation (pre-PAS, mean = 0.020 s, SD = 0.001 s; post-PAS, mean = 0.021 s, SD = 0.001 s; $p = 0.02$; **Fig. 3.7**). No difference was present in the latencies of the MEPs acquired with a PA coil orientation (pre-PAS, mean = 0.020 s, SD = 0.001 s; post-PAS, mean = 0.020 s, SD = 0.001 s; $p = 0.85$).

Effect	F	<i>p</i>
cc-PAS protocol	$F_{1,33} = 3.49$	$p = 0.07$
Action Condition	$F_{2,66} = 41.31$	$p < 0.0001$
Action Condition*cc-PAS protocol	$F_{2,66} = 0.25$	$p = 0.78$
Coil Orientation	$F_{1,33} = 109.94$	$p < 0.0001$
Coil Orientation*cc-PAS protocol	$F_{1,33} = 0.62$	$p = 0.44$
Time	$F_{1,33} = 3.36$	$p = 0.07$
Time*cc-PAS protocol	$F_{1,33} = 0.04$	$p = 0.84$
Action Condition*Coil Orientation	$F_{2,66} = 1.18$	$p = 0.31$
Action Condition*Coil Orientation*cc-PAS protocol	$F_{2,66} = 1.56$	$p = 0.22$
Action Condition*Time	$F_{2,66} = 0.36$	$p = 0.70$
Action Condition*Time*cc-PAS protocol	$F_{2,66} = 1.72$	$p = 0.19$
Coil Orientation*Time	$F_{1,33} = 0.01$	$p = 0.94$
Coil Orientation*Time*cc-PAS protocol	$F_{1,33} = 6.85$	$p = 0.01$
Action Condition*Coil Orientation*Time	$F_{2,66} = 0.43$	$p = 0.65$
Action Condition*Coil Orientation*Time*cc-PAS protocol	$F_{2,66} = 0.79$	$p = 0.46$

Table 3.4. Complete results of ANOVA on motor-evoked potential latency data. Significant results are shown in bold.

Effect of cc-PAS_{PA} on MEP latency

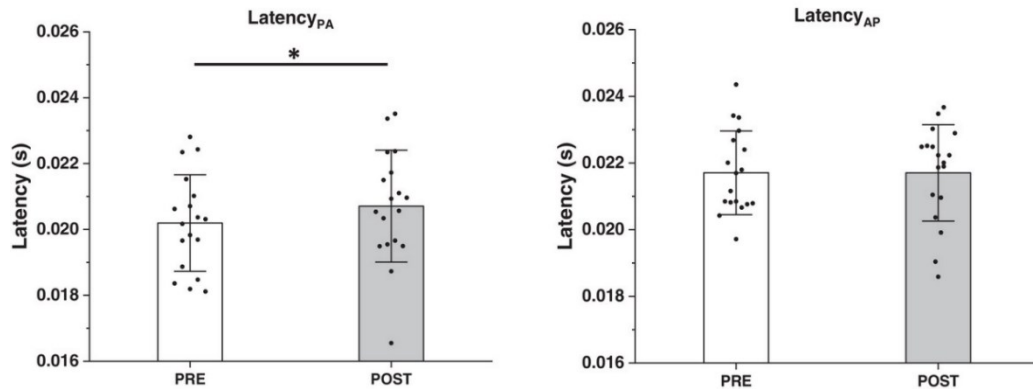


Figure 3.6. Main effect results for MEP latencies in Session 1.

The left panel highlights the significant main effect of time on latency_{PA}. The right panel shows no significant main effect of time on latency_{AP}. In experiment 1, the PMv–M1 cc-PAS was applied with a postero-anterior (PA) orientation. Error bars represent the SD; * $p < 0.05$.

Effect of cc-PAS_{AP} on MEP latency

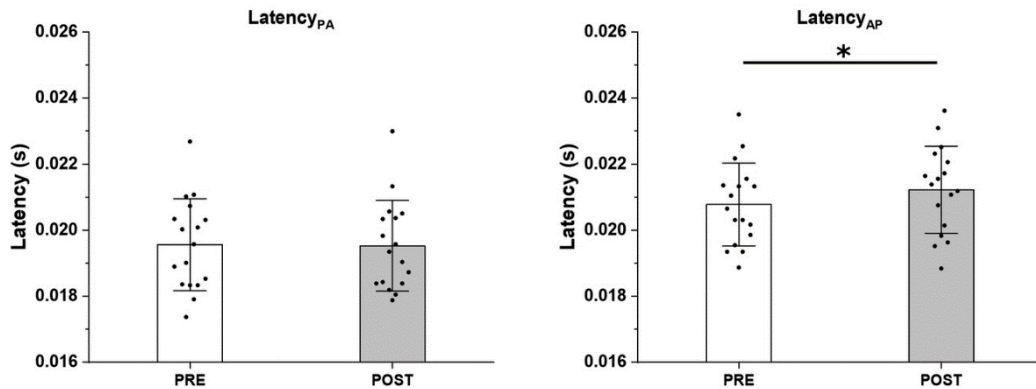


Figure 3.7. Main effect results for MEP latencies in Session 2.

The left panel shows no significant main effect of time on latency_{PA}. The right panel highlights the significant main effect of time on latency_{AP}. In session 2, the PMv–M1 cc-PAS was applied with an antero-posterior (AP) orientation. Error bars represent the SD; * $p < 0.05$.

Discussion

In the present work, we applied a PMv–M1 cc-PAS protocol with two coil orientations (PA vs. AP on M1) to investigate the possibility of modulating specific PMv–M1 connections during the execution of different grasping actions. We found that PMv–M1 cc-PAS with an AP direction resulted in a preferential modulation of precision grip motor drive. Notably, at rest we replicated some of the key results obtained earlier (Casarotto *et al.*, 2023a), whereas in activation, we showed that the cc-PAS protocols modulated MEP latency only when elicited with the same coil orientation used during the cc-PAS stimulations, thus lending additional consistency to our present manipulations and results.

Effects of PMv-to-M1 cc-PAS on corticospinal motor drive

Visually guided grasping actions recruit an extended network, in which different parietal and frontal areas provide key contributions. Previous studies highlighted the visuomotor nature of PMv and its crucial role in grasping actions; in particular, during the precision grip (Davare *et al.*, 2008, 2009; Prabhu *et al.*, 2009; Koch *et al.*, 2010b). Although several parietal areas offer key contributions to the fine execution of grasping actions, these seem to be mediated by the activity of premotor areas (Koch *et al.*, 2010a). The PMv thus represents a converging node for several inputs which, unlike parietal and frontal areas, is connected monosynaptically to M1 (Matelli *et al.*, 1998; Makris *et al.*, 2005; Rozzi *et al.*, 2006).

This extended network converges towards M1 for the control of precision and power grip, possibly involving partially non-overlapping neural populations. Single-unit recordings clearly show that some cortical motor neurons appear to be more active during precision grip, whereas others are more active during power grip (Muir & Lemon, 1983). Precision and power grip are not the two ends of the same action continuum (i.e. grasping) but represent two qualitatively different motor plans. At least in part, these actions engage different PMv and M1 intracortical circuits (Muir & Lemon, 1983; Bennett & Lemon, 1996; Umiltà *et al.*, 2007) and descending systems (Baker & Perez, 2017; Federico & Perez, 2017; Tazoe & Perez, 2017).

Although the origin of the various descending volleys that compose the M1 output remains largely unclear, it is assumed that different neuronal populations might be targeted preferentially by TMS with different coil orientations (Ni *et al.*, 2011a; Hamada *et al.*, 2014; Aberra *et al.*, 2020; Fong *et al.*, 2021). Our results confirm this hypothesis, showing that by varying the coil orientation of a PMv–M1 cc-PAS protocol, we preferentially conditioned M1 neural populations activated or not during the execution of precision grip.

After the cc-PAS_{PA}, we replicated previous results showing that PMv–M1 cc-PAS_{PA} led to an increase of CSE at rest (Casarotto *et al.*, 2023a; Turrini *et al.*, 2023b). However, the PMv–M1 cc-PAS_{PA} did not produce any significant modulation of the corticospinal motor drive during muscle activation (for both the precision and power grip), as indicated by the absence of modulation of both MEP amplitude and cSP duration. Also, in the cc-PAS_{AP} session we replicated our previous results at rest, showing a significant reduction of CSE after the PMv–M1 cc-PAS_{AP} (Casarotto *et al.*, 2023a). More importantly, the specific activity of the neural populations involved in precision or power grip were also modulated differentially by the PMv–M1 cc-PAS_{AP} protocol. Indeed, the populations recruited by PA single pulse stimulation showed no significant modulation but only a generalized trend to a higher excitability during both precision and power grip. Instead, the neural populations recruited by the AP current direction showed a selective increase for precision grip only. Hence, M1 populations, preferentially recruited by the AP stimulation and influenced by PMv input (Casarotto *et al.*, 2023a), seem to be more involved in the execution of precision grip than power grip (**Fig. 3.8**).

The AP stimulation is believed to induce currents flowing from layer VI to layer I that are likely to generate significant depolarizations in dendrites, hence in more superficial layers (Sommer *et al.*, 2013). Given that most synaptic input occurs on dendrites, signalling to the synapse that the neuron has generated an output is believed to be mediated by back-propagating action potentials (Magee & Johnston, 1997). These provide the depolarization that allows relief of the Mg²⁺ block of NMDA receptors (Vargas-Caballero & Robinson, 2003; Kampa *et al.*, 2004), which is essential for induction of STDP (Bi & Poo, 1998; Debanne *et al.*, 1998; Kampa *et al.*, 2007). Here, the depolarization of the dendritic arbor of

pyramidal neurons would improve their ability to integrate various input signals. The combined effect of AP M1 stimulation paired with the PMv stimulation, as in cc-PAS_{AP}, would induce a long-lasting state of dendrite depolarization, specifically strengthening the integration of PMv inputs. In this regard, effective input integration in the superficial layers of M1 might be mediated by the I₂-wave intracortical circuits that interact with projections coming from the PMv (Shimazu *et al.*, 2004; Cattaneo *et al.*, 2005; Koch *et al.*, 2010*b*). As previously demonstrated, the PMv–M1 cc-PAS specifically modifies the activity of I₂-wave circuits at rest (Casarotto *et al.*, 2023*a*).

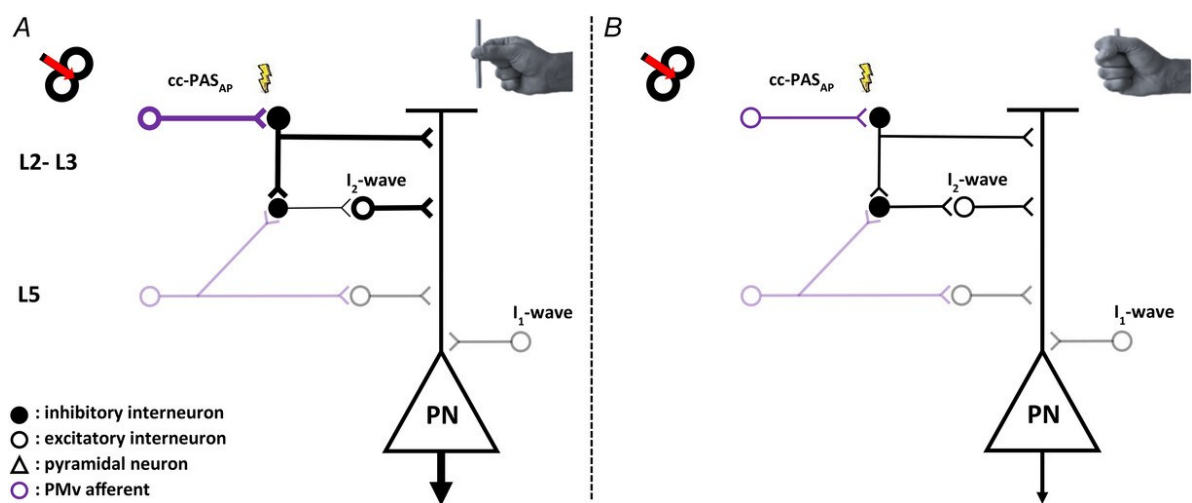


Figure 3.8. Proposed activity of primary motor cortex superficial layers, involving the I₂-wave circuit, during the precision and power grips after cc-PAS_{AP}.

This figure focuses on the preferential contribution of the superficial primary motor cortex (M1) population [layer 2–3 (L2–L3)] to the precision grip (**A**, left) rather than the power grip (**B**, right). After the cc-PAS_{AP}, the superficial M1 neuronal populations (L2–L3) lead to an increase in corticospinal excitability (CSE) only during the precision grip. The precision grip requires finer programming than the power grip, which is likely to be supported by a stronger integration of sensorimotor input. This integration process, after the cc-PAS_{AP}, might be supported by a long-lasting state of dendritic depolarization of the pyramidal neurons and probably occurs in the superficial M1 layers, where dendritic arborizations of layer 5 (L5) pyramidal neurons are located. The effects of PMv–M1 cc-PAS_{AP} on M1 superficial layers are likely to be mediated by the late I-wave circuits, most probably located in these layers. The line thickness indicates increased or decreased motor output.

From a functional perspective, the PMv is more involved in the control of precision grip, as opposed to power grip (Ehrsson *et al.*, 2000; Davare *et al.*, 2008). Integration of a larger variety of signals is also the hallmark of refined motor control, and the precision grip is configured as a finer action than the power grip (**Fig. 3.8**; Witney *et al.*, 2004; Iturrate *et al.*, 2018). In line with this idea, previous work has highlighted a stronger influence of thalamocortical connections on M1 superficial layers during the precision grip than the power grip (Davis *et al.*, 2022), further supporting the need for stronger sensorimotor integration. In our case, previous direct and indirect evidence has shown that the I₂-wave is influenced by the activity of premotor areas (Cerri *et al.*, 2003; Shimazu *et al.*, 2004; Koch *et al.*, 2010a; Casarotto *et al.*, 2023a). It is then reasonable to propose that the effects obtained here, after the cc-PAS_{AP}, are mediated by the late I-wave circuits and that these circuits represent the site of interaction of PMv with M1 specifically for the control of precision grasping actions (**Fig. 3.8**). Conversely, PA stimulation, preferentially targeting the M1 deep layers, might somewhat cloud the contribution of the superficial neuronal populations, providing a more general readout of M1 activity. The contribution of M1 superficial layers could be hidden by the lower threshold for the recruitment of populations targeting the M1 pyramidal neurons closer to the soma with PA stimulations.

Effects of PMv-to-M1 cc-PAS on MEP latency

Further support in favour of a partial separation of neuronal populations recruited with the AP vs. PA current direction can be derived from the results on MEP latencies. The application of the cc-PAS protocol induces specific latency modulation of MEPs elicited with the same coil orientation used for the plasticity-inducing protocol. More specifically, in the *Session 1*, when the cc-PAS was applied with a PA coil orientation, the MEP_{PA} showed a longer latency in the post-PAS acquisition with respect to the pre-PAS acquisition. The MEP_{AP} latency was not affected. In a similar way, after the cc-PAS_{AP} (*Session 2*), only the MEPs elicited with an AP coil orientation presented an altered latency.

The PA and AP stimulations engaged different trans-synaptic sets of inputs (Ni *et al.*, 2011a), probably involving more deep and superficial neural populations, respectively (Koch *et al.*, 2013; Sommer *et al.*, 2013; Aberra *et al.*, 2020). More

precisely, the cortical motoneuronal cells, connected monosynaptically with α -motor neurons, were found predominantly in the anterior bank of the central sulcus (Rathelot & Strick, 2009), which appears to be the portion most activated by the induction of PA current flow. This would justify MEPs with shorter latencies in PA stimulation. In contrast, AP current flow would activate the rostral M1 portion, where the premotor pyramidal cells are located, leading to MEPs with longer latencies (Abera *et al.*, 2020). According to this view, inputs to M1 from the premotor cortex, with conduction latencies matching late descending I-waves, have been identified in monkeys (Tokuno & Nambu, 2000; Shimazu *et al.*, 2004; Maier *et al.*, 2013) and humans (Groppa *et al.*, 2012; Casarotto *et al.*, 2023a; Liao *et al.*, 2023), suggesting that they could be recruited by AP stimulation (Di Lazzaro & Rothwell, 2014).

In this study, modulation of MEP latencies congruent with the cc-PAS orientation support the idea that different coil orientations activate different sets of cortical neurons. Moreover, we demonstrate here that it is possible to apply plasticity-inducing protocols separately to different M1 intracortical circuits. The cc-PAS_{PA} might have conditioned the deep M1 populations specifically, whereas the cc-PAS_{AP} might have modulated the activity of superficial M1 neuronal populations.

Limitations and future perspectives

A limit of the present study might be the isometric execution of grasping actions. Future work should investigate the effects of the induction of plasticity on ecological execution of reaching and grasping actions. In addition, an ecological visually guided grasping action would probably be more suitable to disentangle the differential contributions of premotor and parietal areas.

Here, although the FDI muscle is recruited in a similar manner in both the explored actions, it might play a more important role in precision grip than in power grip. For this reason, future work could explore similar mechanisms in different muscles to understand the generalizability of our results. Finally, the contribution of distinct populations in different M1 layers during specific tasks is far from established, and TMS-based methods are certainly not optimal in solving this issue. However, Kurz *et al.* (2019) demonstrated recently how the temporal combination of single-pulse

TMS protocol with elicitation of the H reflex could provide an interesting tool to investigate the contribution of different M1 layers during specific tasks. Future research might use this procedure to provide further insight into the contribution of different M1 layers during the execution of precision and power grip.

Conclusion

These results provide useful insight into the cortical contribution of isolable neuronal populations to different grasping actions. These findings can be used to induce an action-specific PMv–M1 network plasticity by means of the cc-PAS protocol. Although deep M1 neuronal populations appear to be involved unspecifically in the implementation of precision and power grip, more superficial M1 populations have been shown to play a more prominent role in precision grip. Application of a cc-PAS protocol directed preferentially to these more superficial populations could be particularly suitable for designing specific interventions to improve precision grip performance in various clinical populations. Enhanced synaptic input from PMv, a crucial hub in the grasping parietofrontal network, combined with targeted dendrite depolarization in M1 (Koch *et al.*, 2010*b*; Sommer *et al.*, 2013), might thus represent an important physiological basis for the rehabilitation of fine and independent control of the fingers.

Supplementary Analyses

In this section I will include the supplementary analyses performed to support our findings.

Firstly, we concept this experiment as a within-subject design. We computed two (PA and AP) 3x2 repeated measures ANOVA with “Action Condition” (rest, precision grip, power grip) and “Time” (pre-PAS, post-PAS) as factors on MEP amplitude and MEP latency data. Similarly, we computed two 2x2 repeated measured ANOVA with “Action Condition” (precision grip, power grip) and “Time” (pre-PAS, post-PAS) as factors on cSP duration data. Any significant interaction was further analysed by Newman-Keuls corrected post hoc analysis.

Session 1 – CC-PAS_{PA}

The ANOVA on the MEP_{PA} amplitude showed a significant main effect of “Action Condition” ($F_{2,34} = 8.23$; $p = 0.001$) but no significant main effect of “Time” ($F_{1,17} = 0.36$; $p = 0.56$). We found a significant interaction between the factors ($F_{2,34} = 10.76$; $p = 0.0002$). The post-hoc analyses showed a significant increment of MEP_{PA} at post-PAS ($M = 2.15$ mV; $SD = 1.23$) compared to the pre-PAS acquisition ($M = 1.49$ mV; $SD = 0.69$; $p = 0.0002$) at rest. No significant differences between pre-PAS and post-PAS emerged during precision (pre-PAS: $M = 3.09$ mV; $SD = 1.30$; post-PAS: $M = 2.85$ mV; $SD = 1.48$; $p = 0.12$) and power grip (pre-PAS: $M = 2.35$ mV; $SD = 1.23$; post-PAS: $M = 2.19$ mV; $SD = 1.16$; $p = 0.29$) execution.

The ANOVA on MEP_{AP} amplitude showed a significant main effect of “Action Condition” ($F_{2,34} = 9.99$; $p = 0.0004$) but no significant main effect of “Time” ($F_{1,17} = 0.41$; $p = 0.53$) and interaction between factors ($F_{2,34} = 0.31$; $p = 0.74$ – **Figure 3.9**). The 2x2 ANOVA on the cSP_{PA} duration showed a significant main effect of “Action Condition” ($F_{1,16} = 6.33$; $p = 0.02$; Precision Grip: $M = 0.09$ s; $SD = 0.02$; Power Grip: $M = 0.08$ s; $SD = 0.02$). There was no significant main effect of “Time” ($F_{1,16} = 0.55$; $p = 0.47$) or interaction between “Action Condition” and “Time” ($F_{1,16} = 0.70$; $p = 0.42$). The ANOVA on the cSP_{AP} highlighted no significant main effect of “Action Condition” ($F_{1,16} = 0.08$; $p = 0.78$) and “Time” ($F_{1,16} = 0.01$; $p = 0.91$) or significant interaction between these factors ($F_{1,16} = 0.42$; $p = 0.53$ – **Figure 3.10**).

The 3x2 ANOVA conducted on the latency_{PA} data showed a significant main effect of “Action Condition” ($F_{2,34} = 15.61$; $p < 0.0001$) and “Time” ($F_{1,17} = 6.05$; $p = 0.02$;

pre-PAS: $M = 0.020$ s; $SD = 0.001$; post-PAS: $M = 0.022$ s; $SD = 0.002$). No significant interaction emerged between the factors ($F_{2,34} = 0.74$ $p = 0.49$). The ANOVA computed on the latency_{AP} data showed a significant main effect of “Action Condition” ($F_{2,34} = 12.01$; $p = 0.0001$) and no significant main effect of “Time” ($F_{1,17} < 0.01$; $p > 0.99$; pre-PAS: $M = 0.022$ s; $SD = 0.001$; post-PAS: $M = 0.022$; $SD = 0.001$) or significant interaction ($F_{2,34} = 0.57$; $p = 0.57$ – **Figure 3.11**).

Effect of cc-PAS_{PA} on MEP amplitude

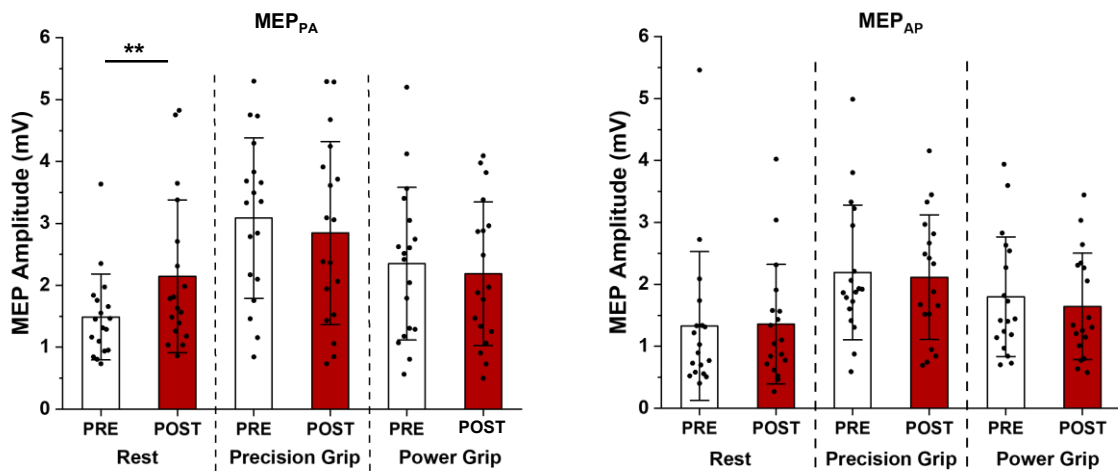


Figure 3.9. MEPs results of Session 1.

The *left* panel reports the effects of PMv-to-M1 cc-PAS_{PA} protocol on MEP tested with a PA coil orientation; the *right* panel reports the results on the MEP data acquired with an AP coil orientation. The error bars represent the standard deviation (SD); ** indicates $p < 0.01$.

Effect of $cc\text{-PAS}_{PA}$ on cSP length

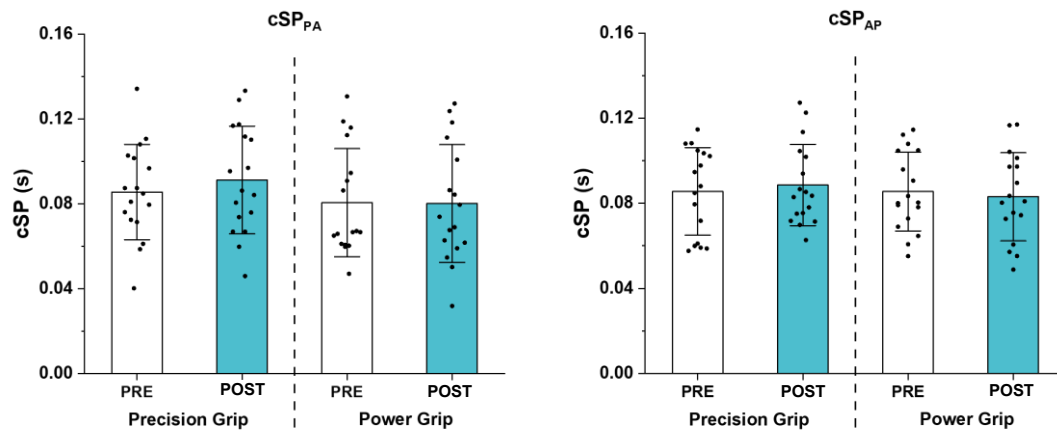


Figure 3.10. Corticospinal silent period results in Session 1.

The *left* panel shows the effects of PMv-to-M1 $cc\text{-PAS}_{PA}$ protocol on cSP tested with a PA coil orientation; the *right* panel report the results on cSP acquired with an AP coil orientation. The error bars of histograms represent the *SD*.

Effect of $cc\text{-PAS}_{PA}$ on MEP latency

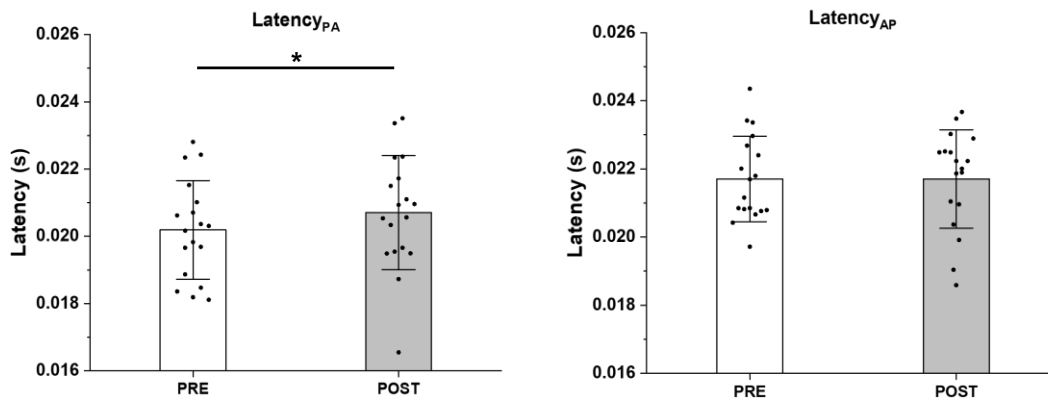


Figure 3.11. Main effect results for MEP latencies in Session 1.

The *left* panel highlights the significant “Time” main effect on $latency_{PA}$. The right panel shows the no significant “Time” main effect on $latency_{AP}$. In *Session 1*, the PMv-M1 $cc\text{-PAS}$ was applied with a PA orientation. The error bars of histograms represent the *SD*; * indicates $p < 0.05$.

Experiment 2 – cc-PAS_{AP}

The 3x2 repeated measured ANOVA of MEP_{PA} data showed a significant main effect of “Action Condition” ($F_{2,32} = 12.40$; $p = 0.001$) and a no significant main effect of “Time” ($F_{1,16} = 1.64$; $p = 0.22$). There was a significant interaction between “Action Condition” and “Time” ($F_{2,32} = 12.37$; $p = 0.0001$). The post-hoc analyses revealed greater CSE_{PA} in the post-PAS acquisition, compared to the pre-PAS acquisition at rest (pre-PAS: $M = 2.00$; $SD = 1.05$; post-PAS: $M = 1.68$ mV; $SD = 0.88$; $p = 0.006$), during the precision (pre-PAS: $M = 2.79$ mV; $SD = 0.98$; post-PAS: $M = 3.15$ mV; $SD = 0.86$; $p = 0.002$) and power grip (pre-PAS: $M = 2.38$ mV; $SD = 0.94$; post-PAS: $M = 2.68$ mV; $SD = 1.03$; $p = 0.008$). The 3x2 repeated measured ANOVA on MEP_{AP} data showed a significant main effect of “Action Condition” ($F_{2,32} = 24.72$; $p < 0.0001$) and no significant main effect of “Time” ($F_{1,16} = 0.07$; $p = 0.80$). Moreover, a significant interaction was present between the two factors ($F_{2,32} = 7.43$; $p = 0.002$). The post-hoc analyses showed a significant greater CSE_{AP}, after the cc-PAS_{AP}, during the precision grip (pre-PAS: $M = 2.48$ mV; $SD = 1.04$; post-PAS: $M = 2.84$ mV; $SD = 1.12$; $p = 0.003$); but no significant modulation during the power grip (pre-PAS: $M = 2.09$ mV; $SD = 1.08$; post-PAS: $M = 2.04$ mV; $SD = 0.98$; $p = 0.64$) or at rest (pre-PAS: $M = 1.37$ mV; $SD = 0.64$; post-PAS: $M = 1.14$ mV; $SD = 0.46$; $p = 0.05$ – **Figure 3.12**).

The 2x2 repeated measured ANOVA computed on cSP_{PA} duration data showed a significant main effect of “Action Condition” ($F_{1,16} = 5.23$; $p = 0.04$; Precision Grip: $M = 0.07$ s; $SD = 0.02$; Power Grip: $M = 0.06$ s; $SD = 0.02$) and a no significant main effect of “Time” ($F_{1,16} = 0.48$; $p = 0.50$) or interaction between “Action Condition” and “Time” ($F_{1,16} = 0.12$; $p = 0.73$). In both *Experiments*, we found a significant longer cSP_{PA} when performing the precision than power grip. This effect was absent in the cSP_{AP}. The global readout of M1 activity provided by the PA orientation highlights the greater inhibition required for the execution of a finer action such as precision grip than power grip.

The 2x2 repeated measured ANOVA computed on cSP_{AP} showed no significant main effect of “Action Condition” ($F_{1,16} = 2.52$; $p = 0.13$) but a significant main effect of “Time” ($F_{1,16} = 7.92$; $p = 0.01$; pre-PAS: $M = 0.07$ s; $SD = 0.02$; post-PAS: $M = 0.08$ s; $SD = 0.03$). The interaction between “Action Condition” and “Time” was not

significant ($F_{1,16} = 1.03$; $p = 0.33$ – **Figure 3.13**). Ultimately, the 3x2 repeated measured ANOVA on latency_{PA} showed a significant main effect of “Action Condition” ($F_{2,32} = 24.51$; $p < 0.0001$) but no significant main effect of “Time” (pre-PAS: $M = 0.020$ s; $SD = 0.001$; post-PAS: $M = 0.020$ s; $SD = 0.001$; $F_{1,16} = 0.05$; $p = 0.84$) or interaction between these factors ($F_{2,32} = 2.22$; $p = 0.12$). The 3x2 repeated measured ANOVA on latency_{AP} highlighted a significant main effect of “Action Condition” ($F_{2,32} = 9.97$; $p = 0.0004$) and “Time” (pre-PAS: $M = 0.020$ s; $SD = 0.001$; post-PAS: $M = 0.021$ s; $SD = 0.001$; $F_{1,16} = 5.44$; $p = 0.03$). No significant interaction between the factors emerged ($F_{2,32} = 0.25$; $p = 0.78$ – **Figure 3.14**).

Effect of cc-PAS_{AP} on MEP amplitude

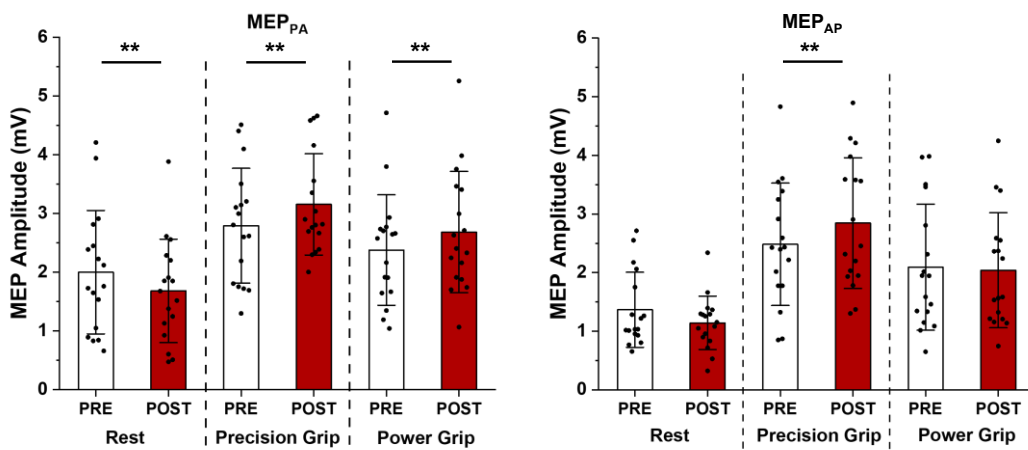


Figure 3.12. MEPs results in Session 2.

The left panel shows the effects on MEP amplitude tested with a PA coil orientation; the right panel reports the results of MEP acquired with an AP coil orientation. The error bars represent the SD ; ** indicates $p < 0.01$.

Effect of $cc\text{-PAS}_{AP}$ on cSP length

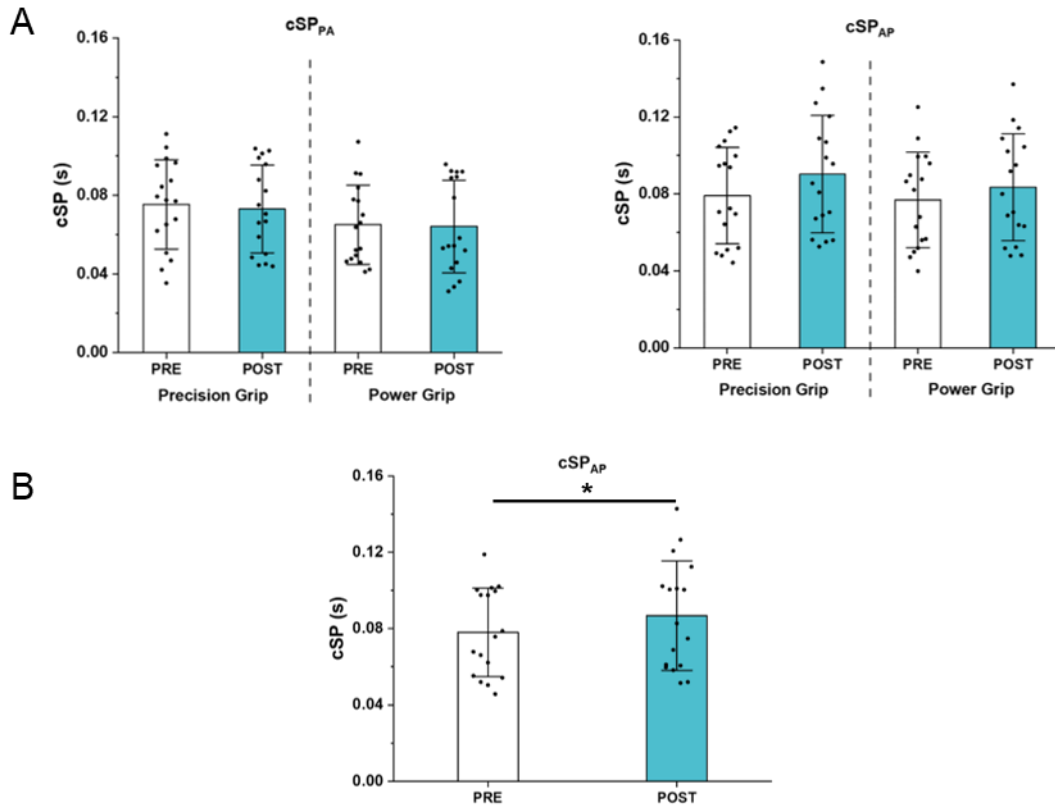


Figure 3.13. Corticospinal silent period results in Session 2.

A) The *left* panel shows the effects of PMv-to-M1 $cc\text{-PAS}_{PA}$ protocol on cSP tested with a PA coil orientation; the *right* panel reports the results on cSP recorded with an AP coil orientation. **B)** Representation of “Time” main effect on cSP length when tested in AP current direction. Error bars represent the *SD*; * indicates $p < 0.05$.

Effect of $cc\text{-PAS}_{AP}$ on MEP latency

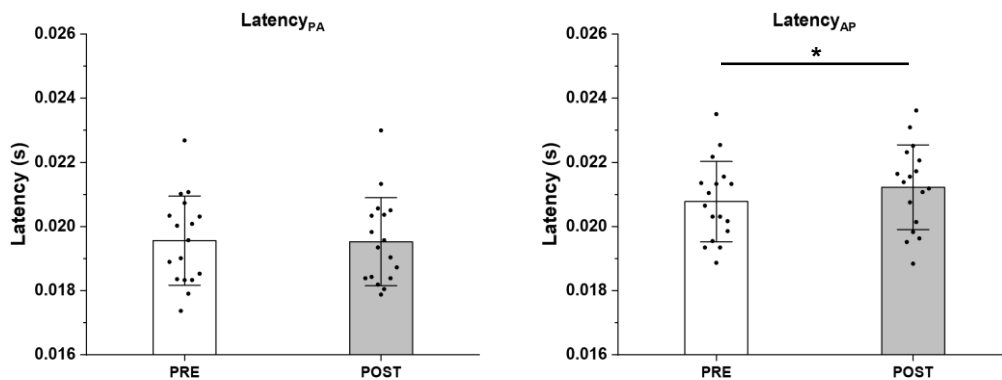


Figure 3.14. Main effects results for MEP latencies in Session 2 (previous page).

The *left* panel shows the no significant “Time” main effect on latency_{PA}. The *right* panel highlights the significant “Time” main effect on latency_{AP}. In *Session 2*, the PMV-M1 cc-PAS was applied with an AP orientation. Error bars represent the *SD*; * indicate $p < 0.05$.

Considering the session in which the cc-PAS was applied with a PA coil orientation, these analyses return the same results as above. The CSE was selectively modulated only at rest and only when tested with a PA coil orientation. The latency only changes for the MEP acquired with a coil orientation congruent with that used during the cc-PAS (i.e., PA). No significant modulations in the length of cSP were observed.

If we consider the session with the cc-PAS protocol administered with an AP coil orientation over M1, we can observe that the results regarding latencies are the same as above. Only the latency of the MEP acquired with a coil orientation congruent with that used during the cc-PAS (i.e. AP) was modulated. Similarly, we have modulation of the CSE tested with an AP coil orientation selectively during the precision grip execution. This confirms our main results.

Nevertheless, in this session, when tested with a PA coil orientation, the CSE was found to be modulated in a non-specific manner during both precision and power grip. These results led us to propose that the deeper layers of M1 (i.e. L5) may be equally involved for both actions studied, while the superficial layers of M1 (i.e. L2-L3) may be preferentially involved in the execution of precision grip.

At this point, by switching from a within-subject experimental design to a mixed-effect design to compare data from the two experimental sessions, we encountered the limitation of having four subjects present in both conditions. These “hybrid” subjects violated the independence of observations assumption for the between-subjects factor.

To account of non-independent observations, we consider a mixed effect model. Although this family of linear models is generally designed to address correlations in the data, they are more straightforwardly applied to hierarchical data. Our data do not naturally fit with this sort of models. However, to add further support to our main results, we performed a mixed effect model on the MEP amplitude data with

“cc-PAS protocol”, “Action Condition”, “Coil Orientation” and “Time” as fixed effects and “Subjects” as random effect. The full results of the mixed-effects model are shown below:

Effect	p
cc-PAS protocol	$p < 0.001$
Action Condition	$p < 0.001$
Coil Orientation	$p < 0.001$
Time	$p < 0.001$
cc-PAS protocol*Coil Orientation	$p = 0.029$
cc-PAS protocol*Action Condition	$p < 0.001$
cc-PAS protocol*Time	$p = 0.073$
Coil Orientation* Action Condition	$p = 0.958$
Coil Orientation*Time	$p = 0.221$
Action Condition*Time	$p = 0.558$
cc-PAS protocol*Coil Orientation*Action Condition	$p = 0.001$
cc-PAS protocol*Coil Orientation*Time	$p = 0.769$
cc-PAS protocol*Action Condition*Time	$p < 0.001$
Coil Orientation*Action Condition*Time	$p = 0.043$
cc-PAS protocol*Coil Orientation*Action Condition*Time	$p = 0.001$

The significant main effects and interactions are bolded. These results are also reported in the “Peer Review History” of the published article.

Here, it can be seen that the interactions found significant in our previous analyses are again significant. The results of the mixed effect model further support our previous results and conclusions.

4. VENTRAL PREMOTOR CORTEX–PRIMARY MOTOR CORTEX PLASTICITY INDUCTION LEADS TO THE MODULATION OF PRECISION GRIP KINEMATICS

The next chapter will present the most recent findings of this research path. As anticipated, one of the main goals of this research was to understand whether the plasticity induction in the PMv-M1 network could modify motor behaviour. In particular, the performance of a precision prehension actions. The aim is not only to increase our knowledge of this network and protocol, but also to understand whether this method might have future clinical relevance. In particular, for those patients who have lost the use of hand fine motor skills. In this last experiment, we study the effect of the cc-PAS protocol on action preparations and on the kinematic of different grasping actions (precision vs. power).

At the beginning of this kinematic study, several pilot studies were conducted focusing only on the execution of different precision grasping actions. I tested different sets of objects with the aim that they would require a gradient of actions ranging from precision grip to power grip. However, the more objects were introduced into the setup, the more noise was introduced. While the objects representing the two extremes of the gradient (pure precision grasp vs. pure power grasp) had clearly different kinematics, the “intermediate” objects, which formed the gradient between the two actions, often had kinematics that were not clearly different. More objects require more trials, and this probably led participants to adopt a more fluid motor plan suitable for interaction with more objects. This evidence led us to build a setup with two actions that required completely separate motor plans (i.e.: precision vs. power grip).

The results to be reported here have not yet been published or presented. Nevertheless, they represent the current end point of our analysis and not just preliminary results. They show modulation of the kinematics, particularly of the precision grip action, after the application of PMv-M1 cc-PAS protocol with an AP

coil orientation. This modulation alters a key property of multi-joint motor control, which is the balance between feedforward and feedback processes.

The following results has been presented at the “7th bi-annual ESCAN meeting” organized by the European Society for Cognitive and Affective Neuroscience in Ghent (Belgium, 22nd and 25th of May 2024) as a contribution at the Symposium “Enhance associative neural plasticity through innovative protocol of non-invasive brain stimulation: cortico-cortical paired associative stimulation”, entitled “PMv – M1 plasticity induction modulates M1 activity during specific grasping actions”.

Introduction

Manipulating and using objects is one of the most common but sophisticated actions performed by human. The study of neural basis has shown that the ventral premotor cortex (PMv) and the primary motor cortex (M1) represent two critical areas of the network that programs and control the execution of these actions (Murata *et al.*, 1997; Raos *et al.*, 2006; Prabhu *et al.*, 2009; Beukelaar *et al.*, 2016). Moreover, previous work has shown that different neuronal populations within M1 are specifically involved in controlling fractioned finger actions rather than power grasping (Muir & Lemon, 1983; Casarotto *et al.*, 2023b). In this view, it has previously been shown how, through the transcranial magnetic stimulation (TMS), it is possible to target the neural populations preferentially involved in the precision grip rather than power grip (Davis *et al.*, 2022; Casarotto *et al.*, 2023b). By changing the TMS coil orientation, it is indeed possible to preferentially stimulates the more superficial (L2 – L3) or the more deep (L5) layers of M1 (Ni *et al.*, 2011a; Federico & Perez, 2017; Spampinato, 2020; Fong *et al.*, 2021). Specifically, the posterior-anterior (PA) coil orientation seems to preferentially target the M1 deeper layers, while the anterior-posterior (AP) coil orientation preferentially targets the M1 superficial layers (Sommer *et al.*, 2013; Aberra *et al.*, 2020; Casarotto *et al.*, 2023a, 2023b).

The AP coil orientation, in particular, seems to be preferential for engaging the M1 neural populations most involved during the precision grip (Davis *et al.*, 2021; Casarotto *et al.*, 2023b). Davis and colleagues (2022) demonstrated how the M1 neuronal populations, stimulated by AP coil orientation, are more sensitive to input from primary somatosensory cortex (S1) during the execution of precision grip rather than power grip. Subsequently, after the application of cortico-cortical paired associative (cc-PAS) protocol in the PMv-M1 network, with an AP coil orientation over M1 (cc-PAS_{AP}), we found that the corticospinal excitability (CSE) tested with an AP coil orientation was selectively modulated during the precision grip (Casarotto *et al.*, 2023b). These results argue in favour of a greater involvement of the superficial M1 layers, recruited by AP stimulation, during the execution of precision grip rather than power grip. In addition to these neurophysiological modulations, previous studies reported behavioural modulations after the application of a PMv-M1 cc-PAS protocol. In these studies, participants became

faster in completing a clinical motor test (i.e. 9-Hole Peg Test - 9-HPT; Fiori *et al.*, 2018; Turrini *et al.*, 2023b). However, the reduction in completion time argues in favour of behavioural modulation but does not provide any further information on how the preparation and execution of a precision prehension may change after the plasticity inductions in the PMv-M1 network.

In the present work, we recorded the upper limb kinematics of the participants while performing precision and power grip actions before and 30 minutes after the application of the PMv-M1 cc-PAS_{AP} protocol. At the same time, to assess the modulations induced on the action preparation, we measured the CSE 50 ms before the “Go signal”. We collected the motor-evoked potential (MEP) amplitude both when participants were preparing a specific type of grasp and when they had to prepare a more general grasping action. For this purpose, we collected the MEP when participants were informed which action (precision vs. power grip) they had to perform, and thus activated a specific motor plan, and when they were not informed which type of grasp they had to perform and thus had to keep at least two motor plans active (i.e. precision grip and power grip). It is well known that during action preparation, the CSE is suppressed. This “inhibitory preparation” (Neige *et al.*, 2021) probably serves to prevent premature release of the action. In previous works, it has been shown that the PMv-M1 cc-PAS modulates the M1 GABAergic inhibitory activity (Casarotto *et al.*, 2023a; Turrini *et al.*, 2023b). For these reasons, we hypothesise that the inhibitory mechanism that is expressed shortly before the action execution may be positively modulated by the cc-PAS.

However, this modulation may be difficult to observe when participants have only one motor plan to prepare and thus suppress. Under these conditions, motor plan inhibition could be optimal even before plasticity induction. Rather, the modulation induced by the plasticity induction may be observable in the not-informed conditions, where the inhibition of at least two motor plans is required. In this case, the competition of motor plans may make preparatory inhibition more challenging and less efficient.

Moving from the preparation to the execution of the actions, based on previous findings, we hypothesised that cc-PAS_{AP} specifically modulates the execution of precision grip (Davis *et al.*, 2021; Casarotto *et al.*, 2023b). We analysed a series of kinematic parameters connected to the transport phase (i.e.: the timing and the

magnitude of peak velocity, the movement time, and the maximum grip aperture) and, in particular, to the acceleration profile (e.g., the timing and the magnitude of the acceleration and deceleration peak). In kinematics, the acceleration and deceleration phases are directly determined by the muscle activations pattern. More precisely, the acceleration phase strictly reflects the first burst of the agonist muscle, while the deceleration phase reflects the subsequent burst of the antagonist muscle and the final weaker second burst of the agonist muscle. This synchronous activation of agonistic and antagonistic muscles, which forms the triphasic pattern activation (Hallett, 1975), is directly linked to the control of voluntary movement by the central nervous system (CNS). Indeed, the acceleration and deceleration phases directly reflect the feedforward and feedback components of movements (Brown & Cooke, 1990).

Differently from the acceleration profile, according to Brown & Cooke (1990), the velocity profiles of different movements will be approximately equivalent regardless of the movement amplitude or duration. For this reason, the induced modulations in *how* the neural control of movement is organized, and thus in the temporal coordination of muscle activation patterns, may not emerge from the velocity profile (Brown & Cooke, 1990), but rather by the analysis of the different phases of the acceleration profile.

After the cc-PAS, there may be an imbalance in favour of the acceleration or deceleration phase of the reaching movement. This possible imbalance, observable in the ratio computed between the acceleration and deceleration component, would directly reflect a change in the muscle activation pattern and consequently in the rules used by the CNS to formulate movement commands (Cooke & Brown, 1994).

Furthermore, the prolonged execution of certain movements usually leads to a decrease in their variability (Georgopoulos *et al.*, 1981; Darling & Cooke, 1987). By analysing the standard deviation of the previously mentioned kinematic features (e.g. the maximum acceleration or deceleration), it might be possible to understand whether cc-PAS can influence this phenomenon in specific actions. Following the previous results, which highlighted the capability of the cc-PAS protocol to modify the PMv-M1 cortical activity (Casarotto *et al.*, 2023a, 2023b; Turrini *et al.*, 2023b), the possibility of modulating the behavioural performance of

grasping actions, and in particular of fractional finger movements, could represent an important basis for the rehabilitation of fine finger control.

Methods

Participants

A total of 19 healthy volunteers (mean \pm SD age, 23.84 ± 1.14 years; 9 males) took part in this study (**Table 4.1**). This sample size is in line with previous studies using similar experimental manipulations (Rizzo *et al.*, 2009; Chiappini *et al.*, 2018; Fiori *et al.*, 2018; Casarotto *et al.*, 2023a; 2023b). All the participants were informed about the experimental procedure and gave their written consent according to the last update of the *Declaration of Helsinki*, except for the registration in a database. The experiment was approved by the ethical committee 'Comitato Etico Unico della Provincia di Ferrara' (approval no. 170592). The participants were compensated for their participation with €30.00.

All the participants were included in the MEPs analyses. However, due to technical problems during the kinematic recording, two participants were not included in the kinematics analyses.

Subject (male)	Age	M1 rMT _{AP}	M1 rMT _{PA}
19 (9)	23.84 ± 1.14	50.37 ± 5.38	44.32 ± 4.77

Table 4.1. The rMT value indicates the percentage of the maximum stimulator output and is reported for all coils used. During the cc-PAS protocol and acquisition of connectivity, the 50 mm coil used for the rMT_{AP} was positioned on M1 while the 50 mm coil used for the rMT_{PA} was on PMv.

Experimental task

Two wooden spheres were positioned on a board in front of the subject's right hand. A small sphere (20 mm diameter) that could be grasped with a precision grip and a large sphere (80 mm diameter) that could be grasped with a power grip. The two spheres were positioned at 30% of the subject's arm length from the hand starting point. Three green LEDs were placed in front of the two spheres: one near each of them and one in between. Participants began each trial by holding a little

touch sensor between their thumb and index. They were instructed to perform a reach-to-grasp action based on the switching on of the lights. Once they had grasped the ball, they had to lift it slightly, reposition it and return to the starting position.

In each trial, participants could be early or late instructed on the action to be performed. When they were early instructed (i.e. “Informed Precision Grip” and “Informed Power Grip”) the trial began with the switching on of one of the two lights near one of the spheres (e.g. the switching on of the light near the small sphere in case of precision grip), this light acted as an “Informative Cue”. After 500 ms the central light switched on and the participant started the action; this light acted as a “Go Signal”. In the trials in which the participants were late instructed (i.e. “Not Informed Precision Grip” and “Not Informed Power Grip”), at the beginning of the trial, the central light, which acted as a “Not-Informative Cue”, was switched on, and after 500 ms, one of the two lights near the spheres, which acted as an “Informative Go”, was switched on.

A total of 160 trials were collected, 40 for each condition. In half of the trials, 50 ms before the “Go Signal”/“Informative Go” a TMS single-pulse was released to evaluate the CSE during the action preparation phase (**Figure 4.1**).

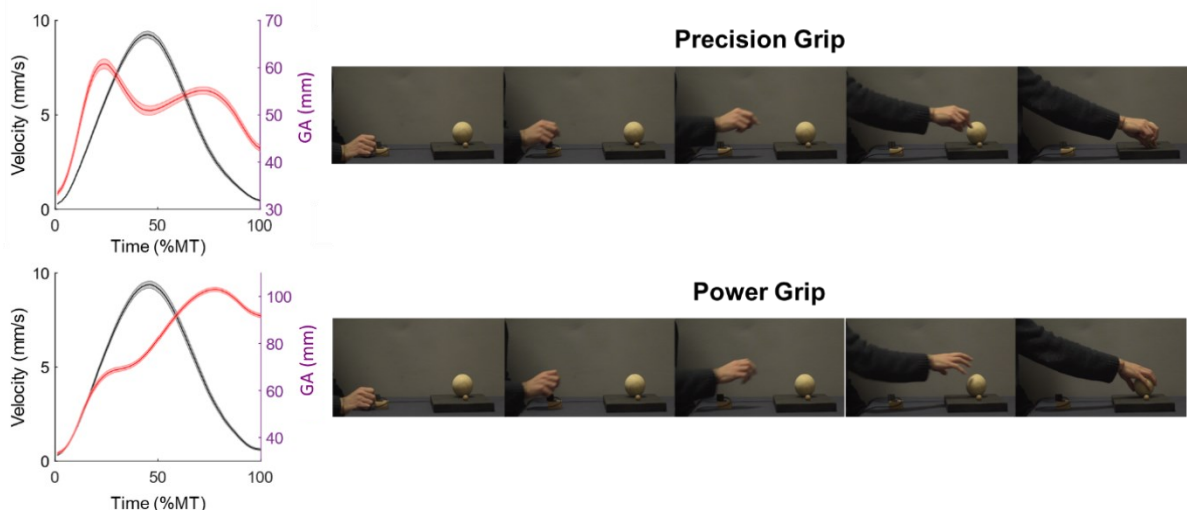


Figure 4.1. Grasping movements required during the experiment.

The *top* panel shows the typical execution of a precision prehension, whereas the *bottom* panel shows the execution of the power grip. On the left side the typical grip aperture (GA; in *red*) and velocity profile (in *black*) of these actions can be observed. The position of the targets was randomised between the subjects.

Kinematic data recording

The right upper arm movement in three axes (anteroposterior, X; mediolateral, Y; and vertical, Z) was continuously recorded using a ten cameras motion capture system (Vicon Nexus; RRID:SCR_015001; sampling rate: 100 Hz). A total of 14 retro-reflective markers were recorded. Eight markers with a diameter of 9.5 mm were used to record the trunk, upper arm, and wrist movements, while six markers with a diameter of 6.4 mm were used to record the hand and fingers movements.

Markers were placed at the following anatomical locations: the sternum body (named “trunk”), the left acromial process (named “shoulder sx”), the right acromial process (named “shoulder dx”), the right triceps muscle (named “arm”), the lateral condyle of the humerus (named “elbow”), the right extensor digitorum muscle (named “forearm”), the styloid process of the radius (named “wrist sx”), the ulnar epiphysis (named “wrist dx”), the first dorsal interosseous (named “hand/thumb”), the condyle of V metacarpal bone (named “hand”), the condyle of III metacarpal bone (named “hand/little finger”), the last thumb phalanx (named “thumb”), the last index phalanx (named “index”) and the last little finger phalanx (named “little finger”).

Transcranial Magnetic Stimulation

Participants were seated during all the experimental sessions. Single-pulse TMS and cc-PAS protocols were administered through a 50 mm figure-of-eight focal coil connected to a Magstim BiStim2 monophasic stimulator (The Magstim Company, Whitland, UK). The FDI optimal scalp position (OSP) was found by moving the coil in 0.5 cm steps over the left primary motor cortex hand area and using a slightly suprathreshold stimulus. Resting motor threshold (rMT) was defined as the lowest intensity that evoked an MEP with $>50 \mu\text{V}$ amplitude in 5 of 10 consecutive trials while the participants kept the FDI muscle relaxed (Rossi *et al.*, 2009; Rossini *et al.*, 2015). The individual OSP and rMT were defined for each coil used. A total of 160 trials were acquired during the action preparation phase in the two behavioural sessions (e.g., “pre-PAS” and “post-30”). Specifically, we recorded 40 MEPs for each experimental condition (i.e.: “Informed Precision Grip”, “Not Informed Precision Grip”, “Informed Power Grip”, “Not Informed Power Grip”).

Cortico-cortical paired associative stimulation

In the cc-PAS protocol, dual-sites TMS repeatedly activated the connection between the left PMv and left M1. One hundred couples of pulses were delivered at a frequency of 0.25 Hz for ~6 min. The left PMv was stimulated at 90% of individual rMT, while the left M1 was stimulated at 120% of rMT (Casarotto et al., 2023a, 2023b). In each pair, the M1 stimulation followed the PMv stimulation by 6 ms (Davare et al., 2008, 2009; Koch et al., 2010; Casarotto et al., 2023a, 2023b). The coil over the left M1 was placed tangentially to the scalp on the FDI OSP, at ~45° with respect to the midline and rotated 180° to induce an AP current flow. To estimate the position of the left PMv, we used the SofTaxic Navigator System (Electro Medical System, Bologna, Italy). The skull landmarks (nasion, inion, right, and two preauricular points) and 23 points on the scalp were digitalized through a Polaris Vicra optical tracker (Northern Digital, Canada). To stimulate the left PMv, the coil was placed over a scalp region corresponding to the Montreal Neurological Institute (MNI) coordinates $x = -52.8$, $y = 11.6$, $z = 25.1$ (Casarotto et al., 2023a, 2023b).

EMG recording

Surface EMG was recorded from the right first dorsal interosseous (FDI) muscle through a wireless system (Zerowire EMG, Aurion, Italy) with a tendon–belly montage. EMG signals were digitized (2 kHz) and acquired by a CED Power1401-3A board (Cambridge Electronic Design, Cambridge, UK). The acquired data were stored for offline analysis using the Signal 3.09 software (Cambridge Electronic Design, Cambridge, UK).

Data Analysis

Corticospinal Excitability

At first, we excluded from the analysis all trials that presented a peak-to-peak MEP amplitude of ≤ 0.05 mV. After this, for each trial, we computed the ratio between the MEP peak-to-peak amplitude and the root mean square (RMS) of the 100 ms pre-TMS window. This was done to avoid any modulation of the CSE due to the pre-movement level of muscle contraction. Indeed, although the participants were

instructed to stay relaxed before the movement, the request to hold the touch sensor between the thumb and finger could lead to a slight muscle contraction. After this, the MEPs were z-scored.

To investigate the effects induced by different PMv–M1 cc-PAS protocols on the CSE during the preparation of different actions we computed a 3x2 repeated measured ANOVA with “Action Condition” (Informed Precision Grip vs. Informed Power Grip vs. Not informed grip), and “Time” (pre-PAS vs. post-30) as factors. The “Not Informed Grip” includes the behavioural “Not Informed Precision Grip” and “Not Informed Power Grip” conditions. These data were collapsed in one condition, as at this point of the action programming the participants were not informed of the action they were to perform, so it was irrelevant which action they would later perform. Any significant interactions were further analysed by Newman–Keuls corrected post hoc analysis.

Kinematics

In order to characterise the movement of the required actions, we considered several features related to the transport phase and the hand preshaping. We considered the “peak velocity” (PV) and the “average velocity” (AV) reached during the movement, the “movement time” (i.e. the time needed to complete the actions - MT). The “reaction time” (RT), computed as the time between the “Go Signal” and the moment when the velocity exceeded the 3% of PV, and the “maximum grip aperture” (MGA; i.e. the maximum aperture between the thumb and the index during the reaching phase). Moreover, we computed the “time to the peak velocity” (TPV) expressed as a percentage of the MT.

We then considered the acceleration profile and extracted the “peak acceleration” (PA) and the “peak deceleration” (PD) as well as the “time to PA” (TPA) and the “time to PD” (TPD) expressed as a percentage of MT. To evaluate a possible imbalance in favour of the feedforward component or in favour of the feedback component, we computed the ratio between the PA and the PD (PA/PD). An increase in the ratio would indicate an imbalance in favour of the feedforward component; otherwise, there would be an imbalance in favour of the feedback component.

In order to observe whether there was a modulation of motion dispersion after the cc-PAS protocol, we computed the standard deviation (*SD*) of these features. All these variables were extracted from the trajectory of the marker placed on the wrist, called “wrist sx”. This marker was preferable to those placed on the fingers (i.e. “thumb”, “index” and “little finger”), which undergo changes in trajectory and acceleration due to the hand preshaping.

For each feature, we computed a 2x2x2 repeated measured ANOVA with the within-subjects factors “Action” (precision vs. power grip), “Information” (informed vs. not-informed) and “Time” (pre-PAS vs. post-30). Any significant interactions were further analysed by Newman–Keuls corrected post hoc analysis. However, particular emphasis will be placed on the main effect of “Time” and the interactions comprising this factor, as the main goal being to investigate the modulations induced by cc-PAS protocol.

Results

Corticospinal Excitability

The 3x2 ANOVA on MEP amplitude showed no significant main effect of “Action Conditions” ($F_{1,19} = 3.06$; $p = 0.06$) or “Time” ($F_{1,19} = 2.21$; $p = 0.15$). However, the interaction between these factors results to be significant ($F_{2,38} = 3.45$; $p = 0.04$). In the pre-PAS, the post hoc analyses showed a significantly greater MEP during the preparation of the not-informed grip compared to the MEP during the preparation of precision (not-informed grip, $M = 0.25$, $SD = 0.26$; precision grip, $M = -0.02$, $SD = 0.37$; $p = 0.01$) and power grip (not-informed grip, $M = 0.25$, $SD = 0.26$; power grip, $M = -0.004$, $SD = 0.41$; $p = 0.01$).

Moreover, the post-hoc showed a significant reduction of the MEPs during the preparation of the not-informed grip after the cc-PAS (pre-PAS, $M = 0.25$, $SD = 0.26$; post-30, $M = -0.10$, $SD = 0.29$; $p = 0.005$; **Figure 4.2**).

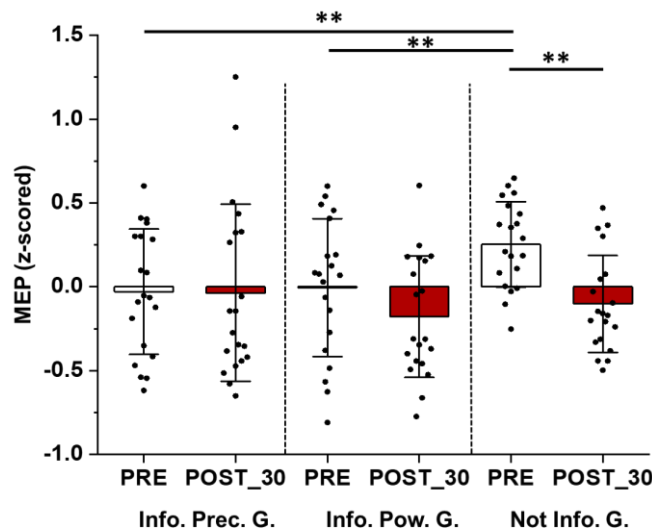


Figure 4.2. Effect of cc-PAS_{AP} on the CSE during the action preparation.

The MEPs are expressed as the ratio between the MEP amplitude and the RMS of the EMG contraction 100 ms before the TMS pulse. The ratio was then z-scored. Error bars represent the *SD*; ** $p < 0.01$. Abbreviation: Info. Prec. G. = Informed Precision Grip; Info. Pow. G. = Informed Power Grip; Not Info. G = Not Informed Grip.

Acceleration Profile Analyses

The ANOVA on the PA showed a significant main effect of “Action” ($F_{1,16} = 9.99$; $p = 0.006$; $\eta^2 = 0.38$) and “Time” ($F_{1,16} = 6.60$; $p = 0.02$; $\eta^2 = 0.29$; pre-PAS, $M = 0.48$ mm/s², $SD = 0.16$; post-30, $M = 0.44$ mm/s², $SD = 0.14$; **Figure 4.3A**) but a not significant main effect of “Information” ($F_{1,16} = 1.03$; $p = 0.33$; $\eta^2 = 0.06$). The interaction between “Action” and “Information” was found to be significant ($F_{1,16} = 5.31$; $p = 0.03$; $\eta^2 = 0.25$). Differently, the interactions between “Information” and “Time” ($F_{1,16} = 0.001$; $p = 0.97$; $\eta^2 = 0.0001$), “Action” and “Time” ($F_{1,16} = 1.92$; $p = 0.18$; $\eta^2 = 0.11$), and between the three factors ($F_{1,16} = 0.43$; $p = 0.52$; $\eta^2 = 0.03$) were found to be not significant.

Moreover, the ANOVA on the PD showed a significant main effect of “Action” ($F_{1,16} = 14.58$; $p = 0.002$; $\eta^2 = 0.48$) and “Time” ($F_{1,16} = 5.56$; $p = 0.03$; $\eta^2 = 0.26$; pre-PAS, $M = -0.44$ mm/s², $SD = 0.16$; post-30, $M = -0.40$ mm/s², $SD = 0.13$) but a not significant main effect of “Information” ($F_{1,16} = 0.03$; $p = 0.87$; $\eta^2 = 0.002$). No significant interaction was found between “Information” and “Action” ($F_{1,16} = 0.84$; $p = 0.37$; $\eta^2 = 0.05$), “Information” and “Time” ($F_{1,16} = 0.31$; $p = 0.58$; $\eta^2 = 0.01$),

“Action” and “Time” ($F_{1,16} = 0.01$; $p = 0.91$; $\eta^2 = 0.001$) or between the three factors ($F_{1,16} = 0.47$; $p = 0.50$; $\eta^2 = 0.03$; **Figure 4.3B**).

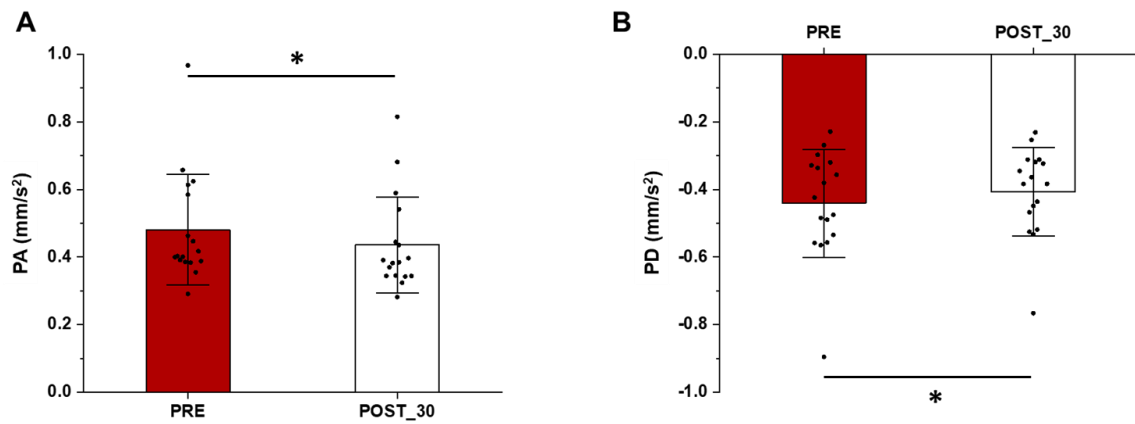


Figure 4.3. Main effect of “Time” for the PA and the PD

A. The *left* panel shows the modulation in the PA peak magnitude. **B.** The *right* panel shows the modulation of the PD. Error bars represent the *SD*; * $p < 0.05$.

The ANOVA on the ratio between PA and PD showed a significant main effect of the factor “Information” ($F_{1,16} = 9.03$; $p = 0.008$ $\eta^2 = 0.36$) and a significant interaction between the “Action” and “Time” factors ($F_{1,16} = 5.62$; $p = 0.03$; $\eta^2 = 0.26$). The post-hoc analyses revealed significant modulation between the pre-PAS and the post-30 session for the precision grip (pre-PAS, $M = 0.30$, $SD = 0.05$; post-30, $M = 0.31$, $SD = 0.05$; $p = 0.02$) but not for the power grip (pre-PAS, $M = 0.32$, $SD = 0.06$; post-30, $M = 0.32$, $SD = 0.05$; $p = 0.39$). The main effect of “Action” ($F_{1,16} = 1.96$; $p = 0.18$; $\eta^2 = 0.26$) and “Time” ($F_{1,16} = 0.13$; $p = 0.73$ $\eta^2 = 0.01$) were not significant, as well as the interaction between “Information” and “Action” ($F_{1,16} = 0.34$; $p = 0.56$; $\eta^2 = 0.02$), “Information” and “Time” ($F_{1,16} = 1.45$; $p = 0.24$; $\eta^2 = 0.08$) or between the three factors ($F_{1,16} = 0.79$; $p = 0.38$; $\eta^2 = 0.05$; **Figure 4.4 and 4.5**).

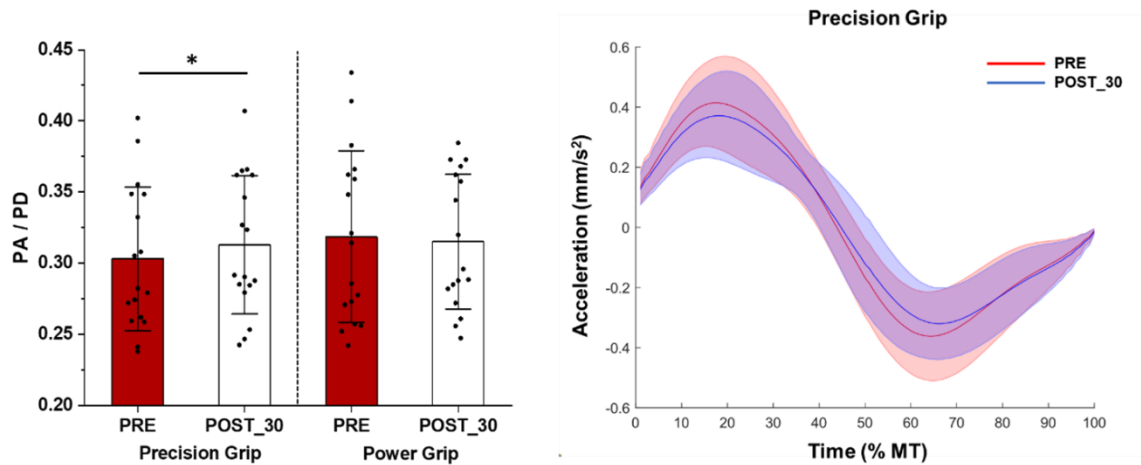


Figure 4.4. Effect of cc-PAS on the PA/PD ratio.

A) The *left* panel reports the modulation, after the cc-PAS_{AP}, of the PA/PD ratio in the precision grip action. For the ratio, the value of the PD, previously reported as negative value, was rectified. Error bars represent the *SD*; * $p < 0.05$. **B)** For exemplification purposes, the *right* panel shows the precision grip acceleration profile. In this graph, the “Informed” and “Not Informed” precision grip conditions have been collapsed. It is possible to observe the modulation of the magnitude of both PA and PD, which leads to the modulation of the ratio between them. The shaded area represents the *SD*.

The ANOVA on the TPA has shown a significant main effect of the factor “Information” ($F_{1,16} = 12.65$; $p = 0.03$; $\eta^2 = 0.44$), “Action” ($F_{1,16} = 18.44$; $p = 0.001$; $\eta^2 = 0.54$) and “Time” factors ($F_{1,16} = 5.67$; $p = 0.03$; $\eta^2 = 0.26$; pre-PAS, $M = 18.84$ %MT, $SD = 3.72$; post-30, $M = 20.41$ %MT, $SD = 3.76$; **Figure 4.6A**). No significant interaction emerged between “Information” and “Action” ($F_{1,16} = 0.41$; $p = 0.53$; $\eta^2 = 0.03$), “Information” and “Time” ($F_{1,16} = 0.58$; $p = 0.46$; $\eta^2 = 0.05$), “Action” and “Time” ($F_{1,16} = 0.84$; $p = 0.37$; $\eta^2 = 0.05$) and between these three factors ($F_{1,16} = 0.05$; $p = 0.84$; $\eta^2 = 0.003$).

The ANOVA on the TPD data has shown a significant main effect of the factor “Information” ($F_{1,16} = 12.04$; $p = 0.001$; $\eta^2 = 0.43$), “Action” ($F_{1,16} = 20.58$; $p = 0.0003$; $\eta^2 = 0.56$) but a not significant main effect of “Time” ($F_{1,16} = 2.39$; $p = 0.14$; $\eta^2 = 0.13$). No significant interaction emerged between “Information” and “Action” ($F_{1,16} = 1.14$; $p = 0.30$; $\eta^2 = 0.007$), “Information” and “Time” ($F_{1,16} = 0.02$; $p = 0.88$; $\eta^2 = 0.001$), “Action” and “Time” ($F_{1,16} = 1.45$; $p = 0.25$; $\eta^2 = 0.08$) or between these three factors ($F_{1,16} = 0.18$; $p = 0.68$; $\eta^2 = 0.01$).

Standard Deviation Analysis

Moving to analyse the *SD* of these variables, the ANOVA on the *SD* of PA showed a significant main effect of the factor “Information” ($F_{1,16} = 10.90$; $p = 0.005$; $\eta^2 = 0.41$) but a not significant main effect of “Action” ($F_{1,16} = 3.11$; $p = 0.10$; $\eta^2 = 0.16$) or “Time” ($F_{1,16} = 1.68$; $p = 0.21$; $\eta^2 = 0.10$). No significant interaction emerged between “Information” and “Action” ($F_{1,16} = 0.01$; $p = 0.92$; $\eta^2 = 0.001$), “Information” and “Time” ($F_{1,16} = 0.04$; $p = 0.84$; $\eta^2 = 0.003$), “Action” and “Time” ($F_{1,16} = 1.09$; $p = 0.31$; $\eta^2 = 0.06$) or between these three factors ($F_{1,16} = 0.01$; $p = 0.93$; $\eta^2 = 0.001$).

The ANOVA on the *SD* of PD data has shown a significant main effect of “Information” ($F_{1,16} = 12.33$; $p = 0.003$; $\eta^2 = 0.44$) and “Action” ($F_{1,16} = 6.65$; $p = 0.02$; $\eta^2 = 0.29$) but a not significant main effect of “Time” ($F_{1,16} = 0.92$; $p = 0.35$; $\eta^2 = 0.05$). No significant interaction was found between “Information” and “Action” ($F_{1,16} = 0.46$; $p = 0.51$; $\eta^2 = 0.03$), “Information” and “Time” ($F_{1,16} = 0.07$; $p = 0.79$; $\eta^2 = 0.004$), “Action” and “Time” ($F_{1,16} = 0.42$; $p = 0.53$; $\eta^2 = 0.03$) or between these three factors ($F_{1,16} = 2.58$; $p = 0.13$; $\eta^2 = 0.14$).

The ANOVA conducted on the *SD* of TPA showed a significant main effect of “Action” ($F_{1,16} = 6.83$; $p = 0.02$; $\eta^2 = 0.30$) and “Time” ($F_{1,16} = 5.20$; $p = 0.04$; $\eta^2 = 0.25$; pre-PAS, $M = 3.75$ %MT; $SD = 0.37$; post-30 = 3.98 %MT, $SD = 0.35$; **Figure 4.6B**), and a not significant main effect of “Information” ($F_{1,16} = 0.99$; $p = 0.34$; $\eta^2 = 0.06$). No significant interaction emerged between “Information” and “Action” ($F_{1,16} = 0.08$; $p = 0.79$; $\eta^2 = 0.01$), “Information” and “Time” ($F_{1,16} = 0.18$; $p = 0.68$; $\eta^2 = 0.01$), “Action” and “Time” ($F_{1,16} = 0.01$; $p = 0.93$; $\eta^2 = 0.001$) or between these three factors ($F_{1,16} = 0.08$; $p = 0.78$; $\eta^2 = 0.01$).

The ANOVA on the *SD* of TPD data has shown a significant main effect of “Action” ($F_{1,16} = 6.86$; $p = 0.02$; $\eta^2 = 0.30$) and a not significant main effect of “Information” ($F_{1,16} = 0.95$; $p = 0.35$; $\eta^2 = 0.06$) and “Time” ($F_{1,16} = 2.02$; $p = 0.17$; $\eta^2 = 0.11$). No significant interaction emerged between “Information” and “Action” ($F_{1,16} = 1.25$; $p = 0.28$; $\eta^2 = 0.07$), “Information” and “Time” ($F_{1,16} = 0.04$; $p = 0.84$; $\eta^2 = 0.003$), “Action” and “Time” ($F_{1,16} = 1.02$; $p = 0.33$; $\eta^2 = 0.06$) or between these three factors ($F_{1,16} = 0.05$; $p = 0.83$; $\eta^2 = 0.003$).

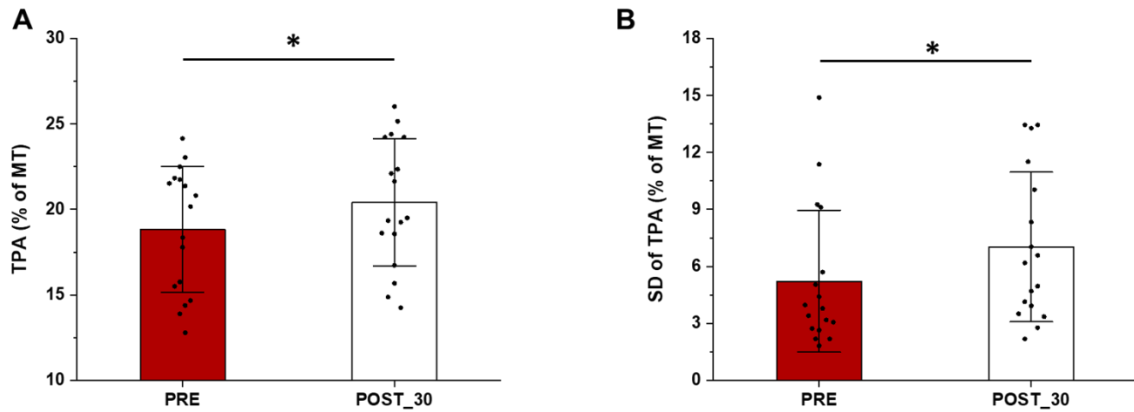


Figure 4.6. “Time” main effect for TPA and its SD.

Time's main effect on the TPA (panel **A**), and on the SD of the TPA (panel **B**). Both are expressed in % of MT. Error bars represent the SD; * $p < 0.05$.

Macroscopic Features Analyses

The ANOVA on the PV data showed a not significant main effect of “Action” ($F_{1,16} = 0.02$; $p = 0.90$; $\eta^2 = 0.05$), “Information” ($F_{1,16} = 2.89$; $p = 0.11$; $\eta^2 = 0.15$) or “Time” ($F_{1,16} = 2.23$; $p = 0.16$; $\eta^2 = 0.12$), and a not significant interaction between “Action” and “Information” ($F_{1,16} = 2.50$; $p = 0.13$; $\eta^2 = 0.14$), “Action” and “Time” ($F_{1,16} = 0.0004$; $p = 0.99$; $\eta^2 < 0.0001$), “Information” and “Time” ($F_{1,16} = 0.02$; $p = 0.89$; $\eta^2 = 0.001$) or between the three factors ($F_{1,16} = 0.001$; $p = 0.97$; $\eta^2 < 0.0001$).

The ANOVA on the AV has shown a significant main effect of “Action” ($F_{1,16} = 5.93$; $p = 0.03$; $\eta^2 = 0.27$) and “Information” ($F_{1,16} = 5.79$; $p = 0.03$; $\eta^2 = 0.27$), but a not significant main effect of “Time” ($F_{1,16} = 1.70$; $p = 0.21$; $\eta^2 = 0.10$). No significant interaction emerged between “Action” and “Information” ($F_{1,16} = 0.94$; $p = 0.35$; $\eta^2 = 0.06$), “Action” and “Time” ($F_{1,16} = 1.20$; $p = 0.29$; $\eta^2 = 0.07$), “Information” and “Time” ($F_{1,16} = 0.33$; $p = 0.58$; $\eta^2 = 0.02$) or between the three factors ($F_{1,16} = 0.02$; $p = 0.90$; $\eta^2 = 0.001$).

The ANOVA on the TPV has shown a significant main effect of “Information” ($F_{1,16} = 5.98$; $p = 0.03$; $\eta^2 = 0.27$) and a not significant main effect of “Action” ($F_{1,16} = 2.73$; $p = 0.12$; $\eta^2 = 0.15$) or “Time” ($F_{1,16} = 2.64$; $p = 0.12$; $\eta^2 = 0.14$). No significant interaction emerged between “Action” and “Information” ($F_{1,16} = 0.73$; $p = 0.41$; $\eta^2 = 0.04$), “Action” and “Time” ($F_{1,16} = 1.77$; $p = 0.20$; $\eta^2 = 0.10$), “Information” and “Time” ($F_{1,16} = 0.73$; $p = 0.41$; $\eta^2 = 0.04$) or between the three factors ($F_{1,16} = 0.03$; $p = 0.86$; $\eta^2 = 0.002$).

The ANOVA on the MT data showed a significant main effect of “Action” ($F_{1,16} = 28.10$; $p < 0.0001$; $\eta^2 = 0.64$) and “Information” ($F_{1,16} = 18.12$; $p = 0.001$; $\eta^2 = 0.53$), and a not significant main effect of “Time” ($F_{1,16} = 0.88$; $p = 0.36$; $\eta^2 = 0.05$). Similarly, no significant interaction emerged between “Action” and “Information” ($F_{1,16} = 0.31$; $p = 0.58$; $\eta^2 = 0.02$), “Action” and “Time” ($F_{1,16} = 3.00$; $p = 0.10$; $\eta^2 = 0.16$), “Information” and “Time” ($F_{1,16} = 0.01$; $p = 0.91$; $\eta^2 = 0.001$) or between the three factors ($F_{1,16} = 0.51$; $p = 0.49$; $\eta^2 = 0.03$).

The ANOVA on the RT showed a significant main of “Time” ($F_{1,16} = 7.70$; $p = 0.01$; $\eta^2 = 0.32$; pre-PAS; $M = 1.26$ s, $SD = 0.003$; post-30, $M = 1.23$, $SD = 0.004$; **Figure 4.7**) and “Information” ($F_{1,16} = 230.08$; $p < 0.0001$; $\eta^2 = 0.93$), but a not significant main effect of “Action” ($F_{1,16} = 0.04$; $p = 0.85$; $\eta^2 = 0.002$). However, no significant interaction emerged between “Action” and “Information” ($F_{1,16} = 0.33$; $p = 0.57$; $\eta^2 = 0.02$), “Action” and “Time” ($F_{1,16} = 1.62$; $p = 0.22$; $\eta^2 = 0.09$), “Information” and “Time” ($F_{1,16} = 1.12$; $p = 0.31$; $\eta^2 = 0.07$) or between the three factors ($F_{1,16} = 1.20$; $p = 0.29$; $\eta^2 = 0.07$). Participants were instructed to perform actions in a naturalistic and not necessarily fast manner. This probably led to higher RT values than those observed in a classical 'two-choice reaction time task'. At the same time, it allows us to emphasise that the modulations observed were obtained in an action performed in a naturalistic manner.

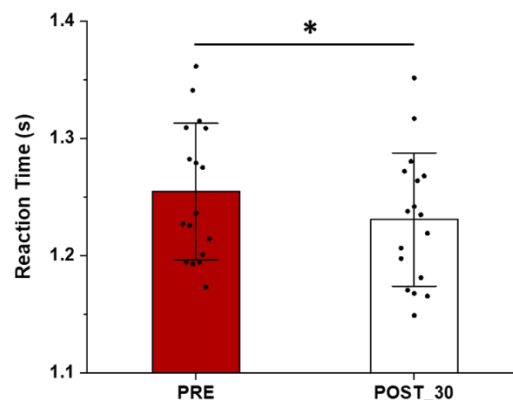


Figure 4.7. Modulation of the RT between pre- and post-30 session.

Participants showed a significant reduction in the RT in all conditions. As mentioned above, participants were instructed to perform an ecological movement. This led to a higher RT but allowed us to evaluate modulations without the experimental constraint of being 'as fast as possible'. Error bars represent the SD ; * $p < 0.05$.

The ANOVA on the MGA showed a significant main effect of “Action” ($F_{1,16} = 245.06$; $p < 0.0001$; $\eta^2 = 0.94$) and a not significant main effect of “Information” ($F_{1,16} = 2.11$; $p = 0.17$; $\eta^2 = 0.12$) and “Time” ($F_{1,16} = 0.001$; $p = 0.97$; $\eta^2 = 0.0002$). Moreover, a significant interaction between “Information” and “Time” emerged ($F_{1,16} = 8.71$; $p = 0.01$; $\eta^2 = 0.35$). No significant interaction emerged between “Action” and “Information” ($F_{1,16} = 3.05$; $p = 0.10$; $\eta^2 = 0.16$), “Action” and “Time” ($F_{1,16} = 1.32$; $p = 0.27$; $\eta^2 = 0.08$) or between the three factors ($F_{1,16} = 0.26$; $p = 0.62$; $\eta^2 = 0.02$). The post hoc analysis showed a significant modulation in the post-30 session of the “Informed” condition ($p = 0.03$; **Figure 4.8**) but not of the “Not Informed” condition ($p = 0.08$).

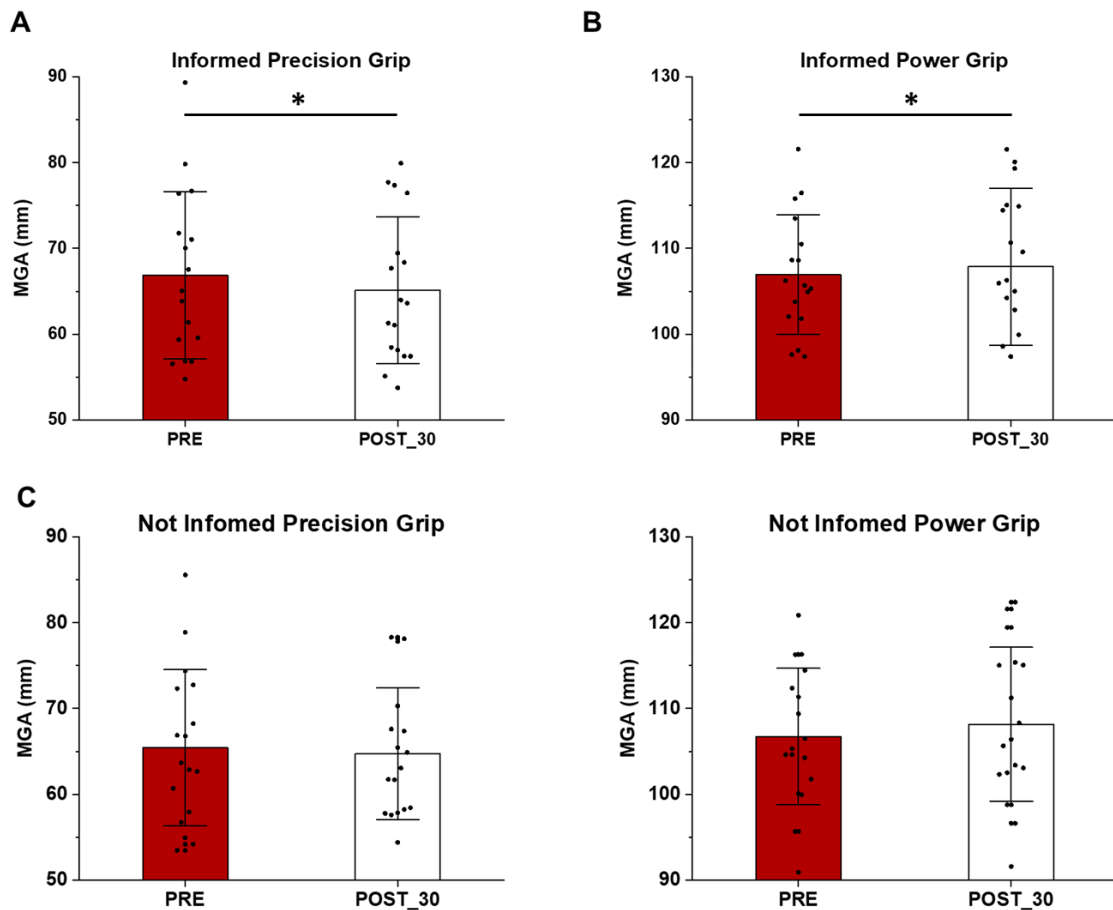


Figure 4.8. MGA modulations after the cc-PASAP.

A) The *left* panel shows a significant reduction in of the MGA in the “Informed” precision grip. **B)** The *right* panel shows the opposite trend in the power grip. Indeed, after the cc-PASAP, there is a significant larger MGA. **C)** The *bottom* panel shows the two “Not

Informed” conditions, which were not significantly modulated by the cc-PAS_{AP}. Here, the precision and power grip are plotted separately as the MGA strictly depend by the dimensions of the target. Collapsing the conditions into a single “Informed” and “Not Informed” condition would not be informative of the effects induced in the two actions. Error bars represent the *SD*; * $p < 0.05$.

Discussion

This work aimed to understand if the PMv-M1 cc-PAS protocol, in particular with an AP coil orientation over M1, could produce changes in the execution of a reach-to-grasp action, particularly in a precision grip action. Although behavioural modulations following the application of cc-PAS have been previously reported (Fiori *et al.*, 2018), this is the first study aimed at investigating the possibility of modulating how a specific type of action is produced. Moreover, the modulation of the kinematic features allowed us to directly link these modulations to the modulation of the rules used by the CNS to sculpt the motor commands (Cooke & Brown, 1994).

Action Preparation

Before the execution of a voluntary action, a series of perceptual, sensory and motor processes interact (Bestmann & Duque, 2015) to enable us to form, select and execute the motor plan congruent with the goal. Although decades of studies have highlighted the role of several regions (e.g., dorsal premotor cortex - PMd, supplementary motor area - SMA, dorsolateral prefrontal cortex - dlPFC) in this procedure, few of these have investigated the role of the PMv (Davare *et al.*, 2009; van Campen *et al.*, 2013). These works suggests that PMv, depending on the demand of the task, can exert both an excitatory and inhibitory influence on M1 during the action preparation phase (van Campen *et al.*, 2013). This effect appears to be muscle specific (Davare *et al.*, 2009).

Here, before the cc-PAS_{AP}, we can observe that the CSE is comparable between the condition in which participants were informed to prepare to perform the precision or power grip. However, the CSE was significantly higher when they were not informed which action they had to prepare. This first result can be attributed to the competition of multiple, at least two, motor plans. Indeed, it is

likely that the participants kept both motor plans of precision grip and power grip active.

It is known that, in the preparation phase, there is an increase of motor inhibition (Neige *et al.*, 2021). This phenomenon, also called “impulse control”, is thought to prevent the initiation of a premature response (Duque *et al.*, 2010, 2017; Derosiere & Duque, 2020). In this case, the need to keep active two motor plans could make the inhibitory capacity of the motor system less effective, resulting in a higher CSE. For the sake of clarity, in this study we do not have a baseline condition in which the participants were completely at rest, in other words where participants did not have to prepare any action. For this reason, we cannot strictly talk about “preparatory inhibition” in the “Informed” conditions and of an “absence of inhibition” in the “Not Informed” conditions. However, comparing our conditions, the higher CSE presents in the “Not Informed” conditions remains evident.

After the cc-PAS_{AP}, we observed a significant reduction of the CSE only in these conditions, whereas nothing changed when the participants were informed. We suggest that, in the “Informed” conditions, the inhibitory control was already optimal before the cc-PAS_{AP} and, for this reason, no modulation is present after the PMv-M1 plasticity induction. In contrast, in the “Not Informed” conditions, where the inhibitory control was lower, the cc-PAS_{AP} application made it more efficient.

Although few studies have investigated the role of PMv during action preparation (Davare *et al.*, 2009; van Campen *et al.*, 2013), previous studies on the PMv-M1 plasticity induction have shown modulations of fast and slow M1 GABAergic activity (i.e. GABA_A and GABA_B receptors mediated; Casarotto *et al.*, 2023a; Turrini *et al.*, 2023b). These neurophysiological modulations find their anatomical basis in the evidence that different PMv projections target M1 inhibitory interneurons (Ghosh & Porter, 1988; Tokuno & Nambu, 2000). These GABAergic inhibitory modulations could represent the cause of this CSE reduction in the “Not Informed” conditions, and thus the cause of the increase in the inhibitory control after the cc-PAS_{AP} application.

Kinematic Modulation

Starting from our preliminary analysis of the more macroscopic features; we observed a not-specific reduction of the RT in the post-30 section and the specific modulation of the MGA for the “Informed” conditions. In this case, although the modulation of the MGA was not action-specific, it showed an opposite pattern in the two actions. More precisely, after the cc-PAS_{AP}, the MGA appears to be reduced in the “Informed Precision Grip”, whereas it was larger in the “Informed Power Grip”. Since the size of the objects did not change between the two sessions, this effect could be interpreted as an optimization of the hand preshaping during the transport phase. In all likelihood, this effect may only appear when participants have been early informed of the action to be performed and can therefore select and fine-tune the specific motor plan in advance.

As mentioned earlier, the actions investigated here are strongly stereotyped, which may mean that the more macroscopic components of their kinematics are less susceptible to modulations. However, although the actions have similar macroscopic kinematics, they may conceal finer modulations due to different muscle activation encoded by the CNS (Brown & Cooke, 1990; Cooke & Brown, 1990, 1994).

After the cc-PAS_{AP}, we have an action unspecific reduction of the maximum acceleration (i.e.: PA) and maximum deceleration (i.e.: PD) reached by the subjects. Moreover, the TPA is temporally shifted forward, although it shows greater variability, as evidenced by the increase in its standard deviation. Taken together, these results seem to highlight a greater smoothness of the movement, with less pronounced acceleration and deceleration peaks.

The most important aspect that emerges from the results is the specific modification in the ratio of PA to PD (i.e. PA/PD) in the precision grip actions. Although the acceleration and the deceleration peaks changes in both precision and power grips, the ratio between the two only changes in the precision grip. As already mentioned, the magnitude of the acceleration and deceleration components of movements is linked to the underlying muscle activation and, in particular, to the interaction between agonist and antagonist muscles (Brown & Cooke, 1990). Here, we have an increase in the PA/PD ratio, after the cc-PAS_{AP}, indicating an imbalance in favour of the acceleration component of the movement.

This phase reflects the feedforward component of the movement – in other words, the part of the movement that is most closely preplanned and requires the least feedback corrections. The precision grip actions, characterised by a fractioned finger configuration and by a finer approach to the target, usually present a pronounced feedback component. Crucially, this result shows a shift in favour of feedforward control rather than in favour of the feedback corrections.

The modulation of the acceleration and deceleration phase could be attributed to a different interplay between the agonist and antagonist muscles. These multi-joint movements are characterised by a “triphasic” pattern (Hallett, 1975; Brown & Cooke, 1990; Cooke & Brown, 1990, 1994). This pattern is composed by a first burst of the agonist muscle, followed by a burst of the antagonist muscle, and ending with a second small burst of the agonist muscle. The first two components of this pattern (i.e.: the agonist muscle burst followed by the antagonist muscle burst) are clearly linkable to the acceleration profile components and correspond to the acceleration and deceleration phases. For this reason, we can assume that the modulation of the PA/PD ratio reflects a different interplay between the recruited muscles during movement; an interplay that here results in being specifically modulated in the precision grip actions. The importance of this modulation lies in the fact that the underlying muscular interaction is determined by the CNS motor output.

Conclusion

The results of this study expand our knowledge of the motor control of different grasping actions and the opportunity to selectively modulate one of them. Here, we demonstrate for the first time that, the PMv-M1 plasticity induction, through the application of the cc-PAS_{AP}, can preferentially modulate the kinematics of precision grip. In particular, the feedforward and feedback control of the action are modulated. The precision prehension, which is configured as a more feedback-based action, after the cc-PAS_{AP} presents a stronger feedforward component.

The possibility to specifically conditioning the neuronal populations that sculpt the precision prehension command has undeniable clinical relevance. It is well known that many patients with hand motor impairments often recover their gross functions but, just as often, do not recover fine motor skills.

These new results further support the future relevance of these TMS protocols for motor rehabilitation.

Furthermore, the increased inhibitory control during the action preparation, after the cc-PAS_{AP}, supports the role of PMv as a key node that can modulate and optimise M1 activity according to context demands. Indeed, after the cc-PAS_{AP}, the CSE was increased if an isometric contraction was required (Casarotto *et al.*, 2023b), but here, during the action preparation phase, when inhibitory control play a crucial role, we found an increased inhibition.

5. DISCUSSION AND FUTURE PERSPECTIVES

Discussion

Here are presented the studies on the PMv-M1 network and the plasticity induction that I have conducted in the past three years. Prehension movements represent the most common actions performed in daily life and allow us to interact with our surroundings and others. Furthermore, the ability to grasp an object is the first step in manipulating and using it. The extensive network supporting these actions has been studied for a long time. However, the possibility to induce a Hebbian-like STDP between different brain areas has only recently been proposed (Rizzo *et al.*, 2009). The opportunity to increase or decreased synaptic efficiency between regions of a network brings with it the possibility of new insights into how different areas work together to sustain a complex function and, not least, could have important clinical implications. The loss of the motor functions of the hand, the principal effector of grasping movements, represents a severe impairment of daily life. With this awareness, several research fields have invested their efforts in implementing rehabilitation methods: from the development of different orthosis to robotic devices, from the more classical physiotherapy rehabilitation to peripheral and central nerve stimulation. The PAS and cc-PAS protocols represent one of the future proposals for hand motor rehabilitation. This perspective will be further explored in the next section.

Over the past three years, we have started with an extensive investigation of neurophysiological modulations resulting from the cc-PAS application between the PMv and M1. This protocol, applied with different M1 coil orientations, can lead to different long-lasting effects. At the neurophysiological level, the application of this protocol with a PA coil orientation led to an LTP-like after-effect, whereas the same protocol applied with an AP coil orientation led to the opposite after-effect (i.e.: LTD-like). These two after-effects appear to be mediated by the I₂-wave circuitry, the activity of which appears to be functionally correlated, at single-subject level, with the magnitude of LTP- or LTD-like after-effect.

Furthermore, the M1 local GABAergic circuits are also modulated by the PMv-M1 plasticity induction. After the cc-PAS_{PA}, we found a GABA_B-receptors mediated inhibitory modulation (Casarotto *et al.*, 2023b); differently, after the same protocol, Turrini and colleagues (2023b) found a GABA_A-receptor mediated inhibition modulation. It is possible that the modulations of inhibitory mechanisms are more subtle and do not involve a single component (i.e. GABA_A receptors and GABA_B receptors). However, this modulation of inhibitory activity becomes evident when the context required an inhibitory control, as demonstrated in the action preparation phase. This supports the idea that PMv does not only exert a specific influence in M1, as could be the selective potentiation of inhibitory or excitatory activity. Rather, it seems that PMv can modulate M1 activity more generally, making it optimal in different contexts. During the executions of an isometric precision prehension, the enhancement of synaptic efficiency between PMv and M1 led to an increase in the CSE, whereas during the action preparation there was an increase in the inhibitory control.

Although initially, for the sake of clarity in reporting results, they were described separately, all these modulations are closely interconnected. The several circuits existing in M1 work in concert with each other, not independently, to sculpt the motor output.

The PMv likely interacts with and modulates the M1 descending motor output through the I₂-wave circuit. Indeed, in the macaque, PMv stimulation prior to M1 stimulation led to the modulation of I₂- and I₃-wave amplitude (Cerri *et al.*, 2003; Shimazu *et al.*, 2004). This circuit is likely composed of inhibitory and excitatory interneurons that repeatedly inhibit and reactivate L5 pyramidal neurons (Di Lazzaro *et al.*, 2012; Ziemann, 2020). In this regards, previous evidence has shown that PMv projections, which reach M1 in both more superficial (i.e.: L2-L3) and deeper (i.e.: L5) layers, target both inhibitory and excitatory neurons (Ghosh & Porter, 1988; Tokuno & Nambu, 2000). The observed modulations of GABAergic activity could represent one of the modulated components into the I₂-wave intracortical circuits. The altered activity of this circuit, which is at least partly responsible for the inhibition and reactivation of pyramidal neurons, is likely to lead to the more general LTP- and LTD-like after-effect.

From these results, it is important to consider that Hebbian-like STDP plasticity is a neurophysiological phenomenon. For this reason, it is hardly possible to carry out reliable behavioural or cognitive investigations related to this phenomenon, if not grounded upon a thorough knowledge of its neurophysiological bases.

Once we had established the neurophysiological effects induced by these protocols, we could use this knowledge to understand the role of different intracortical circuits in different tasks. It has been previously seen that through different coil orientations, it is possible to observe the contribution of different M1 circuits in various tasks (Federico & Perez, 2017; Spampinato, 2020; Spampinato *et al.*, 2020; Davis *et al.*, 2022). Here, in particular, we observed how the application of cc-PAS, with an AP coil orientation, could specifically modulate the M1 motor output during the precision grip execution. This specific modulation was only observable when the CSE was tested with an AP coil orientation. This result further supports the idea that different coil orientations recruit different circuits, and consequently bring out different effects that are otherwise not visible. The PA coil orientation, stimulating the M1 neuronal populations close to L5 pyramidal neurons, could provide a general readout of the CSE that neglects, at least in part, the contribution of the more superficial layers. A contribution emerging through the AP stimulation.

The result obtained related a specific action with a specific circuit and a specific protocol with the modulation of its motor output.

From a methodological and neurophysiological point of view, another important result emerged from the analysis of MEPs latencies. The cc-PAS modulated MEPs latency only when they were elicited with the same coil orientation used during the cc-PAS stimulations. This specificity argues in favour of the possibility of specifically modulating the activity of different intracortical M1 circuits.

The cc-PAS protocol, which modulated the motor output during the isometric execution of the precision grip action, also resulted in the modulation of its kinematics when it was performed naturalistically. By analysing the kinematic of precision and power prehension before and after the PMv-M1 plasticity induction emerged that, although some macroscopic features were modified in both actions, the balance between the acceleration and deceleration component of the actions was selectively modulated during the precision grip. The relevance of this result

can be traced back to the evidence that the acceleration and deceleration phases of movement directly depends by the activity of agonist and antagonist muscles. The underlying muscle activity is the direct expression of how the movement is encoded in motor regions. The modulation observed allows us to propose that, after cc-PAS_{AP}, in the PMv-M1 network the motor plan of precision prehension was encoded, at least in part, differently. This different encoding of the motor plan results in a different encoding of the muscular activation to translate it into an action. This has led to an imbalance in favour of the feedforward component (i.e. the acceleration phase), although precision grasping is a more feedback-based action.

All the actions we are studying, no matter how complex and rich in meaning, when reduced to the bare minimum are composed of a sequence of muscle activations defined by the descending nerve signals produced by the CNS. For this reason, evidence of modulation of the way an action is encoded in motor areas must be sought in the way this action is performed. The kinematics of an action is determined by the muscular activity occurs. In the future, to further support these results, it might be interesting to directly observe, through EMG recording, how the pattern of muscle activation changes after the PMv-M1 plasticity induction. Furthermore, it might be interesting to observe how the descending volley changes during the action execution. In the first study performed, we reported the modulation, at rest, of the SICF at 2.5 ms, which reflects the I₂-wave. In the future, we could be studied how the descending volley changes during the execution of different actions.

Previous studies had already suggested that precision and power grip actions may be supported, at least in part, by different circuits (Baker, 2011; Baker & Perez, 2017; Federico & Perez, 2017; Tazoe & Perez, 2017). Here, we demonstrated the possibility of selectively modulating the neurophysiological activity and the motor expression of one of these circuits. Considering all these results, we can assume that the AP current direction is preferential for inducing a functional motor plasticity in the PMv-M1 network. At least, if we consider the more fractioned finger movements. We can speculate that the modulation of the M1 motor output, observed in our second study (Casarotto *et al.*, 2023b), may represent the neurophysiological modulation that leads to the kinematic changes that emerged

from our last experiment. This initial evidence of the possibility of modulating how an action is performed opens up to different future perspectives.

Future perspectives

The evidence that is possible to modulates not only the neurophysiology of the PMv-M1 network and the M1 motor output, but also how the movements are produced open to different future directions. Indeed, it is not obvious that a TMS protocol that can induce neurophysiological modulations is also able to lead to behavioural modulations such as modulation of kinematics.

One of the next steps of this research is to understand if and how these behavioural modulations can have an impact in a social context. In our daily lives we constantly interact with other people and, if not always, at least very often, our interactions have a motor component. For this reason, one of the next questions might concern how plasticity induction can modulate social motor interactions. It is known that behavioural interactions require reciprocal and continuous motor adaptations and shared cognitive representation of the task and goals. During such interactions, the motor plans require to be continuously updated and corrected. As can be deduced, investigating motor adaptation in the complexity of naturalistic interaction represents a complex challenge. We must first clarify how we correct our actions in a discrete manner, based on context requirements, and how the PMv-M1 plasticity inductions could modify this process. This should be the first step in studying naturalistic interaction in which motor plans must be continuously corrected. In this regards, it has previously been suggested that PMv represents a critical regions when a current action needs to be reprogrammed. (Buch *et al.*, 2010).

We have already conducted an initial study aimed at temporally characterising the action reprogramming. In this study, using the same setup as described in *Chapter 4*, participants were instructed to perform a precision or a power grip action. However, unlike the experiment described above, there were no “Informed” and “Not Informed” conditions, but participants were always informed in advantage of the action to be performed. In some trials, an acoustic cue warned participants to change the target (i.e.: from the small sphere to the big sphere or vice versa). The

acoustic signal could be presented 50 ms, 75 ms, 100 ms or 125 ms after the beginning of the actions. In this way, we aim to investigate the difference in the action reprogramming pattern at different timing, and to understand what might be the correct time to use to observe the possible effects induced by the plasticity induction in this process.

Indeed, although this study is still in progress, it has already allowed us to observe that it is not useful to signal to reprogram the action 125 ms after it has been initiated. At this timing, the current action is almost completed and therefore there is no reprogramming, but rather a complete stop of the action. At the same time, we are trying to understand whether the acoustic cue presented 50 ms after the beginning of the actions may be too early. In this phase of the movement, the action may not yet have developed enough to require visible adjustments.

Once we have defined the timing that makes the action reprogramming evident in the action kinematics, we will study the effect of the PMv-M1 cc-PAS on this process.

As we proposed in our previous studies, the cc-PAS with an AP coil orientation preferentially modulates the activity of the neuronal populations most involved in precision grip. Therefore, we expect that, after the cc-PAS_{AP}, modulations of the reprogramming pattern may be present when participants are required to reprogramme a power grip action into a precision grip action. Modulation of the activity of the most active populations during precision prehension could lead to an advantage in reprogramming towards this action.

Following this line of research, we will then move on to investigate the effect of plasticity induction on the naturalistic motor interactions. In this case, motor plans need to be continuously updated and, for this updating, the sensorimotor information provided by the other kinematic becomes relevant. The enhancement of the synaptic efficiency in the PMv-M1 network could lead to greater sensitivity in the perceiving these sensorimotor signals and, consequently, to better adjustment our motor plans. This could result in a modulation of the motor contagion, which naturally tends to occur (Dumas *et al.*, 2014; D'Ausilio *et al.*, 2015), between the kinematics of the actors involved in the interaction. Indeed, while in the current experiment the correction of the actions occurs in a delimited temporal window

(i.e.: immediately after the acoustic cue), during a prolonged coordination task the modulation could develop during the entire interaction.

Clinical implications

Although the interest on precision grip modulation was certainly driven by the evidence that it is a complex and fine movement, as anticipated earlier this is not the only reason that drove us. Another important aspect that motivated our interest was the awareness that in several clinical populations fractional finger movements are impaired and, usually, never fully recovered. Patients with motor impairments after stroke in the motor regions, usually only partially recover the use of the hand fine motor functions. If, they do recover. The recovery of gross motor functions of the hand, in parallel with the never complete recovery of the fine motor abilities, is probably the strongest evidence that different actions, such as the power grip and precision grip, are supported by different neural circuits. Lesional studies in monkeys clearly showed that the precision prehension is mediated by the corticospinal tract. After the surgical resection of the corticospinal tract, the monkeys reacquired some ability of grasp, but they never recovered the fine and independent finger movements (Lawrence & Kuypers, 1968a). The subsequent lesion of the rubrospinal tract led to a complete loss of the ability to grasp with the hand (Lawrence & Kuypers, 1968b). However, in human the rubrospinal tract appears to be almost absent (Nathan & Smith, 1955). For this reason, the most likely candidate, in human, for the gross hand functions is the reticulospinal tract (Baker, 2011; Baker & Perez, 2017; Tazoe & Perez, 2017). In support of this view there is precisely the evidence that in patients suffering from corticospinal lesions, such as after a stroke, which leaves the reticulospinal tract intact, there is a recovery of gross hand function. In this regard, reticulospinal outputs have been shown to strengthened during the recovery of a corticospinal injury (Zaaimi *et al.* 2009).

However, as mentioned above, these patients never recover the fractioned finger control, which is the hallmark of human and primate dexterity.

Currently, on the one side, different robotics supports have been developed with the aim of improving the hand motor rehabilitation. However, these passive arm mobilization aids have proved to be useful in the after-stroke motor rehabilitation,

they usually target the more proximal joint and muscles (i.e. arm, elbow, and forearm) and not the hand. On the other side, several orthoses are used as passive support for the hand stiffness. However, these do not show significant rehabilitative properties. In this difficult scenario, the PAS and cc-PAS protocols may be a promising alternative for the future of hand fine motor skill rehabilitation. It is well known that after an injury, multiple neurophysiological processes are activated that try to repair the damage. Obviously, we do not think that the TMS or the cc-PAS protocols can repair the lesion. However, reinforcement of inputs from nearby regions could serve to enhance the physiological processes active after injury.

Recent promising evidenced has shown that combining the PAS protocol with physiotherapy programmes promote the functional recovery in patients with chronic spinal cord injury (SCI - Urbin *et al.*, 2017; Jo *et al.*, 2023). In these studies, patients received 20 or 40 sessions of Hebbian (i.e. PAS protocol) or sham stimulation, targeting corticospinal-motoneuronal synapses of multiple leg muscles. Each stimulation session was followed by exercise. Patients who received the PAS stimulation showed significantly greater improvement of their walking speed and corticospinal function than patients who receive the sham stimulation. This improvement was maintained at 9 months after therapy and was greater with more sessions (Urbin *et al.*, 2017; Jo *et al.*, 2023). These results are a source of inspiration for the future development of rehabilitation methods incorporating cc-PAS protocols.

This protocol, combined with various tried-and-tested rehabilitation techniques such as the action observation therapy (AON), the peripheral stimulation or the physiotherapeutic exercise, could promote the hand motor rehabilitation in a similar way to what has been observed in the aforementioned studies.

In this regard, it is interestingly to mention another recent proposal published by MacLennan and colleagues (2023). Considering the results of our works, in particular the specific modulation of the motor output during the precision grip after the cc-PAS_{AP} (Chapter 3), they proposed to use this protocol as treatment for age-related declines in hand function. From this proposal, we can speculate that these stimulation protocols may have a role not only as rehabilitation techniques after

brain injury, but also as maintenance treatment in chronic and neurodegenerative conditions.

In these last two sections, I have tried to highlight what will be the interesting future perspectives of this specific research. Obviously, these proposals are not the only ones possible. The possibility of modulating synaptic efficiency between different areas opens up countless possibilities. Furthermore, I emphasised the perspectives closely related to the network considered in the studies previously presented (i.e. PMv-M1). However, these protocols for the plasticity induction have also been used in different areas of the ventral (e.g. V5-V1; Chiappini *et al.*, 2018) and dorsal stream (e.g. PPC-M1; Koch *et al.*, 2013). The use of these protocols between different regions from those considered here opens up other future possibilities and bodes well for a growing interest in this field of research.

BIBLIOGRAPHY

- Aberra AS, Wang B, Grill WM & Peterchev A V. (2020). Simulation of transcranial magnetic stimulation in head model with morphologically-realistic cortical neurons. *Brain Stimul* **13**, 175–189.
- Aguiar SA & Baker SN (2018). Convergent spinal circuits facilitating human wrist flexors. *J Neurosci* **38**, 3929–3938.
- Allison T, Mccarthy G, Wood CC & Jones SJ (1991). Potentials Evoked in Human and Monkey Cerebral Cortex By Stimulation of the Median Nerve. *Brain* **114**, 2465–2503.
- Amassian VE & Stewart M (2003). *Motor cortical and other cortical interneuronal networks that generate very high frequency waves*. Elsevier B.V. Available at: [http://dx.doi.org/10.1016/S1567-424X\(09\)70214-4](http://dx.doi.org/10.1016/S1567-424X(09)70214-4).
- Andersen RA & Buneo CA (2002). Intentional maps in posterior parietal cortex. *Annu Rev Neurosci* **25**, 189–220.
- Baker SN (2011). The primate reticulospinal tract, hand function and functional recovery. *J Physiol* **589**, 5603–5612.
- Baker SN & Perez MA (2017). Reticulospinal contributions to gross hand function after human spinal cord injury. *J Neurosci* **37**, 9778–9784.
- Battaglini P, Muzur A, Galletti C, Skrap M, Brovelli A & Fattori P (2002). Effects of lesions to area V6A in monkeys. *Exp Brain Res* **144**, 419–422.
- Bäumer T, Schippling S, Kroeger J, Zittel S, Koch G, Thomalla G, Rothwell JC, Siebner HR, Orth M & Münchau A (2009). Inhibitory and facilitatory connectivity from ventral premotor to primary motor cortex in healthy humans at rest - A bifocal TMS study. *Clin Neurophysiol* **120**, 1724–1731.

- Bennett KMB & Lemon RN (1996). Corticomotoneuronal contribution to the fractionation of muscle activity during precision grip in the monkey. *J Neurophysiol* **75**, 1826–1842.
- Bestmann S & Duque J (2015). Transcranial Magnetic Stimulation : Decomposing the Processes Underlying Action Preparation. ; DOI: 10.1177/1073858415592594.
- de Beukelaar TT, Alaerts K, Swinnen SP & Wenderoth N (2016). Motor facilitation during action observation: The role of M1 and PMv in grasp predictions. *Cortex* **75**, 180–192.
- Bi GQ & Poo MM (1998). Synaptic modifications in cultured hippocampal neurons: Dependence on spike timing, synaptic strength, and postsynaptic cell type. *J Neurosci* **18**, 10464–10472.
- Binkofski F & Buxbaum LJ (2013). Two action systems in the human brain. *Brain Lang* **127**, 222–229.
- Borra E, Belmalih A, Calzavara R, Gerbella M, Murata A, Rozzi S & Luppino G (2008). Cortical connections of the macaque anterior intraparietal (AIP) area. *Cereb Cortex* **18**, 1094–1111.
- Bosco A, Breveglieri R, Chinellato E, Galletti C & Fattori P (2010). Reaching activity in the medial posterior parietal cortex of monkeys is modulated by visual feedback. *J Neurosci* **30**, 14773–14785.
- Brochier T & Umiltà MA (2007). Cortical control of grasp in non-human primates. *Curr Opin Neurobiol* **17**, 637–643.
- Brown SH & Cooke JD (1990). Movement-related phasic muscle activation. I. Relations with temporal profile of movement. *J Neurophysiol* **63**, 455–464.
- Brzosko Z, Mierau SB & Paulsen O (2019). Neuromodulation of Spike-Timing-Dependent Plasticity: Past, Present, and Future. *Neuron* **103**, 563–581.
- Buch ER, Johnen VM, Nelissen N, O’Shea J & Rushworth MFS (2011).

- Noninvasive associative plasticity induction in a corticocortical pathway of the human brain. *J Neurosci* **31**, 17669–17679.
- Buch ER, Mars RB, Boorman ED & Rushworth MFS (2010). A network centered on ventral premotor cortex exerts both facilitatory and inhibitory control over primary motor cortex during action reprogramming. *J Neurosci* **30**, 1395–1401.
- Bunday KL, Tazoe T, Rothwell JC & Perez MA (2014). Subcortical control of precision grip after human spinal cord injury. *J Neurosci* **34**, 7341–7350.
- Caminiti R, Johnson PB, Galli C, Ferraina S & Burnod Y (1991). Making arm movements within different parts of space: The premotor and motor cortical representation of a coordinate system for reaching to visual targets. *J Neurosci* **11**, 1182–1197.
- van Campen AD, Neubert FX, van den Wildenberg WPM, Richard Ridderinkhof K & Mars RB (2013). Paired-pulse transcranial magnetic stimulation reveals probability-dependent changes in functional connectivity between right inferior frontal cortex and primary motor cortex during go/no-go performance. *Front Hum Neurosci* **7**, 1–10.
- Caporale N & Dan Y (2008). Spike timing-dependent plasticity: A Hebbian learning rule. *Annu Rev Neurosci* **31**, 25–46.
- Cardellicchio P, Koch G, Fadiga L & D'Ausilio A (2021). Motor overload: GABAergic index of parallel buffer costs. *Brain Stimul* **14**, 1106–1108.
- Casarotto A, Dolfini E, Cardellicchio P, Fadiga L, D'Ausilio A & Koch G (2023a). Mechanisms of Hebbian-like plasticity in the ventral premotor – primary motor network. *J Physiol* **0**, 1–16.
- Casarotto A, Dolfini E, Fadiga L, Koch G & D'Ausilio A (2023b). Cortico-cortical paired associative stimulation conditioning superficial ventral premotor cortex–primary motor cortex connectivity influences motor cortical activity during precision grip. *J Physiol* **601**, 3945–3960.

- Castiello U & Begliomini C (2008). The cortical control of visually guided grasping. *Neuroscientist* **14**, 157–170.
- Cattaneo L, Voss M, Brochier T, Prabhu G, Wolpert DM & Lemon RN (2005). A cortico-cortical mechanism mediating object-driven grasp in humans. *Proc Natl Acad Sci U S A* **102**, 898–903.
- Cavina-Pratesi C, Monaco S, Fattori P, Galletti C, McAdam TD, Quinlan DJ, Goodale MA & Culham JC (2010). Functional magnetic resonance imaging reveals the neural substrates of arm transport and grip formation in reach-to-grasp actions in humans. *J Neurosci* **30**, 10306–10323.
- Cerri G, Shimazu H, Maier MA & Lemon RN (2003). Facilitation from ventral premotor cortex of primary motor cortex outputs to macaque hand muscles. *J Neurophysiol* **90**, 832–842.
- Chiappini E, Silvanto J, Hibbard PB, Avenanti A & Romei V (2018). Strengthening functionally specific neural pathways with transcranial brain stimulation. *Curr Biol* **28**, R735–R736.
- Connolly JD, Andersen RA & Goodale MA (2003). FMRI evidence for a “parietal reach region” in the human brain. *Exp Brain Res* **153**, 140–145.
- Cooke JD & Brown SH (1990). Movement-related phasic muscle activation. II. Generation and functional role of the triphasic pattern. *J Neurophysiol* **63**, 465–472.
- Cooke JD & Brown SH (1994). Movement-related phasic muscle activation - III. The duration of phasic agonist activity initiating movement. *Exp Brain Res* **99**, 473–482.
- Culham JC, Danckert SL, DeSouza JFX, Gati JS, Menon RS & Goodale MA (2003). Visually guided grasping produces fMRI activation in dorsal but not ventral stream brain areas. *Exp Brain Res* **153**, 180–189.
- Culham JC & Valyear KF (2006). Human parietal cortex in action. *Curr Opin*

Neurobiol **16**, 205–212.

D'Ausilio A, Badino L, Cipresso P, Chirico A, Ferrari E, Riva G & Gaggioli A (2015). Automatic imitation of the arm kinematic profile in interacting partners. *Cogn Process* **16**, 197–201.

Dafotakis M, Sparing R, Eickhoff SB, Fink GR & Nowak DA (2008). On the role of the ventral premotor cortex and anterior intraparietal area for predictive and reactive scaling of grip force. *Brain Res* **1228**, 73–80.

Darling WG & Cooke JD (1987). Changes in the variability of movement trajectories with practice. *J Mot Behav* **19**, 291–309.

Davare M, Andres M, Cosnard G, Thonnard JL & Olivier E (2006). Dissociating the role of ventral and dorsal premotor cortex in precision grasping. *J Neurosci* **26**, 2260–2268.

Davare M, Kraskov A, Rothwell JC & Lemon RN (2011). Interactions between areas of the cortical grasping network. *Curr Opin Neurobiol* **21**, 565–570.

Davare M, Lemon R & Olivier E (2008). Selective modulation of interactions between ventral premotor cortex and primary motor cortex during precision grasping in humans. *J Physiol* **586**, 2735–2742.

Davare M, Montague K, Olivier E, Rothwell JC & Lemon RN (2009). Ventral premotor to primary motor cortical interactions during object-driven grasp in humans. *Cortex* **45**, 1050–1057.

Davare M, Rothwell JC & Lemon RN (2010). Causal Connectivity between the Human Anterior Intraparietal Area and Premotor Cortex during Grasp. *Curr Biol* **20**, 176–181.

Davis M, Wang Y, Bao S, Buchanan JJ, Wright DL & Lei Y (2022). The Interactions Between Primary Somatosensory and Motor Cortex during Human Grasping Behaviors. *Neuroscience* **485**, 1–11.

Debanne D, Gähwiler BH & Thompson SM (1998). Long-term synaptic plasticity

between pairs of individual CA3 pyramidal cells in rat hippocampal slice cultures. *J Physiol* **507**, 237–247.

Derosiere G & Duque J (2020). Tuning the Corticospinal System: How Distributed Brain Circuits Shape Human Actions. *Neuroscientist* **26**, 359–379.

Derosiere G, Vassiliadis P & Duque J (2020). Advanced TMS approaches to probe corticospinal excitability during action preparation. *Neuroimage* **213**, 116746.

Dumas G, Laroche J & Lehmann A (2014). Your body, my body, our coupling moves our bodies. *Front Hum Neurosci* **8**, 1–5.

Duque J, Greenhouse I, Labruna L & Ivry RB (2017). Physiological Markers of Motor Inhibition during Human Behavior. *Trends Neurosci*; DOI: 10.1016/j.tins.2017.02.006.

Duque J, Lew D, Mazzocchio R, Olivier E & Ivry RB (2010). Evidence for two concurrent inhibitory mechanisms during response preparation. *J Neurosci* **30**, 3793–3802.

Dutar P & Nicoll RA (1988). A physiological rôle for GABAB receptors in the central nervous system. *Nature* **332**, 156–158.

Ehrsson HH, Fagergren A, Jonsson T, Westling G, Johansson RS & Forssberg H (2000). Cortical activity in precision- versus power-grip tasks: An fMRI study. *J Neurophysiol* **83**, 528–536.

Fattori P, Raos V, Breveglieri R, Bosco A, Marzocchi N & Galletti C (2010). The dorsomedial pathway is not just for reaching: Grasping neurons in the medial parieto-occipital cortex of the macaque monkey. *J Neurosci* **30**, 342–349.

Federico P & Perez MA (2017). Distinct Corticocortical Contributions to Human Precision and Power Grip. *Cereb Cortex* **27**, 5070–5082.

Filimon F, Nelson JD, Hagler DJ & Sereno MI (2007). Human cortical representations for reaching: Mirror neurons for execution, observation, and imagery. *Neuroimage* **37**, 1315–1328.

- Filimon F, Nelson JD, Huang RS & Sereno MI (2009). Multiple parietal reach regions in humans: Cortical representations for visual and proprioceptive feedback during on-line reaching. *J Neurosci* **29**, 2961–2971.
- Fiori F, Chiappini E & Avenanti A (2018). Enhanced action performance following TMS manipulation of associative plasticity in ventral premotor-motor pathway. *Neuroimage* **183**, 847–858.
- Fisher RJ, Nakamura Y, Bestmann S, Rothwell JC & Bostock H (2002). Two phases of intracortical inhibition revealed by transcranial magnetic threshold tracking. *Exp Brain Res* **143**, 240–248.
- Fogassi L, Gallese V, Buccino G, Craighero L, Fadiga L & Rizzolatti G (2001). Cortical mechanism for the visual guidance of hand grasping movements in the monkey: A reversible inactivation study. *Brain* **124**, 571–586.
- Fong PY, Spampinato D, Rocchi L, Hannah R, Teng Y, Di Santo A, Shoura M, Bhatia K & Rothwell JC (2021). Two forms of short-interval intracortical inhibition in human motor cortex. *Brain Stimul* **14**, 1340–1352.
- Gallese V, Fadiga L, Fogassi L & Rizzolatti G (1996). Action recognition in the premotor cortex. *Brain* **119**, 593–609.
- Gallese V, Murata A, Kaseda M, Nanako N & Sakata H (1994). Deficit of hand preshaping after muscimol injection in monkey parietal cortex. (5) 1525-1529.
- Galletti C, Kutz DF, Gamberini M, Breveglieri R & Fattori P (2003). Role of the medial parieto-occipital cortex in the control of reaching and grasping movements. *Exp Brain Res* **153**, 158–170.
- Georgopoulos AP, Kalaska JF & Massey JT (1981). Spatial trajectories and reaction times of aimed movements: Effects of practice, uncertainty, and change in target location. *J Neurophysiol* **46**, 725–743.
- Ghosh B & Porter R (1988). Corticocortical synaptic influences on morphologically identified pyramidal neurones in the motor cortex of the monkey. *J Physiol*

400, 617–629.

Grafton ST (2010). The cognitive neuroscience of prehension: Recent developments. *Exp Brain Res* **204**, 475–491.

Grol MJ, Majdandžić J, Stephan KE, Verhagen L, Dijkerman HC, Bekkering H, Verstraten FAJ & Toni I (2007). Parieto-frontal connectivity during visually guided grasping. *J Neurosci* **27**, 11877–11887.

Groppa S, Werner-Petroll N, Münchau A, Deuschl G, Ruschworth MFS & Siebner HR (2012). A novel dual-site transcranial magnetic stimulation paradigm to probe fast facilitatory inputs from ipsilateral dorsal premotor cortex to primary motor cortex. *Neuroimage* **62**, 500–509.

Hallett M (1975). EMG analysis of stereotyped voluntary movements in man. *J Neurol Neurosurg Psychiatry* **38**, 1154–1162.

Hamada M, Galea JM, Di Lazzaro V, Mazzone P, Ziemann XU & Rothwell JC (2014). Two distinct interneuron circuits in human motor cortex are linked to different subsets of physiological and behavioral plasticity. *J Neurosci* **34**, 12837–12849.

Hannah R, Rocchi L, Tremblay S, Wilson E & Rothwell JC (2020). Pulse width biases the balance of excitation and inhibition recruited by transcranial magnetic stimulation. *Brain Stimul* **13**, 536–538.

Hebb DO (1949). *The Organization of Behavior: a Neuropsychological Theory*. New York Sci Ed; DOI: 10.2307/1418888.

Hupfeld KE, Swanson CW, Fling BW & Seidler RD (2020). TMS-induced silent periods: A review of methods and call for consistency. *J Neurosci Methods* **346**, 108950.

Ilić T V., Meintzschel F, Cleff U, Ruge D, Kessler KR & Ziemann U (2002). Short-interval paired-pulse inhibition and facilitation of human motor cortex: The dimension of stimulus intensity. *J Physiol* **545**, 153–167.

- Iturrate I, Chavarriaga R, Pereira M, Zhang H, Corbet T, Leeb R & Millán J del R (2018). Human EEG reveals distinct neural correlates of power and precision grasping types. *Neuroimage* **181**, 635–644.
- Jeannerod M, Arbib MA, Rizzolatti G & Sakata H (1995). Grasping objects: the cortical mechanisms of visuomotor transformation. *Trends Neurosci* **18**, 314–320.
- Jiang X, Wang G, Lee AJ, Stornetta RL & Zhu JJ (2013). The organization of two new cortical interneuronal circuits. *Nat Neurosci* **16**, 210–218.
- Jo HJ, Kizziar E, Sangari S, Chen D, Kessler A, Kim K, Anshel A, Heinemann AW, Mensh BD, Awadalla S, Lieber RL, Oudega M & Perez MA (2023). Multisite Hebbian Plasticity Restores Function in Humans with Spinal Cord Injury. *Ann Neurol* **93**, 1198–1213.
- Johnen VM, Neubert FX, Buch ER, Verhagen LM, O'Reilly J, Mars RB & Rushworth MFS (2015). Causal manipulation of functional connectivity in a specific neural pathway during behaviour and at rest. *Elife* **2015**, 1–23.
- Johnson MD, Hyngstrom AS, Manuel M & Heckman CJ (2012). Push – Pull Control of Motor Output. **32**, 4592–4599.
- Johnson PB, Ferraina S, Bianchi L & Caminiti R (1996). Cortical networks for visual reaching: Physiological and anatomical organization of frontal and parietal lobe arm regions. *Cereb Cortex* **6**, 102–119.
- Kampa BM, Clements J, Jonas P & Stuart GJ (2004). Kinetics of Mg²⁺ unblock of NMDA receptors: Implications for spike-timing dependent synaptic plasticity. *J Physiol* **556**, 337–345.
- Kampa BM, Letzkus JJ & Stuart GJ (2007). Dendritic mechanisms controlling spike-timing-dependent synaptic plasticity. *Trends Neurosci* **30**, 456–463.
- Klein PA, Olivier E & Duque J (2012). Influence of reward on corticospinal excitability during movement preparation. *J Neurosci* **32**, 18124–18136.

- Koch G, Cercignani M, Pecchioli C, Versace V, Oliveri M, Caltagirone C, Rothwell J & Bozzali M (2010a). In vivo definition of parieto-motor connections involved in planning of grasping movements. *Neuroimage* **51**, 300–312.
- Koch G, Ponzo V, Di Lorenzo F, Caltagirone C & Veniero D (2013). Hebbian and anti-Hebbian spike-timing-dependent plasticity of human cortico-cortical connections. *J Neurosci* **33**, 9725–9733.
- Koch G, Versace V, Bonni S, Lupo F, Gerfo E Lo, Oliveri M & Caltagirone C (2010b). Resonance of cortico-cortical connections of the motor system with the observation of goal directed grasping movements. *Neuropsychologia* **48**, 3513–3520.
- Kurz A, Xu W, Wiegel P, Leukel C, & N. Baker S (2019). Non-invasive assessment of superficial and deep layer circuits in human motor cortex. *The Journal of physiology*, 597(12), 2975-2991.
- Lago A, Koch G, Cheeran B, Márquez G, Sánchez JA, Ezquerro M, Giraldez M & Fernández-del-Olmo M (2010). Ventral premotor to primary motor cortical interactions during noxious and naturalistic action observation. *Neuropsychologia* **48**, 1802–1806.
- Di Lazzaro V, Pilato F, Oliviero A, Dileone M, Saturno E, Mazzone P, Insola A, Profice P, Ranieri F, Capone F, Tonali PA & Rothwell JC (2006). Origin of facilitation of motor-evoked potentials after paired magnetic stimulation: Direct recording of epidural activity in conscious humans. *J Neurophysiol* **96**, 1765–1771.
- Di Lazzaro V, Profice P, Ranieri F, Capone F, Dileone M, Oliviero A & Pilato F (2012). I-wave origin and modulation. *Brain Stimul* **5**, 512–525.
- Di Lazzaro V & Rothwell JC (2014). Corticospinal activity evoked and modulated by non-invasive stimulation of the intact human motor cortex. *J Physiol* **592**, 4115–4128.
- Lehmann SJ & Scherberger H (2013). Reach and gaze representations in

- macaque parietal and premotor grasp areas. *J Neurosci* **33**, 7038–7049.
- Leocani L, Cohen LG, Wassermann EM, Ikoma K & Hallett M (2000). Human corticospinal excitability evaluated with transcranial magnetic stimulation during different reaction time paradigms. *Brain* **123**, 1161–1173.
- Liao W-Y, Opie MG, Ziemann U & Semmler GJ (2023). Modulation of dorsal premotor cortex differentially influences I-wave excitability in primary motor cortex of young and older adults. *J Physiol*; DOI: 10.1113/JP284204.
- Luppino G, Murata A, Govoni P & Matelli M (1999). Largely segregated parietofrontal connections linking rostral intraparietal cortex (areas AIP and VIP) and the ventral premotor cortex (areas F5 and F4). *Exp Brain Res* **128**, 181–187.
- Magee JC & Johnston D (1997). A synaptically controlled, associative signal for Hebbian plasticity in hippocampal neurons. *Science (80-)* **275**, 209–213.
- Maier MA, Kirkwood PA, Brochier T & Lemon RN (2013). Responses of single corticospinal neurons to intracortical stimulation of primary motor and premotor cortex in the anesthetized macaque monkey. *J Neurophysiol* **109**, 2982–2998.
- Makris N, Kennedy DN, McInerney S, Sorensen AG, Wang R, Caviness VS & Pandya DN (2005). Segmentation of subcomponents within the superior longitudinal fascicle in humans: A quantitative, in vivo, DT-MRI study. *Cereb Cortex* **15**, 854–869.
- Malenka RC (1994). Synaptic plasticity in the hippocampus: LTP and LTD. *Cell* **78**, 535–538.
- Mao T, Kusefoglou D, Hooks BM, Huber D, Petreanu L & Svoboda K (2011). Long-Range Neuronal Circuits Underlying the Interaction between Sensory and Motor Cortex. *Neuron* **72**, 111–123.
- Markram H, Gerstner W & Sjöström PJ (2011). A history of spike-timing-

- dependent plasticity. *Front Synaptic Neurosci* **3**, 1–24.
- Markram H, Lübke J, Frotscher M & Sakmann B (1997). Regulation of synaptic efficacy by coincidence of postsynaptic APs and EPSPs. *Science (80-)* **275**, 213–215.
- Matelli M, Govoni P, Galletti C, Kutz DF & Luppino G (1998). Superior area 6 afferents from the superior parietal lobule in the macaque monkey. *J Comp Neurol* **402**, 327–352.
- McDonnell MN, Orekhov Y & Ziemann U (2006). The role of GABAB receptors in intracortical inhibition in the human motor cortex. *Exp Brain Res* **173**, 86–93.
- Mott DD & Lewis D V. (1991). Facilitation of the induction of long-term potentiation by GABAB receptors. *Science (80-)* **252**, 1718–1720.
- Muir RB & Lemon RN (1983). Corticospinal neurons with a special role in precision grip. *Brain Res* **261**, 312–316.
- Müller-Dahlhaus JFM, Liu Y & Ziemann U (2008). Inhibitory circuits and the nature of their interactions in the human motor cortex - A pharmacological TMS study. *J Physiol* **586**, 495–514.
- Murata A, Fadiga L, Fogassi L, Gallese V, Raos V & Rizzolatti G (1997). Object representation in the ventral premotor cortex (Area F5) of the monkey. *J Neurophysiol* **78**, 2226–2230.
- Murata A, Gallese V, Luppino G, Kaseda M & Sakata H (2000). Selectivity for the shape, size, and orientation of objects for grasping in neurons of monkey parietal area AIP. *J Neurophysiol* **83**, 2580–2601.
- Neige C, Rannaud Monany D & Lebon F (2021). Exploring cortico-cortical interactions during action preparation by means of dual-coil transcranial magnetic stimulation: A systematic review. *Neurosci Biobehav Rev* **128**, 678–692.
- Ni Z, Charab S, Gunraj C, Nelson AJ, Udupa K, Yeh IJ & Chen R (2011a).

- Transcranial magnetic stimulation in different current directions activates separate cortical circuits. *J Neurophysiol* **105**, 749–756.
- Ni Z, Gunraj C, Wagle-Shukla A, Udupa K, Mazzella F, Lozano AM & Chen R (2011*b*). Direct demonstration of inhibitory interactions between long interval intracortical inhibition and short interval intracortical inhibition. *J Physiol* **589**, 2955–2962.
- Pauly MG, Barlage M, Hamami F, Steinhardt J, Baarbé J, Tran S, Hanssen H, Herzog R, Tadic V, Brüggemann N, Chen R, Münchau A, Bäumer T & Weissbach A (2022). Subthalamic nucleus conditioning reduces premotor-motor interaction in Parkinson's disease. *Parkinsonism Relat Disord* **96**, 6–12.
- di Pellegrino G, Fadiga L, Fogassi L, Gallese V & Rizzolatti G (1992). Understanding motor events: a neurophysiological study. *Exp Brain Res* **91**, 176–180.
- Pisella L, Gréa H, Tilikete C, Vighetto A, Desmurget M, Rode G, Boisson D & Rossetti Y (2000). An 'automatic pilot' for the hand in human posterior parietal cortex: toward reinterpreting optic ataxia. *Nat Neurosci* **7**, 729–736.
- Poole BJ, Mather M, Livesey EJ, Harris IM & Harris JA (2018). Motor-evoked potentials reveal functional differences between dominant and non-dominant motor cortices during response preparation. *Cortex* **103**, 1–12.
- Prabhu G, Shimazu H, Cerri G, Brochier T, Spinks RL, Maier MA & Lemon RN (2009). Modulation of primary motor cortex outputs from ventral premotor cortex during visually guided grasp in the macaque monkey. *J Physiol* **587**, 1057–1069.
- Prado J, Clavagnier S, Otzenberger H, Scheiber C, Kennedy H & Perenin MT (2005). Two cortical systems for reaching in central and peripheral vision. *Neuron* **48**, 849–858.
- Raos V, Umiltá MA, Gallese V & Fogassi L (2004). Functional properties of grasping-related neurons in the dorsal premotor area F2 of the macaque

- monkey. *J Neurophysiol* **92**, 1990–2002.
- Raos V, Umiltá MA, Murata A, Fogassi L & Gallese V (2006). Functional properties of grasping-related neurons in the ventral premotor area F5 of the macaque monkey. *J Neurophysiol* **95**, 709–729.
- Rathelot JA & Strick PL (2009). Subdivisions of primary motor cortex based on cortico-motoneuronal cells. *Proc Natl Acad Sci U S A* **106**, 918–923.
- Rice NJ, Tunik E & Grafton ST (2006). The anterior intraparietal sulcus mediates grasp execution, independent of requirement to update: New insights from transcranial magnetic stimulation. *J Neurosci* **26**, 8176–8182.
- Rizzo V, Siebner HS, Morgante F, Mastroeni C, Girlanda P & Quartarone A (2009). Paired associative stimulation of left and right human motor cortex shapes interhemispheric motor inhibition based on a hebbian mechanism. *Cereb Cortex* **19**, 907–915.
- Rizzolatti G & Craighero L (2004). The mirror neuron system. *Annu Rev Neurosci* **27**, 169–192.
- Rizzolatti G & Luppino G (2001). The cortical motor system. *Neuron* **31**, 889–901.
- Rizzolatti G, Luppino G & Matelli M (1998). The organization of the cortical motor system: new concepts. *Electroencephalogr Clin Neurophysiol* **106**, 283–296.
- Rizzolatti G & Matelli M (2003). Two different streams form the dorsal visual system: Anatomy and functions. *Exp Brain Res* **153**, 146–157.
- Roshan L, Paradiso GO & Chen R (2003). Two phases of short-interval intracortical inhibition. *Exp Brain Res* **151**, 330–337.
- Rossi S et al. (2009). Safety, ethical considerations, and application guidelines for the use of transcranial magnetic stimulation in clinical practice and research. *Clin Neurophysiol* **120**, 2008–2039.
- Rossini PM et al. (2015). Non-invasive electrical and magnetic stimulation of the

brain, spinal cord, roots and peripheral nerves: Basic principles and procedures for routine clinical and research application: An updated report from an I.F.C.N. Committee. *Clin Neurophysiol* **126**, 1071–1107.

Rozzi S, Calzavara R, Belmalih A, Borra E, Gregoriou GG, Matelli M & Luppino G (2006). Cortical connections of the inferior parietal cortical convexity of the macaque monkey. *Cereb Cortex* **16**, 1389–1417.

Rozzi S, Ferrari PF, Bonini L, Rizzolatti G & Fogassi L (2008). Functional organization of inferior parietal lobule convexity in the macaque monkey: Electrophysiological characterization of motor, sensory and mirror responses and their correlation with cytoarchitectonic areas. *Eur J Neurosci* **28**, 1569–1588.

Sanchez-Vives M V., Barbero-Castillo A, Perez-Zabalza M & Reig R (2021). GABAB receptors: modulation of thalamocortical dynamics and synaptic plasticity. *Neuroscience* **456**, 131–142.

Schwenkreis P, Liepert J, Witscher K, Fischer W, Weiller C, Malin JP & Tegenthoff M (2000). Riluzole suppresses motor cortex facilitation in correlation to its plasma level. A study using transcranial magnetic stimulation. *Exp Brain Res* **135**, 293–299.

Shimazu H, Maier MA, Cerri G, Kirkwood PA & Lemon RN (2004). Macaque Ventral Premotor Cortex Exerts Powerful Facilitation of Motor Cortex Outputs to Upper Limb Motoneurons. *J Neurosci* **24**, 1200–1211.

Sjöström PJ & Häusser M (2006). A Cooperative Switch Determines the Sign of Synaptic Plasticity in Distal Dendrites of Neocortical Pyramidal Neurons. *Neuron* **51**, 227–238.

Sommer M, Norden C, Schmack L, Rothkegel H, Lang N & Paulus W (2013). Opposite optimal current flow directions for induction of neuroplasticity and excitation threshold in the human motor cortex. *Brain Stimul* **6**, 363–370.

Spampinato D (2020). Dissecting two distinct interneuronal networks in M1 with

- transcranial magnetic stimulation. *Exp Brain Res* **238**, 1693–1700.
- Spampinato D, Celnik PA & Rothwell JC (2020). Cerebellar-motor cortex connectivity: One or two different networks? *J Neurosci* **40**, 4230–4239.
- Spinks RL, Kraskov A, Brochier T, Umiltà MA & Lemon RN (2008). Selectivity for grasp in local field potential and single neuron activity recorded simultaneously from M1 and F5 in the awake macaque monkey. *J Neurosci* **28**, 10961–10971.
- Stark E & Abeles M (2007). Predicting movement from multiunit activity. *J Neurosci* **27**, 8387–8394.
- Stefan K, Kunesch E, Cohen LG, Benecke R & Classen J (2000). Induction of plasticity in the human motor cortex by paired associative stimulation. *Brain* **123**, 572–584.
- Tazoe T & Perez MA (2017). Cortical and reticular contributions to human precision and power grip. *J Physiol* **595**, 2715–2730.
- Tokuno H & Nambu A (2000). Organization of nonprimary motor cortical inputs on pyramidal and nonpyramidal tract neurons of primary motor cortex: An electrophysiological study in the macaque monkey. *Cereb Cortex* **10**, 58–68.
- Tunik E, Frey SH & Grafton ST (2005). Virtual lesions of the anterior intraparietal area disrupt goal-dependent on-line adjustments of grasp. *Nat Neurosci* **8**, 505–511.
- Turella L & Lingnau A (2014). Neural correlates of grasping. *Front Hum Neurosci* **8**, 1–8.
- Turrini S, Bevacqua N, Cataneo A, Chiappini E, Fiori F, Battaglia S, Romei V & Avenanti A (2023a). Neurophysiological Markers of Premotor – Motor Network Plasticity Predict Motor Performance in Young and Older Adults. *Front Aging Neurosci*.
- Turrini S, Fiori F, Chiappini E, Lucero B, Santarnecchi E & Avenanti A (2023b).

- Cortico-cortical paired associative stimulation (ccPAS) over premotor-motor areas affects local circuitries in the human motor cortex via Hebbian plasticity. *Neuroimage* **271**, 120027.
- Umiltà MA, Brochier T, Spinks RL & Lemon RN (2007). Simultaneous recording of macaque premotor and primary motor cortex neuronal populations reveals different functional contributions to visuomotor grasp. *J Neurophysiol* **98**, 488–501.
- Urbán MA, Özdemir RA, Tazoe T & Perez MA (2017). Spike-timing-dependent plasticity in lower-limb motoneurons after human spinal cord injury. *J Neurophysiol* **118**, 2171–2180.
- Vargas-Caballero M & Robinson HPC (2003). A slow fraction of Mg²⁺ unblock of NMDA receptors limits their contribution to spike generation in cortical pyramidal neurons. *J Neurophysiol* **89**, 2778–2783.
- Veniero D, Ponzio V & Koch G (2013). Paired associative stimulation enforces the communication between interconnected areas. *J Neurosci* **33**, 13773–13783.
- Vingerhoets G (2014). Contribution of the posterior parietal cortex in reaching, grasping, and using objects and tools. *Front Psychol* **5**, 1–17.
- Vucic S, Cheah BC & Kiernan MC (2011). Dissecting the mechanisms underlying short-interval intracortical inhibition using exercise. *Cereb Cortex* **21**, 1639–1644.
- Werhahn KJ, Kunesch E, Noachtar S, Benecke R & Classen J (1999). Differential effects on motorcortical inhibition induced by blockade of GABA uptake in humans. *J Physiol* **517**, 591–597.
- Witney AG, Wing A, Thonnard JL & Smith AM (2004). The cutaneous contribution to adaptive precision grip. *Trends Neurosci* **27**, 637–643.
- Wolters A, Sandbrink F, Schlottmann A, Kunesch E, Stefan K, Cohen LG, Benecke R & Classen J (2003). A temporally asymmetric Hebbian rule

governing plasticity in the human motor cortex. *J Neurophysiol* **89**, 2339–2345.

Ziemann U (2020). I-waves in motor cortex revisited. *Exp Brain Res* **238**, 1601–1610.

Ziemann U, Chen R, Cohen LG & Hallett M (1998). Dextromethorphan decreases the excitability of the human motor cortex. *Neurology* **51**, 1320–1324.

Ziemann U, Lönnecker S, Steinhoff BJ & Paulus W (1996a). The effect of lorazepam on the motor cortical excitability in man. *Exp Brain Res* **109**, 127–135.

Ziemann U, Reis J, Schwenkreis P, Rosanova M, Strafella A, Badawy R & Müller-Dahlhaus F (2015). TMS and drugs revisited 2014. *Clin Neurophysiol* **126**, 1847–1868.

Ziemann U, Rothwell JC & Ridding MC (1996b). Interaction between intracortical inhibition and facilitation in human motor cortex. *J Physiol* **496**, 873–881.